Error estimates of discontinuous Galerkin methods on moving meshes for the advection-diffusion equation

Ezra Serge Adam Rozier
February 26, 2024

DOCTORAL DISSERTATION
in
The Faculty of Mathematics, Informatics and Natural Sciences
(Mathematics)
Universität Hamburg

Assessors

Prof. Dr. Tobias Dyckerhoff

Prof. Dr. Hendrik Ranocha

Prof. Dr. Jörn Behrens

Prof. Dr. Thomas Rung

Prof. Dr. Winnifried Wollner

Date of the disputation: December 15th 2023

I, Ezra Serge Adam Rozier, hereby declare upon oath that I have written the present dissertation independently and have not used further resources and aids than those stated in the dissertation.

Hamburg, August 21st 2023

Signature

Summary

This dissertation is concerned with the development of a discontinuous Galerkin semi-discretisation of moving mesh methods for the advection-diffusion equation. *A priori* and *a posteriori* error estimations are derived that can both drive the choice of the mesh velocity and an h-refinement strategy.

Zusammenfassung

Diese Dissertation beschäftigt sich mit der Entwicklung einer diskontinuierlichen Galerkin-Semi-Diskretisierung von Moving-Mesh-Methoden für die Advektions-Diffusions-Gleichung. Es werden *a priori* und *a posteriori* Fehlerabschätzungen abgeleitet, die sowohl die Wahl der Gittergeschwindigkeit als auch eine h-Verfeinerungsstrategie steuern können.

List of publications

The work done along the development of the present dissertation gave rise to a publication [40]. The work done in this paper is my own for the theoretical framework, mathematical study and method's implementation. The co-author Prof. Dr. Jörn Behrens worked as a scientific advisor and reviewed the work at several steps.

Acknowledgement

First of all, I would like to thank the colleagues who surrounded me during my doctorate, in particular Joern Behrens, who was able to advise me and guide me through my difficult entry into the world of research.

I acknowledge the support by the Deutsche Forschungsgemeinschaft (DFG) within the Research Training Group GRK 2583 "Modeling, Simulation and Optimization of Fluid Dynamic Applications". I would also like to thank the PhD students in the research training group 2583, with whom it was easy to work on a day-to-day basis over these three years, as well as the group's scientific coordinator Petra Gunnewig.

I would also like to thank the doctoral students and post-docs in the NumGeo group at the University of Hamburg for the emulation they have fostered.

Last but not least, I would like to thank Armelle Chretien, who gave me a lot of support and helped me get through the last two years of my life.

Abstract

In convection-dominated flows, large-scale trends necessarily coexist with small-scale effects. While reducing the convection-dominance by moving the mesh, also called Arbitrary Lagrangian-Eulerian (ALE), already proved efficient, Adaptive Mesh Refinement (AMR) is able to catch the small scale effects. But ALE introduces an exponential error term that cannot be neglected compared to the small-scale effects, so that it is unsatisfying to use AMR in an ALE situation in the same way as it is used on static meshes.

This thesis is concerned with the development of *a priori* and *a posteriori* error estimations for the discretisation of the unsteady advection-diffusion equation on velocity-based moving meshes.

The development of the discontinuous Galerkin method is done using the developments of interior penalty Galerkin methods with non-constant diffusion tensors. In particular, the computation of the numerical fluxes will be emphasized.

The technique used towards the h-refinement criteria follows three main tracks: the error term caused by the mesh movement, the error sources, and the error propagation. Whereas the mesh movement's error term and the error sources are easily measurable, having a precise understanding of the error propagation remains difficult. The cheap and efficient way to have a faithful picture of the error propagation in a dynamic situation is by measuring the residual of the approximation solution.

These residuals, weighted according to the mesh's deformation, provide with local information on the error that can help building an h-refinement strategy. They in particular have the property to be robust in terms of the mesh's Peclet number and to be scaled by the remaining advection velocity.

Taking good care of this scaling, supplemented by an *a priori* error estimate leads us towards a balance between the remaining advection speed and the gradient of the mesh velocity.

Additionally, we compare the ALE formulation to the existing semi-Lagrangian discontinuous Galerkin methods and conclude that we can make them more accurate by paying attention to the numerical flux.

We present a series of numerical examples based on a Python implementation of our method. These numerical results indicate that the ALE-DG method inherits the ability to resolve boundary layers and that the error criteria detects them. They also confirm the existence of a balance between the advection speed and the gradient of the moving mesh velocity that are predicted in the *a priori*

estimate.

Contents

List of Figures

Chapter 1

Motivation

Advection-dominated flow problems play an important role in many applications such as gas and fluid dynamics, pollutant transport in porous media, meteorology, etc. Finding accurate and efficient methods for approximating their solutions is therefore of great importance.
One method that has become famous in recent decades for solving elliptic problems is the finite element method. However, this method faced stability problems when applied to advection-dominated flows. In fact, the finite element method becomes unstable when faced with regions of large gradients (either at the outflow boundary or internally where the advection velocity is steep). Two main strategies are used to solve this problem for transient advection-diffusion:

- The semi-Lagrangian (SL) method, which splits the advection, solved as an ODE, and the diffusion, solved as a PDE. This removes the advection term in the elliptic equation and consequently the instabilities.
- Stabilisation methods of the finite elements such as the streamline upwind Petrov-Galerkin (SUPG), the continuous interior penalty (CIP) or the local discontinuous Galerkin (LDG) methods, which add a stabilisation term to the finite element formulation, or Discontinuous Galerkin (DG) methods, which use discontinuous and piecewise polynomial basis functions.

The first method gives very good results. However, by solving the ODE when the advection velocity is spatially steep, it can lead to what is later called entanglement ([28]).
Among the methods used for stabilisation, the DG methods have been much studied because of the simplicity with which one can achieve *hp*-refinement. In addition, DG methods are still perturbed by advection-dominance.

To illustrate these two limitations of the DG method and the SL method, consider the following advection-diffusion problem:

$$\partial_t u + a(x)\partial_x u - \varepsilon \partial_{xx} u = f(t,x) \text{ on } [0,T] \times [0,1]$$

With a being steep in the centre: $a(x) = \alpha + 2\tanh(\frac{0.5-x}{\varepsilon})$, where α is a constant that we will change to control the advection-dominance. The solution u has an internal layer in the centre: $u(t,x) = \tanh(\frac{0.5-x}{\varepsilon})$, and we will look at the problem when $\varepsilon = 1 \times 10^{-2}$, discretised with time step $\Delta t = 1 \times 10^{-3}$ on a regular mesh with size $h = 0.04$. This is calculated using linear polynomials.

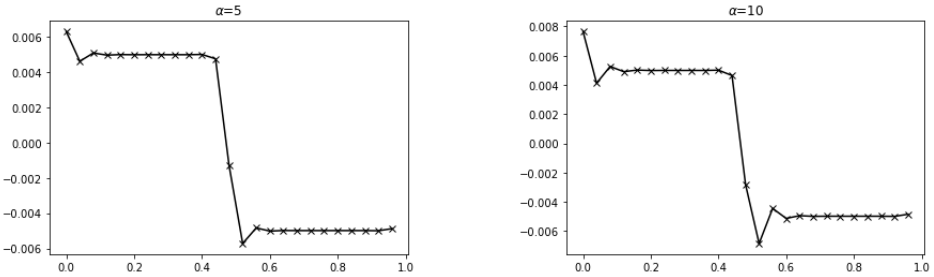

Figure 1.1: Plot of the mean value of the computed solution after four time steps of the approximated solution with a linear polynomial NIPG method with $\alpha = 5$ (left) and $\alpha = 10$ (right)

In Figure 1.1 the oscillations downwind of the steepness are larger when $\alpha = 10$ than when $\alpha = 5$. This shows that for such layers the local stability depends on the value of the Peclet number. One sees that near the boundaries the quality of the solution is improved when $\alpha = 5$. Finally the value in the centre is closer to 0 for $\alpha = 5$ than for $\alpha = 10$. We conclude that the DG method can also be improved by a strategy that would reduce the advection-dominance, such as SL methods.

For the same test case solved with the SL method, the characteristics in the centre lead to some entanglement when calculated forward. The discretisation would have to pay close attention to this effect. We can conclude that the steeper the advection velocity, the more likely the SL method is to lead to entanglement.

In conclusion, DG methods are good tools to deal with steepness and discontinuities in the solution, but they can be enhanced by a procedure that reduces the advection-dominance. A procedure that reduces advection-dominance, and which is also a theoretical basis for the study of SL methods, is the so-called Arbitrary Lagrangian-Eulerian (ALE). This consists of applying a dynamically deforming transformation to the space, so that the mesh would be considered static at the computational level, but deforming at the natural level.

In addition to such stabilisation methods, another way to approximate the small scale effects in the solution is through h-refinement. This consists of slicing or merging the cells of the mesh where the error of the approximation is larger or smaller in order to efficiently achieve higher accuracy. The basis for such a refinement method is *a posteriori* error estimation ([22], [20], [49], [15], [21], [19], [11], [24]), but these error estimators, as well as the DG method, have to be adapted to the ALE situation.

This thesis is concerned with the development of a DG method computed in an ALE dynamically deforming space. The study will outline the effect of the ALE deformation on the error *a priori* and consequently set out a procedure to avoid entanglement. Finally, *a posteriori* error estimators will be derived for refinement.

Chapter 2

The advection-diffusion equation on a moving mesh

In the computation of fluids, several paradigms can be used to reduce the computational cost. In particular, for advection-dominated flows, the use of SL methods can help to treat advection and diffusion separately. This ensures stability and give very accurate results. This approach can be used with all types of spatial integration such as finite volume, finite element or DG.

In addition, an interesting way of dealing with all kinds of small-scale problems, such as boundary layers, is to use adaptive mesh refinement (AMR).

In this chapter we will review the different tools that we need to use in order to achieve an efficient h-refinement procedure for SL methods and velocity-based moving mesh methods in general, discretising advection-dominated flows.

1 Model problem

We consider a unsteady advection-diffusion equation:

$$\begin{aligned} &\tfrac{\partial u}{\partial t} + V \cdot \nabla u - \varepsilon \Delta u = f && [0,T] \times \Omega \\ &u = u_D && [0,T] \times \Gamma_D \\ &\varepsilon \tfrac{\partial u}{\partial n} = u_N && [0,T] \times \Gamma_N \\ &u(x,0) = u_0(x) && \Omega \end{aligned} \tag{2.1}$$

in a bounded space-time cylinder with a convex cross-section $\Omega \subset \mathbb{R}^2$, having a Lipschitz boundary Γ consisting of two disjoint connected parts Γ_D and Γ_N. The final time T is arbitrary, but kept fixed in what follows. We assume that the data

satisfy the following conditions:

(A1) $f \in C(0,T;L^2(\Omega))$, $u_D \in C(0,T;L^2(\Gamma_D))$, $u_N \in C(0,T;L^2(\Gamma_N))$, $V \in C(0,T;W^{1,\infty}(\Omega)^2)$.

(A2) $0 < \varepsilon \ll 1$.

(A3) $\forall t \in [0,T]$, $-\int_\Omega \nabla \cdot V(t,x)dx \coloneqq \alpha(t) > 0$.

(A4) The Dirichlet boundary Γ_D has a positive 1-dimensional measure and includes the inflow boundary $\{x \in \Gamma \,|\, V(t,x) \cdot \mathbf{n}(x) < 0\}$ for all t.

Assumption (A2) means that we are interested in the advection-dominated regime. Assumption (A1) can be replaced by weaker conditions concerning the temporal smoothness.

In this formulation, V is a prescribed velocity (for instance if (2.1) is the equation for the concentration of a chemical species, then V is the velocity of the solute). In this case the advection-dominance means that $V \gg \varepsilon$. Another feature of this advection velocity is that it lies in the space $C(0,T;W^{1,\infty}(\Omega)^d)$ which means that the velocity can be steep in its spatial variations.

2 Semi-Lagrangian methods for advection-dominated problems

In the analysis of schemes for approximating the advection-diffusion equation, the diffusion constant ε often appears in the denominator. In particular, in [1], Theorem 4.11 gives an *a priori* error bound for the solution of a general advection-diffusion problem approximated by the DG method that involves a term $\exp(Ct/\varepsilon)$. The work of [25] for a finite element approximation estalishes

$$||u - u_h|| \leq C \inf_{v_h \in U_h} ||u - v_h|| \text{ with } C \propto \exp(t||V||_\infty/\varepsilon)$$

For advection-dominated problems these terms can become too strong to consider the error estimate reliable. One way to get around this problem has been to use SL methods, in particular Lagrange-Galerkin methods ([26], [27], [28], [78], [79], [80], [81]), which make the exponential dependence vanish in $1/\varepsilon$ (see [28]). But these methods present their own problems:

- The error estimates depend exponentially on the higher derivatives of the advection velocity, which can be prescribed with large gradient (see [28]).
- SL methods are often analysed as moving mesh methods with remeshing at each step (see [28], [53]) and the discontinuity of the higher derivatives of the advection field (remember that $V \in; W^{1,\infty}(\Omega)^2$) can cause entanglement

even with a very short time step. Here, we can mention different methods designed to avoid this: [53] tries to track the entanglement, and the so-called MMSISL ([75]) method avoids it with a location-based moving mesh method (also called r-refinement).

It is this ability to remove advection-dominance that explains why SL approaches are used for all kinds of flow problems (see the reviews [72] and [73]).

Another problem that arises for advection-dominated flows is the resolution of the solution as the Peclet number of the mesh becomes large. In cases where the diffusion coefficient is small, the solutions are not regular in the sense that higher Sobolev norms of the solution are unbounded as $\varepsilon \to 0$, and the approach requires some hp-refinement. The hp-refinement needs to be done according to some error estimates.

Here we prefer to work with DG methods to achieve h-refinement, and some DG approaches for SL methods already exist (see [74], [76], [53]).
In these works done on SLDG methods, there are two competing paradigms, the one based on the characteristic Galerkin weak formulation and the one based on the flux difference form. The flux difference form advects the approximate solution u_h on a static mesh and the characteristic Galerkin weak formulation uses a deformed mesh and deformed polynomial basis functions (see [77]). In [53] the authors adopt an approach close to the flux difference form, whereas in [76], [74], Chapter 5 from [71], the authors adopt a characteristic Galerkin approach. Here, like in [82] and following the approach taken in [28], we prefer to work with the characteristic Galerkin weak formulation since it makes the calculation of the Laplacian of the advection-diffusion problem more consistent and it allows us to have an interior penalty approach to the diffusion term. This approach involves a velocity-based moving mesh framework.

3 Velocity-based moving mesh methods

Following what is done for the study of finite elements with the Lagrange-Galerkin method (see [26], [27], [28]), we want to implement a velocity-based moving mesh method with DG spatial discretisation in order to orient the analysis of this method.

Moving mesh methods (see [44] and [50]) are known to be a dynamic adaptation of the mesh. Unlike p- or h-refinement, which are based on the addition of degrees of freedom (either spatial or polynomial), moving mesh methods consist in relocating the mesh points to a nearby location at each time step with the

aim of minimising the error. There are two main paradigms: location-based and velocity-based moving mesh methods. While location-based methods consist of setting up a functional equation or PDE that drives the movement of the mesh points ([62], [63]), velocity-based methods move the mesh points at a given velocity. An important challenge behind this method is to control the tendency towards entanglement ([44]), and this is what SL methods need to avoid. Since the time-stepping is not forced by any CFL condition, the mesh can be deformed so that the mesh tangles. For a review of such methods, we refer the reader to [51].

A large number of studies of this paradigm exist, many of them in connection with the study of ALE methods. Introduced in [61] and further studied in [68] and [69] with the geometric conservation law, the use of ALE can be very useful for time-dependent domains or problems with flexible boundaries ([34]) and there is a lot of literature focusing on the order of the ALE framework ([53], [52]) and its relation to time discretisation (see [27], [31], [32], [33] and [76] for a stochastic approach). The spatial discretisation can be applied either to conservation laws with finite elements ([58]), LDG ([60]) or finite volume and DG methods ([52], [56], [57], [38], [65]) or to the advection-dominated advection-diffusion equation using finite elements ([26], [59], [27], [28]) with local projection stabilization ([35]), LDG ([39]), SUPG ([67], [37], [36]) or even space-time DG ([64], [34]).

In most of these situations, the choice that is made is to consider that the points of the mesh move either with a velocity defined at the vertices (see for example [66]) or cell-centred ([70], [55] and references therein). These situations call for specific attention to the entanglement of the mesh and to the computation of the fluxes. What we decide to do is to consider a total Lagrangian approach where the computational mesh is static and with a dynamically deforming mapping on it (see [54], [28]). This means that the characteristics of the problem as well as the Jacobi matrix of the transformation must be calculated accurately. This helps to remove entanglement and to control the volumes of the deformed cells. Additionally the fluxes of the upwind contribution and the interior penalty term are computable, but this also makes the CFL condition more difficult to achieve, since it is complicated to estimate *a priori* the modified advection velocity (called W in section **4 - 1**).

Finally, as for the Lagrange Galerkin approach, the use of a total Lagrangian approach helps us to build a theoretical framework for the error approximation. Combining this with the advances in Interior Penalty Galerkin methods [43], we could build an Interior Penalty Galerkin method on moving meshes.

4 *h*-refinement for mesh-based methods

With the moving mesh method we expect to solve the large trends of the flow. To resolve the small-scale effects, one can imagine a tailoring strategy at the cell level. AMR offers this approach ([20]), which consists in splitting or merging the cells of the mesh depending on a local error indicator. In the present situation, the mesh motion introduces an error multiplier of the order of $e^{\|\nabla \tilde{V}\|_\infty T}$, which become significant after some time T. Since the AMR deals with small-scale effects, the strategy has to be adapted to the moving mesh situation.

AMR involves developing a refinement strategy that goes along with a refinement criterion based on error indicators. The η indicator is ideally:

- local: $\eta^2 = \sum \eta_K^2$
- reliable: $|u - u_h| \lesssim \eta$
- efficient: $\eta \lesssim |u - u_h|$

There are three strategies: Feature-based refinement, which relies on the values of the features and benefits from *apriori* error estimates ([9], [13]), goal-oriented estimators, which are based on solving an optimisation problem ([14]), and residual-error-based estimators, which deal with the residual of the problem ([11], [16], [19], [20], [21], [22]). [12] provides a comparison of these three paradigms in the situation of p-refinement. Since the aim of this study is to develop an efficient and low-cost h-refinement strategy, a residual error-based estimator (analogous to [24] on static meshes) is developed here. This strategy has been shown to be able to identify the small scale effects of the flow such as boundary layers or internal layers due to a steep advection velocity. The development of this strategy involves the design and use of tools to approximate the error in the situation of moving meshes so as to end up with a *a posteriori* error estimator.

5 Discontinuous Galerkin methods for advection-diffusion problems

The Discontinuous Galerkin (DG) method is a class of finite element methods in which the basis functions are discontinuous piecewise polynomials. Reed and Hill introduced the first DG method to solve the neutron equation ([5]), while

Cockburn *et al.* extended the method to Runge-Kutta DG (RKDG) for nonlinear conservation laws ([3]).

Although the first DG methods were used to discretise hyperbolic equations, there are a number of DG methods for second order elliptic equations. A first unified analysis of these methods for elliptic problems is given in [6]. One solution for the discretisation of elliptic problems is the interior penalty method. There are several versions of the interior penalty method, but we can highlight two main methods: the symmetric and the non-symmetric interior penalty method ([7], SIPG and NIPG respectively).

These interior penalty methods have then been studied for more complex diffusion tensors in advection-dominated problems ([47], [48] for the weighted interior penalty method) and even used on complex geometries ([43]).

Although DG methods use additional degrees of freedom, they are suitable for high order accuracy and *hp*-refinement. These refinement methods are based on indicators, *a posteriori* indicators being particularly efficient ([20], [24]).

A posteriori error estimation for stationary linear equations is now relatively well understood, as shown by work on pure diffusion problems for DG methods ([22]). For stationary advection-diffusion equations, work on robust *a posteriori* estimators for DG methods can be cited ([20] for constant diffusion, [49] for the weighted penalty method).

In the case of non-stationary advection-diffusion, we refer to the work of ([15], [21], [19]) for various space discretisations, and [11] and [24] for the interior penalty method. Here, following the work of [24] and [20] adapted to the case of a complex diffusion tensor ([43]), we derive a reliable *a posteriori* error estimator for the moving mesh DG method. Since our moving mesh method is velocity based, we want to keep track of the effect of the modified advection velocity, which means that we need to discuss the robustness of the estimator.

6 Flow maps

We consider the ALE method as a classical DG method defined on a deforming space (what is called total Lagrangian in section **2 - 3**). In this case, the complexity of the geometry occurring from the fact that the mesh moves will be featured in the equation itself. In order to do so, we define a smooth velocity $\tilde{V} = \tilde{V}(t, x)$ s.t.

$$\text{(A)} \qquad \begin{cases} \tilde{V} \in C(0,T;C^1(\Omega)^2) \\ \tilde{V}\cdot\mathbf{n} = 0 \text{ on } \Gamma\times[0,T] \\ \tilde{V} = 0 \text{ on } \Gamma_D \cap \Gamma_N \\ -\frac{1}{2}\nabla\cdot(V(t,x)-\tilde{V}(t,x)) \coloneqq \beta(t) > 0 \\ ||\nabla\cdot(V(t,x)-\tilde{V}(t,x))|| \leq c_*\beta \end{cases}$$

for a constant c_* independent of time. The existence of such a function $\tilde{V}$ is ensured by assumption (A3). We also decide that $\tilde{V}$ vanishes on the boundary between Γ_N and Γ_D.

The second assumption on the parametrized velocity $\tilde{V}$ is done so that the whole computational domain does not change.

We introduce the flow map to distinguish a Lagrangian (or reference) variable X and an Eulerian (or spatial) variable x. X lives in a space Ω_r that is later defined (and x lives in Ω). We carry out all the computations in Ω_r and express them back in Ω.

Given $\tilde{V}$ the associated flow map, $x = \chi(t,X)$, satisfies:

$$\dot{x}(t,X) = \tilde{V}(t,x(t,X)), \quad x(0,X) = X$$

As $\tilde{V}$ is smooth we have $\chi(t,.) : \Omega_r \to \Omega$ is a C^1-diffeomorphism and the Jacobian $F = F(t,X) \coloneqq [\frac{\partial x_i}{\partial X_j}]_{i,j}$ satisfies:

$$\dot{F}(t,X) = (\nabla\tilde{V}(t,x))F(t,X), \quad F(0,X) = I, \quad x = \chi(t,X).$$

The determinant $J \coloneqq \det(F)$ satisfies $\dot{J} = J(\nabla\cdot\tilde{V})$.

For a fixed domain $\Omega_r \coloneqq \Omega$ with Lipschitz boundary $\Gamma_r \coloneqq \Gamma$ let $\Omega(t) \coloneqq \chi(t,\Omega_r)$. The unit normal outward $\mathbf{n}_r \coloneqq \mathbf{n}_r(X)$ to Γ_r and the unit normal outward $\mathbf{n} \coloneqq \mathbf{n}(t,x)$ to Γ are related by the formula:

$$\mathbf{n}(t,x) = (\frac{F^{-T}\mathbf{n}_r}{|F^{-T}\mathbf{n}_r|})(t,X), \quad X \in \partial\Omega_r, \quad x = \chi(t,X).$$

Because of the value of $\tilde{V}$ on Γ_r, $\Omega_r = \Omega(t) = \Omega$, $\chi(t,\Gamma_D) = \Gamma_D$ and $\chi(t,\Gamma_N) = \Gamma_N$.

For any function $v(t,x)$ we introduce the $\hat{}$ notation s.t. $\hat{v}(t,X) \coloneqq v(t,x(t,X))$ and reciprocally v can be defined thanks to $\hat{v}$.

This notation also works for functions independent of time, $\hat{v}(t,X) \coloneqq v(x)$ and $v(t,x) \coloneqq \hat{v}(X)$.

$$\hat{v}_t = v_t + \tilde{V}\cdot\nabla v, \quad \nabla v = F^{-T}\nabla_X\hat{v}, \quad \Delta v = \frac{1}{J}\nabla_X\cdot(JF^{-1}F^{-T}\nabla_X\hat{v}) \tag{2.2}$$

Writing

$$\hat{f}(t,X) \coloneqq f(t,x(t,X)), \qquad \hat{u}_D(t,X) \coloneqq u_D(t,x),$$
$$\hat{u}_N(t,X) \coloneqq u_N(t,x), \qquad \hat{u}_0(X) \coloneqq u_0(x(0,X)).$$

The problem becomes:

$$\begin{aligned}
&\tfrac{\partial \hat{u}}{\partial t} + (V - \tilde{V}) \cdot F^{-T}\nabla_X \hat{u} - \tfrac{\varepsilon}{J}\nabla_X \cdot \{JF^{-1}F^{-T}\nabla_X \hat{u}\} = \hat{f} && [0,T]\times\Omega_r \\
&\hat{u} = \hat{u}_D && [0,T]\times\Gamma_D \\
&\varepsilon F^{-T}\nabla_X \hat{u} \cdot \tfrac{F^{-T}\mathbf{n}_r}{|F^{-T}\mathbf{n}_r|} = \hat{u}_N && [0,T]\times\Gamma_N \\
&\hat{u}(0,X) = \hat{u}_0(X) && \Omega_r
\end{aligned} \tag{2.3}$$

In the following we will discretise (2.3) with a DG method in space.

Remark 6.1. *When semi-discretised with finite elements (continuous or discontinuous), two weak formulations of* (2.3) *can be discretised. Write $\mathcal{A}_h$ the finite element operator and U_h the finite element space so that there is:*

The conservative form

$$\text{Find } \hat{u}_h \in C^1(0,T;U_h) \text{ s.t. } \forall \hat{v}_h \in U_h \quad \int_{\Omega_r} \frac{\partial (J\hat{u}_h)}{\partial t}\hat{v}_h - \int_{\Omega_r} (J\hat{u}_h)(\nabla\cdot\tilde{V})\hat{v}_h + \mathcal{A}_h(\hat{u}_h,\hat{v}_h) = 0$$

The non-conservative form

$$\text{Find } \hat{u}_h \in C^1(0,T;U_h) \text{ s.t. } \forall \hat{v}_h \in U_h \ \int_{\Omega_r} J\tfrac{\partial \hat{u}_h}{\partial t}\hat{v}_h + \mathcal{A}_h(\hat{u}_h,\hat{v}_h) = 0$$

One formulation can be related to the other by the relation $\dot{J} = J(\nabla\cdot\tilde{V})$.
In this study we prefer to use the non-conservative form for two main reasons: it allows the assumption (A3) (with the conservative form, (A3) would be replaced by a stronger assumption, $\nabla\cdot V < 0$ pointwise), and since we are working with DG spaces, the mass matrix is block diagonal and easy to compute and invert.

7 Comparison between moving mesh and semi-Lagrangian methods: a justification

In this section we attempt to describe the existing SLDG methods with a characteristic Galerkin approach in terms of flow maps. We simply modify the spatial operator of [82]: we look at the modelling choices they make, replace their LDG operator with an interior penalty formulation and compare this approach with the moving mesh approach based on a flow map discretisation in sections **3 - 3.2** and **4 - 5.2**.
There are two main differences between the existing [82] and the moving mesh method developed here: the existing SLDG methods based on the Galerkin characteristic approach uses the conservative form of the ALE equation and the authors use polynomial interpolation to approximate the values of the function advected along the characteristics (the approximation of the solution u_h and the test functions), whereas in our method, we use the non-conservative form and prefer to interpolate the Jacobi matrix of the transformation using relations (2.2). In the rest of this section we present how to interpret SL methods in terms of ALE formulation.

Tracing characteristics: This part of a SL method is similar to the flow map from section **2 - 6**. We consider a time step $[t_n, t_{n+1}]$ and look at the following flow map. Given $\tilde{V}$ the associated flow map, $x = \chi(t, X)$, satisfies:

$$\forall t \in \mathrm{R},\ \dot{x}(t, X) = \tilde{V}(t, x(t, X))$$

Since $\tilde{V}$ is smooth, we have $\chi(t, .) : \Omega_r \to \Omega$ is a C^1-diffomorphism. The mesh can be considered to be either static at the beginning as $x(t_n, X) = X$ and the ODE is solved forward, or static at the end as $x(t_{n+1}, X) = X$ and the ODE is solved backwards. In the test cases done in sections **3 - 3.2** and **4 - 5.2**, we decide to take the static mesh at the foot of the characteristics. There are several methods to integrate the characteristics and it is at this stage that tangling must be avoided. Here we show that tangling can be avoided by controlling the smoothness of $\tilde{V}$ and by adopting a total Lagrangian approach.

Integrating the spatial operator: The second step in a classical SL method is to integrate the spatial operator. In [82], similar to the ALE-LDG formulation

in [39], the authors choose to model the spatial operator as an LDG problem on a static mesh: the authors do integrate the inner-cell contribution in deformed cells but consider the fluxes as the flux on a static mesh. Everything happens as if they were working with $F = \mathrm{Id}$.
With this motivation in mind, in the test cases of sections **3 - 3.2** and **4 - 5.2**, we compare these two modelling choices and answer the questions: what is the effect of choosing the conservative form of the ALE formulation and what difference does it make to model the fluxes of the Laplacian operator according to the deformation or not ?

8 Conclusion

This thesis bridges the gap between low-cost, reliable h-refinement criteria and discontinuous Galerkin method on moving meshes for the resolution of unsteady advection-dominated flows. For this purpose it deals with the development of a velocity-based moving mesh method semi-discretised with the interior penalty Galerkin method. The study includes an *a priori* estimation of the error in order to orient the moving mesh velocity and an *a posteriori* error estimator that can suit h-refinement.
This thesis is structured as follows. In chapter 3, 1D provides a first approach, laying particular emphasis on the formulation and demonstration of the *a posteriori* error estimation. Chapter 4 focuses on the 2D case, explaining the differences with 1D and giving an *a priori* error estimation to guide the choice of the ALE velocity. Conclusions will be laid out in Chapter 5.

Chapter 3

The interior penalty discretisation for the 1D unsteady advection-diffusion equation on a moving mesh

As established in [16] and [1] , when measuring the error of an advection-diffusion problem's DG approximation, a term proportional to $\|V\|_\infty^2/\varepsilon$ appears. In the situation of advection-dominated flows (where $\|V\| \gg \varepsilon$) this term, that occurs in the interaction between transport and diffusion effect on the edges of the mesh, becomes significant. Reducing this effect implies to understand what composes the velocity V : in turbulent cases, it is composed of a large scale trend and small scale turbulences. Removing a large scale velocity $\tilde{V}$ from the term of interaction to $\|V-\tilde{V}\|_\infty^2/\varepsilon$ (see [28]) can be done by the computation of characteristics that is involved in ALE methods. This way, we can focus our study on the interactions between small scale turbulences and diffusion.

To resolve these small scale effects, one can imagine a tailoring strategy on the cells' level. h-refinement proposes this approach ([20]), which consists in splitting or merging the mesh's cells depending on a local error indicator. In the situation here, the computation of characteristics introduces an error multiplier of order $e^{\|\nabla\tilde{V}\|_\infty T}$ that become significant after some time. Therefore, the AMR strategy has to be adapted to the ALE situation.

The remainder-based refinement criteria from [20], used for the unsteady case in [24], has the ability to capture internal layers that occur when the advection velocity has discontinuities. This is exactly the case we are interested in: by

resolving the large scale smooth parts of the advection velocity with the velocity-based moving mesh, only the small scale discontinuous (or steep) parts of the advection velocity $V - \tilde{V}$ remain to be captured by the mesh refinement strategy. An additional feature of the error criteria that we develop is non-robustness in the sense that the criteria depend on the the local value of $||V - \tilde{V}||^2$. This is important both because we are interested in cases where the remaining advection velocity has spatial variations, and also because we want to develop criteria to parameterise the mesh velocity.

The aim of this 1D study is to fill a gap between SL methods and error estimation based AMR. Following the strategy developed in [28] and taking into account the reasoning of section **2 - 7**, we interpret a SL method as a velocity-based moving mesh method with occasional mesh reconstructions. In this framework, instead of continuously estimating an interpolation of the solution and inducing the gradient, the approximate solution will be a discontinuous polynomial on a regular mesh and only the features of the equation will be estimated by the characteristics. The regularity of the approximate solution allows us to use the well-established results that exist for polynomials on triangular and polygonal meshes (for instance the results of [2], [18], [22], [23], [43]).

In section **2 - 3** we exhibit how in the velocity-based moving mesh method, entanglement can occur when the mesh velocity is discontinuous (see [44]). This is solved here since we consider the mesh velocity to solve only large trends in the advection velocity (with the condition $\tilde{V} \in C^1(\Omega)$), and by explicitly considering the moving mesh in the error estimates, we can develop criteria depending on the steepness of the mesh velocity and on the time step between two mesh reconstructions that not only avoid tangling but also ensure some control over the total error.

As seen in the introductory sections **2 - 4** and **2 - 5**, DG methods provide a suitable framework for mesh adaptation, so in the following sections we will develop a DG method for the space semi-discretisation of (3.1) (section **3 - 1**). In section **2 - 4**, the use of remainder-based criteria over other kinds of criteria is justified. The development of a velocity-based moving mesh DG method, by linking mesh motion and space discretisation in the equation, allows us to compare the formulation of the DG method with the physical solution and then measure where the error is created and propagated.

This chapter is a continuation of the work done in [40]. There the method is slightly different but we can see that the performances of the error criteria are

close to the one here in example 3 (section **3 - 3.3**).
The main difference between 1 and 2D is the fact that in one spatial dimension $J = F$, so it is interesting to construct a specific framework for 1D that gives the expression (3.1).

Following (2.3) in 1D, let $y_0, y_1 \in \mathbf{R}$, $\Omega_r = \Omega = [y_0, y_1]$ and $n_r(X)$ be the outward normal vector of Ω_r in X defined by $n_r(X) = \mathbb{1}_{X=y_1} - \mathbb{1}_{X=y_0}$.
Then the system is given by

$$\begin{aligned} &\partial_t \hat{u} + (V - \tilde{V})\tfrac{\partial_X \hat{u}}{J} - \tfrac{\varepsilon}{J}\partial_X\{\tfrac{\partial_X \hat{u}}{J}\} = \hat{f} && [0,T]\times\Omega_r \\ &\hat{u} = \hat{u}_D && [0,T]\times\Gamma_D \\ &\varepsilon n_r(X)\tfrac{\partial_X \hat{u}}{J} = \hat{u}_N && [0,T]\times\Gamma_N \\ &\hat{u}(0,X) = \hat{u}_0(X) && \Omega_r \end{aligned} \tag{3.1}$$

Finally $V - \tilde{V} \in C(0,T;W^{1,\infty}(\Omega))$ motivates the definition of

$$\delta_\omega(t) = \|(V - \tilde{V})(t,\cdot)\|^2_{L^\infty(\omega)} \text{ for } \omega \subset \Omega_r.$$

The DG method proposed uses upwind discretisation of the transport term and a classical interior penalty method for the diffusive term. Based on a study of the error propagation for this semidiscretisation, a complete *a posteriori* error estimator is derived that can help to parametrize the mesh movement and to define a refinement strategy.
In the following, we will study various properties of the bilinear operator (section **3 - 1**), before developing an *a posteriori* error estimator for the unsteady 1D advection-diffusion (section **3 - 2**), and finally testing this method and the error criteria with three test cases (section **3 - 3**).

A first result that we can mention is that since the *a priori* error estimator only depends on the initial information for the problem, the estimator developed in Chapter 4 (see **Theorem 3.1**) also applies to the 1D case.

1 The semi-discrete formulation

The first step we need to achieve to approximate (3.1) is to give the functional spaces involved for both the solution and the approximation. The space-time solution will then involve the evaluation of a bilinear form defined on the functional space. The same goes for the approximation: the space-time approximation, being only semi-discretised, is defined by an ODE where the right-hand side is the result of a discretised bilinear form. Here, the spatial discretisation will involve

Sobolev spaces for the solution and discontinuous piecewise polynomials on a fixed mesh for the approximation.

1 - 1 Notation and weak form

We define the functional spaces for the solution of the weak formulation of (3.1). For any bounded open subset ω of Ω with boundary γ, we denote by $H^k(\omega)$, $k \in \mathbb{N}$, the usual Sobolev and Lebesgue spaces equipped with the standard norm $\|\cdot\|_{k;\omega} = \|\cdot\|_{H^k(\omega)}$ as well as the standard seminorm $|\cdot|_{H^1(\omega)} = \|\partial_x \cdot\|_{0,\omega}$. Similarly, $(\cdot,\cdot)_\omega$ denote the scalar product of $L^2(\omega)$. If $\omega = \Omega$, we will omit the index Ω.

Let $\omega_r \subset \Omega_r$ with boundary γ_r (recall that $\Omega_r = \Omega$), for a fixed t, denoting $\omega(t) \coloneqq \chi(t, \omega_r)$ and $\gamma(t)$ its boundary ($\gamma(t) = \chi(t, \gamma_r)$). ω is a bounded, open space and the $\hat{}$ operator introduced in section **2 - 6** defines a bijection from $H^k(\omega(t))$ into $H^k(\omega_r)$. Defining

$$\|\hat{v}\|^2_{H_{\omega_r}(t)} \coloneqq \int_{\omega_r} \hat{v}^2 J(t,\cdot), \quad |\hat{v}|^2_{U_{\omega_r}(t)} \coloneqq \int_{\omega_r} \frac{(\nabla_X \hat{v})^2}{J(t,\cdot)}$$

there is

$$\|v(t,\cdot)\|_{0;\omega} = \|\hat{v}\|_{H_{\omega_r}(t)}, \text{ and } |v(t,\cdot)|_{H^1(\omega)} = |\hat{v}|_{U_{\omega_r}(t)}.$$

Remark 1.1. *This property shows that the approximation constructed are given with respect to the reference variable X. By denoting e the approximation error, the bounds on $\|\hat{e}\|_{H(t)}$ and $|\hat{e}|_{U(t)}$ represent L^2- and H^1-bounds on e.*

For a Banach space X we define the spaces $L^p(0,T;X)$ as the standard Bochner spaces, i.e. for a measurable function $v\colon [0,T] \to X$:

$$||v||^p_{L^p(0,T;X)} \coloneqq (\int_0^T ||v(t)||^p_X \mathrm{d}t) < +\infty \text{ for } 1 \leq p < +\infty$$
$$||v||_{L^\infty(0,T;X)} \coloneqq \operatorname*{ess\,sup}_{0\leq t\leq T} ||v(t)||_X < +\infty \text{ for } p = +\infty$$

Additionally set

$$H^1_D(\Omega_r) \coloneqq \{\hat{v} \in H^1(\Omega_r)\colon \hat{v} = 0 \text{ on } \Gamma_D\}$$
$$H^1_0(\Omega_r) \coloneqq \{\hat{v} \in H^1(\Omega_r)\colon \hat{v} = 0 \text{ on } \Gamma\}$$

We can now formulate the definition of the weak form of (3.1).

$$\text{Find } \hat{u} \in C(0,T;H^1_D(\Omega_r)) \cap C^1(0,T;H^{-1}(\Omega_r))$$
$$\text{s.t. } \forall t \in [0,T],\ \forall \hat{v} \in H^1_D(\Omega_r) \quad \int_{\Omega_r} J \frac{\partial \hat{u}}{\partial t} \hat{v} = l(\hat{v}) - A(\hat{u},\hat{v}) \quad (3.2)$$

$$A(\hat{u},\hat{v}) \coloneqq \int_{\Omega_r} J[\varepsilon \tfrac{\partial_X \hat{u}}{J}\tfrac{\partial_X \hat{v}}{J} + (V-\tilde{V})\tfrac{\partial_X \hat{u}}{J}\hat{v}]$$
$$l(\hat{v}) \coloneqq \int_{\Omega_r} J\hat{f}\hat{v} + \sum_{\Gamma_N} \hat{u}_N \hat{v}$$

Remark 1.2. *Each bilinear form here are time-dependent but for clarity it will not always be explicitly stated.*

Notice that by integration by part

$$A(\hat{u},\hat{v}) = \int_{\Omega_r} J[\varepsilon \tfrac{\partial_X \hat{u}}{J}\tfrac{\partial_X \hat{v}}{J} - (V-\tilde{V})\tfrac{\partial_X \hat{v}}{J}\hat{u} - \partial_x(V-\tilde{V})\hat{u}\hat{v}] + \sum_{\Gamma_N} n_r V \hat{u}\hat{v}$$

1 - 2 Bilinear forms and function spaces for the semi-discretisation

The discretisation of (3.2) will be done in a space of discontinuous polynomials, therefore we consider $(n+1)$ points $y_0 = X_0 < \cdots < X_n = y_1$ that meshes Ω into $\mathcal{T}_h = \{K_1, \ldots, K_n\}$ with $K_i = [X_{i-1}, X_i]$ locally quasi-uniform and introduce the notation

$$X_i^{\text{out}} = \begin{cases} X_i^- & \text{if } (V-\tilde{V})(t, x(t, X_i)) > 0 \\ X_i^+ & \text{if } (V-\tilde{V})(t, x(t, X_i)) < 0 \end{cases} \quad \text{and } h_i = \max(|K_i|, |K_{i+1}|).$$

$$\hat{u}(X_n^{\text{out}}) = \begin{cases} \hat{u}(y_1) & \text{if } V(t, y_1) > 0 \\ 0 & \text{if } V(t, y_1) < 0 \end{cases} \text{ and } \hat{u}(X_0^{\text{out}}) = \begin{cases} 0 & \text{if } V(t, y_0) > 0 \\ \hat{u}(y_0) & \text{if } V(t, y_0) < 0 \end{cases}$$

.

We will also write: $H_K = |K|$ and $H_i = \max(|X_i - X_{i-1}|, |X_i - X_{i+1}|)$, and for the lagrangian elements: $h_K = h_{K_i} = |x_{i-1} - x_i|$ and $h_i = \max(|x_i - x_{i-1}|, |x_i - x_{i+1}|)$. In addition let:

$$\zeta_K = \frac{\int_K \frac{1}{J}}{H_K},\ \zeta_i = \max(\zeta_{K_i}, \zeta_{K_{i+1}}) \tag{3.3}$$

Remark 1.3. *We have the following relations between h_K, H_K and ζ_K:*

$$h_K = \int_K J \text{ and } \frac{H_K}{h_K} \leq \zeta_K \tag{3.4}$$

The broken Sobolev spaces associated with the mesh $\mathcal{T}_h$:

$$H^k(\mathcal{T}_h) = \{\varphi \in L^2(\Omega_r) \colon \forall K \in \mathcal{T}_h, \quad \varphi|_K \in H^k(K)\}$$

And

$$V_h \coloneqq \{\varphi \in H^1(\mathcal{T}_h) \colon \forall K \in \mathcal{T}_h \quad \varphi|_K \in \mathcal{S}_p(K)\}$$

with $\mathcal{S}_p$ the space of polynomials of degree $\leq p$.
Finally we denote $U_h \coloneqq V_h + H_D^1(\Omega_r)$ and $V_h^c \coloneqq V_h \cap H_D^1(\Omega_r)$.
In an inner mesh point X_i, the average and jump of a function $\hat{v} \in H^0(\mathcal{T}_h)$ across the point are defined as

$$\{\{\hat{v}\}\} = \tfrac{1}{2}(\hat{v}(X_i^+) + \hat{v}(X_i^-)),\ [\![\hat{v}]\!] = \hat{v}(X_i^+) - \hat{v}(X_i^-) \text{ and } [\![\hat{v}]\!] = \hat{v}(X) \text{ on } \Gamma.$$

We consider the DG method that is based on an upwind discretisation for the convective term and on a (non-)symmetric interior penalty discretisation for the Laplacian

$$\begin{aligned}\text{Find } \hat{u}_h \in C^1(0,T;V_h) \text{ s.t. } \forall t \in [0,T],\ \forall \hat{v}_h \in V_h \\ \int_{\Omega_r} J \frac{\partial \hat{u}_h}{\partial t}\hat{v}_h = l_h(\hat{v}_h) - A_h(\hat{u}_h, \hat{v}_h) \\ \text{where } \hat{u}_h(0,\cdot) \in V_h \text{ is a projection of } \hat{u}_0(\cdot) \text{ onto } V_h. \quad (3.5)\end{aligned}$$

$$\begin{aligned}A_h(\hat{u},\hat{v}) \coloneqq & \sum_{i=1,\dots,n} \int_{K_i} J[\varepsilon \frac{\partial_X \hat{u}}{J}\frac{\partial_X \hat{v}}{J} - (V-\tilde{V})\frac{\partial_X \hat{v}}{J}\hat{u} - \partial_x(V-\tilde{V})\hat{u}\hat{v}] \\ & + \sum_{i=1,\dots,n-1} \varepsilon(\{\{\Pi_{L^2}(\frac{\partial_X \hat{u}}{J^{\frac{1}{2}}})\}\}\frac{[\![\hat{v}]\!]}{J^{\frac{1}{2}}} + \theta\{\{\Pi_{L^2}(\frac{\partial_X \hat{v}}{J^{\frac{1}{2}}})\}\}\frac{[\![\hat{u}]\!]}{J^{\frac{1}{2}}})|_{X_i} + \frac{\gamma\varepsilon}{H_i}\frac{[\![\hat{u}]\!][\![\hat{v}]\!]}{J}|_{X_i} \\ & + \sum_{\Gamma_D}(-1)^{\delta_{ni}}\varepsilon(\Pi_{L^2}(\frac{\partial_X \hat{u}}{J^{\frac{1}{2}}})\frac{\hat{v}}{J^{\frac{1}{2}}} + \theta\Pi_{L^2}(\frac{\partial_X \hat{v}}{J^{\frac{1}{2}}})\frac{\hat{u}}{J^{\frac{1}{2}}})|_{X_i} + \frac{\gamma\varepsilon}{H_i}\frac{\hat{u}\hat{v}}{J}|_{X_i} \\ & - \sum_{i=1,\dots,n-1}(V-\tilde{V})[\![\hat{v}]\!]\hat{u}(X_i^{\text{out}}) + V\hat{v}|_{X_n}\hat{u}(X_n^{\text{out}}) - V\hat{v}|_{X_0}\hat{u}(X_0^{\text{out}})\end{aligned}$$

$$l_h(\hat{v}) \coloneqq l(\hat{v}) + \sum_{\Gamma_D}\theta(-1)^{\delta_{ni}}\varepsilon\Pi_{L^2}(\tfrac{\partial_X \hat{v}}{J^{\frac{1}{2}}})\tfrac{\hat{u}_D}{J^{\frac{1}{2}}}|_{X_i} - \tfrac{\gamma\varepsilon}{H_i}\tfrac{\hat{u}_D\hat{v}}{J}|_{X_i} - V^-\hat{v}|_{X_n}\hat{u}_D + V^+\hat{v}|_{X_0}\hat{u}_D.$$

V^+ and V^- are respectively the positive and negative parts of V ($V^- \leq 0 \leq V^+$) and $\gamma > 0$ the interior penalty parameter that is described in the literature to be depending on the degree of the polynomials. $\theta \in \{-1, 1\}$, the method is called symmetric interior penalty (SIPG) when $\theta = 1$ and nonsymmetric interior penalty when $\theta = -1$. Π_{L^2} denotes the orthogonal L^2-projection onto the finite element space V_h.

For the study that will follow, we decompose the DG operator A_h into several

operators. For $\hat{u}, \hat{v} \in H^1(\mathcal{T}_h)$

$$
\begin{aligned}
D_h(\hat{u},\hat{v}) \coloneqq & \sum_{i=1,\dots,n} \int_{K_i} J[\varepsilon \frac{\partial_X \hat{u}}{J}\frac{\partial_X \hat{v}}{J} - \partial_x(V-\tilde{V})\hat{u}\hat{v}] \\
O_h(\hat{u},\hat{v}) \coloneqq & -\sum_{i=1,\dots,n} \int_{K_i} (V-\tilde{V})\hat{u}\partial_X\hat{v} \\
& -(V-\tilde{V})[\![\hat{v}]\!]|_{X_i}\hat{u}(X_i^{\text{out}}) + V\hat{v}|_{X_n}\hat{u}(X_n^{\text{out}}) - V\hat{v}|_{X_0}\hat{u}(X_0^{\text{out}}) \qquad (3.6)\\
J_h(\hat{u},\hat{v}) \coloneqq & \sum_{i=1,\dots,n-1} \frac{\gamma\varepsilon}{H_i}\frac{[\![\hat{u}]\!][\![\hat{v}]\!]}{J}|_{X_i} + \sum_{\Gamma_D}\frac{\gamma\varepsilon}{H_i}\frac{\hat{u}\hat{v}}{J}|_{X_i} \\
\tilde{A}_h(\hat{u},\hat{v}) \coloneqq & D_h(\hat{u},\hat{v}) + O_h(\hat{u},\hat{v}) + J_h(\hat{u},\hat{v}) \\
\tilde{K}_h(\hat{u},\hat{v}) \coloneqq & \sum_{i=1,\dots,n-1} \varepsilon(\{\{\Pi_{L^2}(\frac{\partial_X\hat{u}}{J^{\frac{1}{2}}})\}\}\frac{[\![\hat{v}]\!]}{J^{\frac{1}{2}}} + \theta\{\{\Pi_{L^2}(\frac{\partial_X\hat{v}}{J^{\frac{1}{2}}})\}\}\frac{[\![\hat{u}]\!]}{J^{\frac{1}{2}}})|_{X_i} \\
& + \sum_{\Gamma_D}(-1)^{\delta_{ni}}\varepsilon(\Pi_{L^2}(\frac{\partial_X\hat{u}}{J^{\frac{1}{2}}})\frac{\hat{v}}{J^{\frac{1}{2}}} + \theta\Pi_{L^2}(\frac{\partial_X\hat{v}}{J^{\frac{1}{2}}})\frac{\hat{u}}{J^{\frac{1}{2}}})|_{X_i} \\
A_h(\hat{u},\hat{v}) \coloneqq & \tilde{A}_h(\hat{u},\hat{v}) + \tilde{K}_h(\hat{u},\hat{v})
\end{aligned}
$$

Note that

$$\forall t \in [0,T],\ \forall \hat{u},\hat{v} \in H^1_D(\Omega_r)\ \ \tilde{A}_h(\hat{u},\hat{v}) = A(\hat{u},\hat{v})$$

We state the ODEs defining the solution and its approximation, we will call $\hat{u}$ (resp. $\hat{u}_h$) the solution to (3.2) (resp. (3.5)) and define $\hat{u}^s\colon [0;T] \to H^1_D(\Omega_r)$ and $\hat{u}^s_h\colon [0;T] \to V_h$ the pointwise solution of the space-discrete problem:

$$
\begin{cases}
\forall \hat{v} \in H^1_D(\Omega_r) & A(t;\hat{u}^s(t),\hat{v}) = l(\hat{v}) - \int_{\Omega_r} J\frac{\partial \hat{u}_h}{\partial t}\hat{v} \\
\forall \hat{v}_h \in V_h & A_h(t;\hat{u}^s_h(t),\hat{v}_h) = l_h(\hat{v}_h) - \int_{\Omega_r} J\frac{\partial \hat{u}_h}{\partial t}\hat{v}_h
\end{cases} \qquad (3.7)
$$

In the following, we will find error estimates for the spatial operator by studying the stationary problem defining $\hat{u}^s$ and $\hat{u}^s_h$ and then use these error bounds to build refinement criteria for the nonstationary problem.

In the semi-discrete formulation, we can see that we focused on building the fluxes according to the moving mesh framework. In section **3 - 3.2** we will compare this DG operator on a moving mesh with the DG operator for a classical SL method and measure how it changes the quality of the approximation.

2 *A posteriori* error estimate

In this section, after showing some fundamental properties for the bilinear forms, which will imply the well-posedness and stability of the problem. We develop reliable *a posteriori* error estimators for the steady-state formulation governing $\hat{u}^s(t) - \hat{u}_h^s(t)$ in **Theorem 2.9** before integrating them to have *a posteriori* error estimators for $\hat{u} - \hat{u}_h$ in **Theorem 2.17**.

2 - 1 Error bound for the stationary problem

The procedure for the proof and results are inspired by [20] with a difference, the diffusion coefficient will be taken to be $\frac{\varepsilon}{J}$, continuous and positive. Following [20] we first approach the advection-diffusion error estimate in the steady-state case. After giving some fundamental properties of the bilinear operator, we give an *a posteriori* estimate depending both on the approximate solutions and on the features at some fixed time t. To do so, we first have to define norms on the functional spaces. These error estimate will finally be integrated in section **3 - 2.2** that will give the final estimates.
For $Y \subset \Omega_r$ we define $\omega_S \coloneqq \{K \in \mathcal{T}_h \colon S \cap K \neq \emptyset\}$. ω_K will be the subsets of Ω_r on which we maximize or average the features $(V - \tilde{V},\, J)$ to be used in the error estimate.
We introduce for $\hat{v} \in H^1(\mathcal{T}_h)$ and $q \in H^0(\Omega_r)$ the quantities

$$
\begin{aligned}
|||\hat{v}|||_t^2 &\coloneqq \sum_{K\in\mathcal{T}_h} [\varepsilon|\hat{v}|_{U_K(t)}^2 + \beta(t)\|\hat{v}\|_{H_K(t)}^2] + \sum_{i=1,\dots,n-1} \frac{\gamma\varepsilon}{H_i}\frac{[\![\hat{v}]\!]^2}{J}|_{X_i} + \sum_{\Gamma_D}\frac{\gamma\varepsilon}{H_i}\frac{\hat{v}^2}{J}|_{X_i} \\
|q|_{t;*} &\coloneqq \sup_{\hat{v}\in H_0^1(\Omega_r)-\{0\}} \frac{\int_{\Omega_r} q\partial_X\hat{v}}{|||\hat{v}|||_t} \\
|\hat{v}|_{t;A}^2 &\coloneqq |(V-\tilde{V})\hat{v}|_{t,*}^2 + \sum_{i=1,\dots,n-1} (\beta + \frac{\delta_{X_i}}{\varepsilon})h_i[\![\hat{v}]\!]_{X_i}^2 + \sum_{\Gamma_D}(\beta + \frac{\delta_{X_i}}{\varepsilon})h_i\hat{v}|_{X_i}^2
\end{aligned}
$$

Remark 2.1. *As well as for the bilinear forms, the $_t$ will be omitted in the notation.*

The first norm is the energy norm associated with the DG discretisation of the advection–diffusion problem (2.1). In [20] the seminorm $|\cdot|_*$ is linked to the Helmholtz decomposition, in particular, this quantity is equal to 0 when q is divergence-free. The third norm measures the error of the transport behaviour.

By (3.41) in [10] there exist inverse and trace inequalities for the eulerian framework.

Lemma 2.2. *Let $\hat{v} \in V_h$, $K \in \mathcal{T}_h$*
- *Inverse inequality: $|\hat{v}|_{U_K(0)} \lesssim \frac{1}{H_K}\|\hat{v}\|_{H_K(0)}$.*
- *Trace inequality: for a mesh cell $K_i = [X_{i-1}; X_i]$,*

$$\hat{v}(X_{i-1})^2 + \hat{v}(X_i)^2 \lesssim \tfrac{1}{H_K}\|\hat{v}\|^2_{H_K(0)}.$$

The proof of the following two lemma and two properties is the topic of section **4 - 1.3**, they will be given here without any proof.

Property 2.3. *(Coercivity) For large enough γ (depending on the value of the scalar in the inverse trace inequality) then A_h is $|||\cdot|||$-coercive. For all $v_h \in U_h$*

$$|||\hat{v}_h|||^2 \lesssim A_h(v_h, v_h) \tag{3.8}$$

Remark 2.4. *As we will see in section **4 - 1.3**, the condition (A4), i.e. $\beta(t) \geq 0$, ensures the stability of the Galerkin semi-discretisation.*

Lemma 2.5. *(Inconsistency) Let $\hat{u} \in H^1(\Omega_r)$ an analytical solution to (3.1) and $\hat{u}_h$ solve (3.5). Then*

$$\forall \hat{v}_h \in V_h,\ A_h(\hat{u} - \hat{u}_h, \hat{v}_h) = \varepsilon \sum_{\mathcal{E}_D} \{\{ \frac{\nabla \hat{u}}{J^{\frac{1}{2}}} - \Pi_{L^2}(\frac{\nabla \hat{u}}{J^{\frac{1}{2}}})\}\} \cdot \frac{[\![\hat{v}_h]\!]}{J^{\frac{1}{2}}} \tag{3.9}$$

Properties 2.6. *(Continuity) For $\hat{v} \in H^1_D(\Omega_r)$, $\hat{w}_1, \hat{w}_2 \in U_h$*

$$|D_h(\hat{w}_1, \hat{w}_2)| \lesssim |||\hat{w}_1||| \cdot |||\hat{w}_2||| \tag{3.10}$$

$$|J_h(\hat{w}_1, \hat{w}_2)| \lesssim |||\hat{w}_1||| \cdot |||\hat{w}_2||| \tag{3.11}$$

$$|O_h(\hat{w}_1, \hat{v})| \leq |(V - \tilde{V})\hat{w}_1|_* \cdot |||\hat{v}||| \tag{3.12}$$

Property 2.7. *(Inf-sup) We have the following inf-sup inequality:*
$$\inf_{\hat{v} \in H^1_D(\Omega_r)\setminus\{0\}} \sup_{\hat{w} \in H^1_D(\Omega_r)\setminus\{0\}} \frac{\tilde{A}_h(\hat{v}, \hat{w})}{(|||\hat{v}||| + |(V-\tilde{V})\hat{v}|_*) \cdot |||\hat{w}|||} \geq C > 0$$

The fact that the mesh motion adds an exponential term makes the DG method inconsistent but the inconsistency can be controlled. **Lemma 2.5** along with the approximations constructed in **Lemma 3.2** (4.40) ensures the a priori control of

this inconsistency. We notice that the control of this inconsistency also depends on the smoothness of J. This also implies that the steeper J is, the less consistent the method becomes. We will study the situation of $\tilde{V} \in W^{1,\infty}(\Omega) \setminus C^1(\Omega)$ in **Remark 3.3** for the 2D case and see that for a very deformed mesh, this increases. This is coherent with the fact that, depending on the flux that we use, the more deformed the mesh, the less stable or consistent is the formulation.

Let $\rho_S(t) \coloneqq \min(h_S \varepsilon^{-\frac{1}{2}}, \beta^{-\frac{1}{2}})$, $S = i$ or K_i and

$$\begin{cases} \eta_{J_i} & \coloneqq \frac{1}{2}[(\beta(t) + \frac{\delta_{\omega_{i-1}}}{\varepsilon})h_{i-1} + \frac{\gamma\varepsilon}{JH_{i-1}}(1 + J\zeta_{i-1} + \zeta_{i-1})][\![\hat{u}_h^s]\!]^2_{X_{i-1}} \\ & \quad + \frac{1}{2}[(\beta(t) + \frac{\delta_{\omega_i}}{\varepsilon})h_i + \frac{\gamma\varepsilon}{JH_i}(1 + J\zeta_i + \zeta_i^2)][\![\hat{u}_h^s]\!]^2_{X_i} \\ \eta_{E_i} & \coloneqq \frac{1}{2}\frac{\rho_{i-1}}{\sqrt{\varepsilon}}[\![\frac{\varepsilon}{J}\partial_X \hat{u}_h^s]\!]^2_{X_{i-1}} + \frac{1}{2}\frac{\rho_i}{\sqrt{\varepsilon}}[\![\frac{\varepsilon}{J}\partial_X \hat{u}_h^s]\!]^2_{X_i} \\ \eta_{R_i} & \coloneqq \rho^2_{K_i}||\hat{f} - \partial_t \hat{u}_h + \frac{\varepsilon}{J}\partial_X\{\frac{\partial_X \hat{u}_h^s}{J}\} - (V - \tilde{V})\frac{\partial_X \hat{u}_h^s}{J}||^2_{H_{K_i}(t)} \end{cases} \tag{3.13}$$

and for the boundary points $i = 0$ or $i = n$

$$\begin{cases} \eta_{J_i} & \coloneqq \mathbb{1}_{\{X_i \in \Gamma_D\}}[(\beta(t) + \frac{\delta_{\omega_i}}{\varepsilon})h_i + \frac{\gamma\varepsilon}{JH_i}(1 + J\zeta_i + \zeta_i^2)](\hat{u}_h^s - \hat{u}_D)|^2_{X_i} \\ & \quad + \frac{1}{2}[(\beta(t) + \frac{\delta_{\omega_{i\pm1}}}{\varepsilon})h_{i\pm1} + \frac{\gamma\varepsilon}{JH_{i\pm1}}(1 + J\zeta_{i\pm1} + \zeta_{i\pm1}^2)][\![\hat{u}_h^s]\!]^2_{X_{i\pm1}} \\ \eta_{E_i} & \coloneqq \mathbb{1}_{\{X_i \in \Gamma_N\}}\frac{\rho_i}{\sqrt{\varepsilon}}(\frac{\varepsilon}{J}\partial_X \hat{u}_h^s - \hat{u}_N)|^2_{X_i} + \frac{1}{2}\frac{\rho_{i\pm1}}{\sqrt{\varepsilon}}[\![\frac{\varepsilon}{J}\partial_X \hat{u}_h^s]\!]^2_{X_{i\pm1}} \end{cases} \tag{3.14}$$

Finally $\eta_i = \eta_{J_i} + \eta_{E_i} + \eta_{R_i}$

Remark 2.8. *What we see in the error criterion η_{J_K} and that we will meet again for the 2D case, for the a priori estimation and in the test cases, is this dependence in $\frac{\delta}{\varepsilon}$. This term, as we will see later in the test cases, is crucial for estimating the error.*

We will now prove the reliability of the local estimators $\sum_i \eta_i$.

Theorem 2.9. *Let $\hat{u}^s \colon [0;T] \to H^1_D(\Omega_r)$ and $\hat{u}_h^s \colon [0;T] \to V_h$ be the pointwise solutions defined in* (3.7)*, η_i be defined in* (3.13) *and* (3.14) *then*

$$|||\hat{u}^s - \hat{u}_h^s||| + |\hat{u}^s - \hat{u}_h^s|_A \lesssim (\sum_i \eta_i)^{\frac{1}{2}}$$

2 - 2 Proof of Theorem 2.9

The outline of the proof for the stationary case is as follow: separate our solution into a continuous and a discontinuous part (**Lemma 2.10**), give a bound to the discontinuous part (**Lemma 2.11**), derive a bound for the bilinear forms as an estimate multiplied by the energy-norm of the continuous function (**Lemma 2.13**, **Lemma 2.14**) and conclude with **Property 2.7**.

We will now study an approximation of elements of V_h by elements of V_h^c. A similar theorem for the eulerian problem is stated in **Theorem 2.2** in [22]. In the 1D case, this theorem depends on static and moving sizes of the cells of the mesh. Since this method involves computing the characteristics and J, these quantities (h_i and H_i), as well as ζ_i are computable *a posteriori*.

Lemma 2.10. *There exists an approximation operator $\mathcal{A}_h : V_h \to V_h^c$ satisfying:*

$$\forall \hat{v}_h \in V_h \begin{cases} \sum\limits_{K\in\mathcal{T}_h} ||\hat{v}_h - \mathcal{A}_h\hat{v}_h||^2_{H_K(t)} & \lesssim \sum\limits_{\{1,\dots,n-1\}\cup\Gamma_D} h_i [\![\hat{v}_h]\!]^2 \\ \sum\limits_{K\in\mathcal{T}_h} |\hat{v}_h - \mathcal{A}_h\hat{v}_h|^2_{U_K(t)} & \lesssim \sum\limits_{\{1,\dots,n-1\}\cup\Gamma_D} \frac{\zeta_i}{H_i} [\![\hat{v}_h]\!]^2 \end{cases}$$

with ζ defined in (3.3).

Proof. We build the approximation with lagrangian nodes and use the property of polynomials to conclude.
For each $K \in \mathcal{T}_h$, $\mathcal{N}_K \coloneqq \{x_K^{(j)} : j = 1, \dots, m\}$ the set of distinct nodes of K with nodes on both ends. Let $\{\phi_K^{(j)} : j = 1, \dots, m\}$ be a local basis of functions satisfying $\phi_K^{(i)}(x_K^{(j)}) = \delta_{ij}$.
Let $\mathcal{N} \coloneqq \bigcup\limits_{K\in\mathcal{T}_h} \mathcal{N}_K$ be the set of nodes and

$$\begin{aligned} \mathcal{N}_D &\coloneqq \{\nu \in \mathcal{N} : \ \nu \in \Gamma_D\} \\ \mathcal{N}_N &\coloneqq \{\nu \in \mathcal{N} : \ \nu \in \Gamma_N\} \\ \mathcal{N}_i &\coloneqq \{\nu \in \mathcal{N} - \mathcal{N}_D : \ |\omega_\nu| = 1\} \\ \mathcal{N}_v &\coloneqq \mathcal{N} - (\mathcal{N}_i \cup \mathcal{N}_D) \end{aligned}$$

Additionally define $\omega_\nu \coloneqq \{K \in \mathcal{T}_h : \nu \in K\}$ for each $\nu \in \mathcal{N}$.
To each $\nu \in \mathcal{N}$ we associate a basis function $\phi^{(\nu)}$:

$$\operatorname{supp}\phi^{(\nu)} \subset \bigcup_{K\in\omega_\nu} K, \ \phi^{(\nu)}|_K = \phi_K^{(j)}, \ x_K^{(j)} = \nu.$$

Write $\hat{v}_h \in V_h$ as $\hat{v}_h = \sum\limits_{K\in\mathcal{T}_h}\sum\limits_{j=1}^{m} \alpha_K^{(j)}\phi_K^{(j)}$ we define

$$\mathcal{A}_h\hat{v}_h \coloneqq \sum_{\nu\in\mathcal{N}}\beta^{(\nu)}\phi^{(\nu)}, \text{ where } \beta^{(\nu)} \coloneqq \begin{cases} 0 & \text{if } \nu \in \mathcal{N}_D \\ \frac{1}{2}\sum_{x_K^{(j)}=\nu}\alpha_K^{(j)} & \text{if } \nu \in \overset{o}{\mathcal{N}} - \mathcal{N}_D \end{cases}$$

We define now $\beta_K^{(j)} \coloneqq \beta^{(\nu)}$ if $x_K^{(j)} = \nu$.

We have $||\phi_K^{(j)}||_\infty \lesssim 1$, $\int_K J = h_K$ and $||\partial_X\phi_K^{(j)}||_\infty \lesssim H_K^{-1}$.
Thus

$$\begin{aligned}
\sum_{K\in\mathcal{T}_h}|\hat{v}_h - \mathcal{A}_h\hat{v}_h|^2_{U_K(t)} &\lesssim \sum_{K\in\mathcal{T}_h}||\partial_X\phi_K^{(j)}||^2_\infty\int_K\frac{1}{J}\sum_{j=1}^m|\alpha_K^{(j)} - \beta_K^{(j)}|^2 \\
&\lesssim \sum_{K\in\mathcal{T}_h}\frac{\zeta_K}{H_K}\sum_{j=1}^m|\alpha_K^{(j)} - \beta_K^{(j)}|^2 \\
&\lesssim \sum_{\nu\in\mathcal{N}}\frac{\zeta_\nu}{H_\nu}\sum_{x_K^{(j)}=\nu}|\alpha_K^{(j)} - \beta^{(\nu)}|^2 \\
&\lesssim \sum_{\nu\in\mathcal{N}_v}\frac{\zeta_\nu}{H_\nu}\sum_{x_K^{(j)}=\nu}|\alpha_K^{(j)} - \beta^{(\nu)}|^2 + \sum_{\nu\in\mathcal{N}_D}\frac{\zeta_\nu}{H_\nu}\sum_{x_K^{(j)}=\nu}|\alpha_K^{(j)}|^2 \\
\sum_{K\in\mathcal{T}_h}||\hat{v}_h - \mathcal{A}_h\hat{v}_h||^2_{H_K(t)} &\lesssim \sum_{K\in\mathcal{T}_h}||\phi_K^{(j)}||^2_\infty\int_K J\sum_{j=1}^m|\alpha_K^{(j)} - \beta_K^{(j)}|^2 \\
&\lesssim \sum_{K\in\mathcal{T}_h}h_K\sum_{j=1}^m|\alpha_K^{(j)} - \beta_K^{(j)}|^2 \\
&\lesssim \sum_{\nu\in\mathcal{N}}h_\nu\sum_{x_K^{(j)}=\nu}|\alpha_K^{(j)} - \beta^{(\nu)}|^2 \\
&\lesssim \sum_{\nu\in\mathcal{N}_v}h_\nu\sum_{x_K^{(j)}=\nu}|\alpha_K^{(j)} - \beta^{(\nu)}|^2 + \sum_{\nu\in\mathcal{N}_D}h_\nu\sum_{x_K^{(j)}=\nu}|\alpha_K^{(j)}|^2
\end{aligned}$$

Where we defined $H_\nu \coloneqq \max_{\omega_\nu}(H_K)$ in the third line and used $\alpha_K^{(j)} = \beta^{(\nu)}$ for $\nu \in \mathcal{N}_i$ in the fourth and last lines. For $\nu \in \mathcal{N}_v$ we write $\omega_\nu = \{K^+, K^-\}$.
Finally

$$\begin{aligned}
\sum_{K\in\mathcal{T}_h}|\hat{v}_h - \mathcal{A}_h\hat{v}_h|^2_{U_K(t)} &\lesssim \sum_{\nu\in\mathcal{N}_v}\frac{\zeta_\nu}{H_\nu}|\alpha_{K^+}^{(j_+)} - \alpha_{K^-}^{(j_-)}|^2 + \sum_{\nu\in\mathcal{N}_D}\frac{\zeta_\nu}{H_\nu}|\alpha_K^{(j)}|^2 \\
\sum_{K\in\mathcal{T}_h}||\hat{v}_h - \mathcal{A}_h\hat{v}_h||^2_{H_K(t)} &\lesssim \sum_{\nu\in\mathcal{N}_v}h_\nu|\alpha_{K^+}^{(j^+)} - \alpha_{K^-}^{(j^-)}|^2 + \sum_{\nu\in\mathcal{N}_D}h_\nu|\alpha_K^{(j)}|^2
\end{aligned}$$

Since $|\alpha_{K^+}^{(j_+)} - \alpha_{K^-}^{(j_-)}| = |[\![\hat{v}_h]\!]|$.
Then

$$\begin{cases} \sum\limits_{K\in\mathcal{T}_h} ||\hat{v}_h - \mathcal{A}_h\hat{v}_h||^2_{H_K(t)} & \lesssim \sum\limits_{\{1,\dots,n-1\}\cup\Gamma_D} h_i[\![\hat{v}_h]\!]^2 \\ \sum\limits_{K\in\mathcal{T}_h} |\hat{v}_h - \mathcal{A}_h\hat{v}_h|^2_{U_K(t)} & \lesssim \sum\limits_{\{1,\dots,n-1\}\cup\Gamma_D} \frac{\zeta_i}{H_i}[\![\hat{v}_h]\!]^2 \end{cases}$$

□

Let's now project $\hat{u}_h^s$ via $\mathcal{A}_h$:

$$\hat{u}_h^s = \hat{u}_h^c + \hat{u}_h^r \text{ with } \hat{u}_h^c = \mathcal{A}_h\hat{u}_h^s \tag{3.15}$$

Here, $\hat{u}_h^c$ is a continuous projection of $\hat{u}_h^s$ and $\hat{u}_h^r$ catches the jumps. With this we will find a bound for

$$\kappa \coloneqq |||\hat{u}^s - \hat{u}_h^s||| + |\hat{u}^s - \hat{u}_h^s|_A \tag{3.16}$$

By definition and triangular inequality,

$$\kappa \leq |||\hat{u}^s - \hat{u}_h^c||| + |\hat{u}^s - \hat{u}_h^c|_A + |||\hat{u}_h^r||| + |\hat{u}_h^r|_A.$$

We then bound κ with these error estimators. We first bound the jump term by applying **Lemma 2.10** to $\hat{u}_h^r$.

Lemma 2.11. $|||\hat{u}_h^r||| + |\hat{u}_h^r|_A \lesssim (\sum\limits_i [\frac{1}{\gamma}+1]\eta_{J_i})^{\frac{1}{2}}$ *with* $\hat{u}_h^r$ *defined in* (3.15).

Proof. Knowing that $[\![\hat{u}_h^r]\!] = [\![\hat{u}_h^s]\!]$ on $\Gamma_D \cup \{1,\dots,n-1\}$:

$$\begin{aligned} |||\hat{u}_h^r|||^2 + |\hat{u}_h^r|_A^2 = &\sum_{K\in\mathcal{T}_h} [\varepsilon|\hat{u}_h^r|^2_{U_K(t)} + \beta||\hat{u}_h^r||^2_{H_K(t)}] + |(V-\tilde{V})\hat{u}_h^r|_*^2 \\ &+ \sum_{\Gamma_D\cup\{1,\dots,n-1\}} [(\beta + \frac{\delta_{X_i}}{\varepsilon})h_i + \frac{\gamma\varepsilon}{JH_i}][\![\hat{u}_h^s]\!]^2_{X_i} \end{aligned}$$

By **Lemma 2.10**

$$\begin{cases} \sum\limits_{K\in\mathcal{T}_h} \varepsilon|\hat{u}_h^r|^2_{U_K(t)} & \lesssim \gamma^{-1} \sum\limits_{\Gamma_D\cup\{1,\dots,n-1\}} \frac{\gamma\varepsilon}{H_i}\zeta_i[\![\hat{u}_h^r]\!]^2_{X_i} \lesssim \gamma^{-1}\sum\limits_i \eta_{J_i} \\ \sum\limits_{K\in\mathcal{T}_h} \beta||\hat{u}_h^r||^2_{H_K(t)} & \lesssim \sum\limits_{\Gamma_D\cup\{1,\dots,n-1\}} \beta h_i[\![\hat{u}_h^r]\!]^2_{X_i} \lesssim \sum\limits_i \eta_{J_i} \end{cases}$$

$$
\begin{aligned}
|(V-\tilde{V})\hat{u}_h^r|_*^2 &\leq \sup_{\hat{v}\in H_0^1(\Omega_r):\ |||\hat{v}|||=1} (||(V-\tilde{V})\hat{u}_h^r||_{H(t)}^2 \cdot |\hat{v}|_{U(t)}^2) \\
&\leq \frac{1}{\varepsilon}||(V-\tilde{V})\hat{u}_h^r||_{H(t)}^2 \\
&\leq \frac{1}{\varepsilon}\sum_{K\in\mathcal{T}_h}\delta_K(t)||\hat{u}_h^r||_{H_K(t)}^2 \\
&\lesssim \sum_{\Gamma_D\cup\{1,\dots,n-1\}} \frac{h_i\delta_{\omega_i}}{\varepsilon}[\![\hat{u}_h^r]\!]_{X_i}^2 \\
&\lesssim \sum_i \eta_{J_i}
\end{aligned}
$$

□

Finally, we want to use the inf-sup condition to bound the continuous part of κ, namely $|||\hat{u}^s-\hat{u}_h^c|||+|\hat{u}^s-\hat{u}_h^c|_A$. To do so we present a lemma of approximation of function of $H_D^1(\Omega_r)$ by continuous, piecewise polynomials. This is done for static meshes in [19] with Clement-type interpolant. The specificity here will be that we will compare these Clement-type interpolants both in the eulerian and in the lagrangian variables. These interpolants are based on the following continuous piecewise linear polynomials that we first define for the eulerian variable.

For $i\in\{1,\dots,n-1\}$

$$
\Lambda_i = \begin{cases} \frac{X-X_{i-1}}{X_i-X_{i-1}} & \text{if } X\in[X_{i-1};X_i] \\ \frac{X-X_{i+1}}{X_i-X_{i+1}} & \text{if } X\in[X_i;X_{i+1}] \\ 0 & \text{else} \end{cases}
$$

$$
\Lambda_0 = \mathbb{1}_{\{X_0\notin\Gamma_D\}} \begin{cases} \frac{X-X_1}{X_0-X_1} & \text{if } X\in[X_0;X_1] \\ 0 & \text{else} \end{cases}
$$

$$
\Lambda_n = \mathbb{1}_{\{X_n\notin\Gamma_D\}} \begin{cases} \frac{X-X_{n-1}}{X_n-X_{n-1}} & \text{if } X\in[X_{n-1};X_n] \\ 0 & \text{else} \end{cases}.
$$

And then we denote:

$$
\begin{aligned}
\mathcal{I}_h(t)\colon L^1(\Omega_r) &\to \{\hat{\varphi}\in C(\Omega_r)\colon \hat{\varphi}|_K\in S_1(K), \hat{\varphi}=0 \text{ on } \Gamma_D\} \\
\hat{v} &\mapsto \sum_i \left\{\frac{1}{\int_{\omega_i}J}\int_{\omega_i}J\hat{v}\right\}\Lambda_i.
\end{aligned}
$$

Lemma 2.12. *Let $\hat{v}\in H_D^1(\Omega_r)$, we have $\varepsilon||\partial_X\mathcal{I}_h\hat{v}||_{H_K(0)}^2 \lesssim \frac{h_K}{H_K}|||\hat{v}|||^2$ and*

$$\begin{cases} \sum\limits_{K\in\mathcal{T}_h} [\rho_K]^{-2}||\hat{v}-\mathcal{I}_h(t)\hat{v}||^2_{H_K(t)} & \lesssim |||\hat{v}|||^2 \\ \sum\limits_i \frac{\sqrt{\varepsilon}}{\rho_i}(\hat{v}-\mathcal{I}_h(t)\hat{v})|^2_{X_i} & \lesssim |||\hat{v}|||^2 \end{cases}$$

$\forall \hat{v} \in H^1_D(\Omega_r)$.

Proof. The following proof will have two steps: first we build a Clement-type interpolant on the moving mesh and bound its difference with a function of $H^1_D(\Omega_r)$, then we bound the difference between the static mesh's interpolant and the moving mesh's interpolant.

We first build the same operator in the lagrangian variable:

For $i \in \{1,\dots,n-1\}$ let

$$\lambda_i = \begin{cases} \frac{x-x_{i-1}}{x_i-x_{i-1}} & \text{if } x \in [x_{i-1};x_i] \\ \frac{x-x_{i+1}}{x_i-x_{i+1}} & \text{if } x \in [x_i;x_{i+1}] \\ 0 & \text{else} \end{cases}$$

$$\lambda_0 = \mathbb{1}_{\{x_0\notin\Gamma_D\}} \begin{cases} \frac{x-x_1}{x_0-x_1} & \text{if } x \in [x_0;x_1] \\ 0 & \text{else} \end{cases}$$

$$\lambda_n = \mathbb{1}_{\{x_n\notin\Gamma_D\}} \begin{cases} \frac{x-x_{n-1}}{x_n-x_{n-1}} & \text{if } x \in [x_{n-1};x_n] \\ 0 & \text{else} \end{cases}.$$

and denote

$$\begin{aligned} \mathcal{J}_h(t)\colon L^1(\Omega) &\to \{\hat{\varphi}\in C(\Omega)\colon \varphi|_K \in S_1(K), \varphi = 0 \text{ on } \Gamma_D\} \\ v &\mapsto \sum_i \left\{ \tfrac{1}{\int_{\omega_i} dx} \int_{\omega_i} v dx \right\} \lambda_i. \end{aligned}$$

Lemma 5.3 [19] for $\mathcal{J}_h(t)$ gives the following estimates:

$$\begin{cases} \varepsilon|\hat{\mathcal{J}_h(t)}v|_{U_K(t)} \lesssim |||\hat{v}|||_{\omega_K} \\ \sum\limits_{K\in\mathcal{T}_h} [\rho_K]^{-2}||\hat{v}-\hat{\mathcal{J}_h(t)}v||^2_{H_K(t)} & \lesssim |||\hat{v}|||^2_{\omega_K} \\ \sum\limits_i \frac{\sqrt{\varepsilon}}{\rho_i}(v-\mathcal{J}_h(t)v)|^2_{X_i} & \lesssim |||\hat{v}|||^2_{\omega_K} \end{cases}$$

Since $\frac{\int_{\omega_i} v dx}{\int_{\omega_i} dx} = \frac{\int_{\omega_i} J\hat{v}}{\int_{\omega_i} J}$:

- the first inequality comes because

$$|\hat{\mathcal{J}_h(t)}v|_{U_K(t)} = |\mathcal{J}_h(t)v|_{H^1(K)} = \tfrac{H_K}{h_K}||\partial_X \mathcal{I}_h\hat{v}||_{H_K(0)}$$

- the last inequality comes by point evaluation

For the second inequality we notice that

$$\begin{cases} ||\hat{v}-\mathcal{I}_h(t)\hat{v}||_{H_K(t)} \le ||\hat{v}-\hat{\mathcal{J}_h(t)}v||_{H_K(t)} + ||\mathcal{I}_h(t)\hat{v}-\hat{\mathcal{J}_h(t)}v||_{H_K(t)} \\ |\lambda-\Lambda| < 1 \end{cases}$$

Then
$$\begin{cases} \frac{\varepsilon}{h^2}||\mathcal{I}_h(t)\hat{v} - \hat{\mathcal{J}_h}(t)v||^2 \leq |||\hat{\mathcal{J}_h}(t)v|||^2 \\ \beta||\mathcal{I}_h(t)\hat{v} - \hat{\mathcal{J}_h}(t)v||^2 \leq |||\hat{v}|||^2 \end{cases}$$

□

We will now state a lemma that gives a bound to $\tilde{K_h}$.

Lemma 2.13. *For all $\hat{v} \in V_h$ and for all $\hat{s} \in H^1_D(\Omega_r)$ satisfying*
$$\begin{cases} \hat{w} = \mathcal{I}_h(t)\hat{s} \\ B_h(\hat{v},\hat{w}) \coloneqq \tilde{K_h}(\hat{v},\hat{w}) + \sum\limits_{\Gamma_D}(-1)^{\delta_{ni}}\varepsilon\Pi_{L^2}(\frac{\partial_X\hat{w}}{J^{\frac{1}{2}}})\frac{\hat{u}_D}{J^{\frac{1}{2}}}|_{X_i} \end{cases}$$

The bilinear form B_h fulfills the following inequality

$$|B_h(\hat{v},\hat{w})| \lesssim \gamma^{-\frac{1}{2}}(\sum_{\{1,\dots,n-1\}}\frac{\varepsilon\gamma\zeta_i^2}{JH_i}[\![\hat{v}]\!]^2_{H_i} + \sum_{\Gamma_D}\frac{\varepsilon\gamma\zeta_i^2}{JH_i}(\hat{v}-\hat{u}_D)^2)^{\frac{1}{2}}|||\hat{s}|||$$

Proof. $B_h(\hat{v},\hat{w}) = -\sum\limits_{i=1,\dots,n-1}\varepsilon\{\{\Pi_{L^2}(\frac{\partial_X\hat{w}}{J^{\frac{1}{2}}})\}\}\frac{[\![\hat{v}]\!]}{J^{\frac{1}{2}}} - \sum\limits_{\Gamma_D}(-1)^{\delta_{ni}}\varepsilon\Pi_{L^2}(\frac{\partial_X\hat{w}}{J^{\frac{1}{2}}})\frac{\hat{v}-\hat{u}_D}{J^{\frac{1}{2}}}|_{X_i}$
and by Cauchy-Schwarz

$$|B_h(\hat{v},\hat{w})| \leq \gamma^{-\frac{1}{2}}(\sum_{\{1,\dots,n-1\}}\zeta_i^2\frac{\varepsilon\gamma}{JH_i}[\![\hat{v}]\!]^2 + \sum_{\Gamma_N}\zeta_i^2\frac{\varepsilon\gamma}{JH_i}(\hat{v}-\hat{u}_D)^2)^{\frac{1}{2}} \\ (\sum_{\{1,\dots,n-1\}\cup\Gamma_D}\frac{\varepsilon H_i}{\zeta_i^2}\{\{\Pi_{L^2}(\frac{\partial_X\hat{w}}{J^{\frac{1}{2}}})\}\}^2)^{\frac{1}{2}}$$

Since $\hat{w}$ is piecewise linear, we have $\partial_X\hat{w} = \mu_K$ with $\varepsilon\mu_K^2H_K \lesssim \zeta_K|||\hat{s}|||^2_{\omega_K}$ (see **Lemma 2.12**).
Using the inverse inequality and (3.4)

$$\begin{aligned}\sum_{\{1,\dots,n-1\}\cup\Gamma_D}\frac{\varepsilon H_i}{\zeta_i^2}\{\{\Pi_{L^2}(\frac{\partial_X\hat{w}}{J^{\frac{1}{2}}})\}\}^2|_{X_i} &\lesssim \sum_{\{1,\dots,n-1\}\cup\Gamma_D}\frac{\varepsilon H_i}{\zeta_i^2}\{\{\mu_K\Pi_{L^2}(\frac{1}{J^{\frac{1}{2}}})\}\}^2|_{X_i} \\ &\lesssim \sum_{K\in\mathcal{T}_h}\frac{\varepsilon}{\zeta_K^2}\mu_K^2\int_K[\Pi_{L^2}(\frac{1}{J^{\frac{1}{2}}})]^2 \\ &\lesssim \sum_{K\in\mathcal{T}_h}\frac{\varepsilon}{\zeta_K^2}\mu_K^2\int_K\frac{1}{J} \\ &\lesssim \sum_{K\in\mathcal{T}_h}\frac{\varepsilon}{\zeta_K}\mu_K^2H_K \\ &\lesssim \sum_{K\in\mathcal{T}_h}|||\hat{s}|||^2_{\omega_K} \lesssim |||\hat{s}|||^2\end{aligned}$$

proves the Lemma. □

Using the inf-sup condition and the previous lemmata, we can now bound the continuous projection of κ, namely $|||\hat{u}^s - \hat{u}_h^c||| + |\hat{u}^s - \hat{u}_h^c|_A$.

Lemma 2.14. $|||\hat{u}^s - \hat{u}_h^c||| + |\hat{u}^s - \hat{u}_h^c|_A \lesssim (\sum_i \eta_i)^{\frac{1}{2}}$ *with* $\hat{u}_h^c$ *defined in* (3.15).

with $\eta_i \coloneqq (1 + \frac{1}{\gamma})\eta_{J_i} + \eta_{E_i} + \eta_{R_i}$.

Proof. We will first bound:

$$T(\hat{v}) \coloneqq l(\hat{v} - \mathcal{I}_h\hat{v}) - \int_{\Omega_r} J\frac{\partial \hat{u}_h}{\partial t}(\hat{v} - \mathcal{I}_h\hat{v}) - \tilde{A}_h(\hat{u}_h^s, \hat{v} - \mathcal{I}_h\hat{v}) \text{ for } \hat{v} \in H_D^1(\Omega_r).$$

Since $T = T_1 + T_2 + T_3$ with:

$$\begin{cases} T_1(\hat{v}) & \coloneqq \sum_{K\in\mathcal{T}_h} \int_K J(\hat{f} - \partial_t\hat{u}_h + \frac{\varepsilon}{J}\partial_X\{\frac{\partial_X\hat{u}_h^s}{J}\} - (V - \tilde{V})\frac{\partial_X\hat{u}_h^s}{J})(\hat{v} - \mathcal{I}_h\hat{v}) \\ T_2(\hat{v}) & \coloneqq \sum_{\Gamma_N}(\hat{u}_N - \frac{\varepsilon}{J}\partial_X\hat{u}_h^s)(\hat{v} - \mathcal{I}_h\hat{v}) + \sum_{i=1,\dots,n-1} \frac{\varepsilon}{J}[\![\partial_X\hat{u}_h^s]\!](\hat{v} - \mathcal{I}_h\hat{v})|_{X_i} \\ T_3(\hat{v}) & \coloneqq -\sum_{i=1,\dots,n-1} (V - \tilde{V})[\![\hat{u}_h^s]\!](\hat{v} - \mathcal{I}_h\hat{v})|_{X_i} \end{cases}$$

Because of

$$\begin{aligned} |T_1| &\leq (\sum_i \eta_{R_i})^{\frac{1}{2}}(\sum_{K\in\mathcal{T}_h} [\rho_K||\hat{v} - \mathcal{I}_h\hat{v}||^2_{H_K(t)})^{\frac{1}{2}} \\ &\lesssim (\sum_i \eta_{R_i})^{\frac{1}{2}}|||\hat{v}||| \\ |T_2| &\lesssim (\sum_i \eta_{E_i})^{\frac{1}{2}}|||\hat{v}||| \\ |T_3| &\lesssim (\sum_i \eta_{J_i})^{\frac{1}{2}}|||\hat{v}||| \end{aligned}$$

Thus $\forall \hat{v} \in H_D^1(\Omega_r)$

$$\begin{aligned} \tilde{A}_h(\hat{u}^s - \hat{u}_h^c, \hat{v}) &= l(\hat{v}) - \int_{\Omega_r} J\frac{\partial \hat{u}_h}{\partial t}\hat{v} - \tilde{A}_h(\hat{u}_h^c, \hat{v}) \\ &= l(\hat{v}) - \int_{\Omega_r} J\frac{\partial \hat{u}_h}{\partial t}\hat{v} - \tilde{A}_h(\hat{u}_h^s, \hat{v}) + \tilde{A}_h(\hat{u}_h^r, \hat{v}) \end{aligned}$$

And

$$\begin{aligned} l(\mathcal{I}_h\hat{v}) - \int_{\Omega_r} J\frac{\partial \hat{u}_h}{\partial t}\mathcal{I}_h\hat{v} &= [l_h(\mathcal{I}_h\hat{v}) - \int_{\Omega_r} J\frac{\partial \hat{u}_h}{\partial t}\mathcal{I}_h\hat{v}] + \sum_{\Gamma_D}(-1)^{\delta_{ni}}\varepsilon\frac{\partial_X\mathcal{I}_h\hat{v}}{J}\hat{u}_D|_{X_i} \\ &= \tilde{A}_h(\hat{u}_h^s, \mathcal{I}_h\hat{v}) + \tilde{K}_h(\hat{u}_h^r, \mathcal{I}_h\hat{v}) + \sum_{\Gamma_D}(-1)^{\delta_{ni}}\varepsilon\frac{\partial_X\mathcal{I}_h\hat{v}}{J}\hat{u}_D|_{X_i} \\ &= \tilde{A}_h(\hat{u}_h^s, \mathcal{I}_h\hat{v}) + B_h(\hat{u}_h^r, \mathcal{I}_h\hat{v}) \end{aligned}$$

Then $\tilde{A}_h(\hat{u}^s - \hat{u}_h^c, \hat{v}) = T(\hat{v}) + \tilde{A}_h(\hat{u}_h^r, \hat{v}) + B_h(\hat{u}_h^s, \mathcal{I}_h\hat{v})$
Finally

$$|\tilde{A}_h(\hat{u}^s - \hat{u}_h^c, \hat{v})| \lesssim (\sum_i \eta_i)^{\frac{1}{2}}|||\hat{v}|||$$

And by noticing that: $|\hat{u}^s - \hat{u}_h^c|_A = |(V - \tilde{V})(\hat{u}^s - \hat{u}_h^c)|_*$:

$$|||\hat{u}^s - \hat{u}_h^c||| + |\hat{u}^s - \hat{u}_h^c|_A \lesssim \sup_{\hat{v}\in H_D^1(\Omega_r)-\{0\}} \frac{\tilde{A}_h(\hat{u}^s - \hat{u}_h^c, \hat{v})}{|||\hat{v}|||} \tag{3.17}$$

□

Lemma 2.15. $\kappa^2 \lesssim \sum_i \eta_i$ *with* κ *defined in* (3.16).

Proof. The result follows directly from **Lemma 2.11** for the discontinuous part and for the continuous part we use (3.17) and **Property 2.7**.

□

2 - 3 Error bound for the semidiscrete nonstationary problem

Finally we will integrate these error estimators and prove that the total error strongly depends on the values of these criteria and on other criteria.

To go from the stationary to the nonstationary problem, we will use a similar argument as in [24], we define the space-time functions $\hat{u}^s(t,\cdot) \coloneqq \hat{u}^s(t)$ and $\hat{u}_h^s(t,\cdot) \coloneqq \hat{u}_h^s(t)$. Now for every $t \in [0,T]$ we have $\hat{u}_h(t,\cdot)$ the unique solution of the same problem as $\hat{u}_h^s(t)$ i.e. $\hat{u}_h = \hat{u}_h^s$.

We define $\hat{e} \coloneqq \hat{u} - \hat{u}_h = \hat{\rho} + \hat{\theta}$ with $\hat{\rho} \coloneqq \hat{u} - \hat{u}^s$ and $\hat{\theta} \coloneqq \hat{u}^s - \hat{u}_h^s = \hat{u}^s - \hat{u}_h$ and let

$$\begin{cases} \eta_{J_i}^t & := \frac{1}{2}[(\beta(t)+\frac{\delta_{\omega_{i-1}}}{\varepsilon})h_{i-1}+\frac{\gamma\varepsilon}{JH_{i-1}}(1+J\zeta_{i-1}+\zeta_{i-1}^2)][[\hat{u}_h]]|_{X_{i-1}}^2 \\ & \quad +\frac{1}{2}[(\beta(t)+\frac{\delta_{\omega_i}}{\varepsilon})h_i+\frac{\gamma\varepsilon}{JH_i}(1+J\zeta_i+\zeta_i^2)][[\hat{u}_h]]|_{X_i}^2 \\ \eta_{E_i}^t & := \frac{1}{2}\frac{\rho_{i-1}}{\sqrt{\varepsilon}}[[\frac{\varepsilon}{J}\partial_X\hat{u}_h]]|_{X_{i-1}}^2+\frac{1}{2}\frac{\rho_i}{\sqrt{\varepsilon}}[[\frac{\varepsilon}{J}\partial_X\hat{u}_h]]|_{X_i}^2 \\ \eta_{R_i}^t & := \rho_{K_i}^2||\hat{f}-\partial_t\hat{u}_h+\frac{\varepsilon}{J}\{\frac{\partial_X\hat{u}_h}{J}\}-(V-\tilde{V})\frac{\partial_X\hat{u}_h}{J}||_{H_{K_i}(t)}^2 \\ \eta_i^t & := [(1+\frac{1}{\gamma})\eta_{J_i}^t+\eta_{E_i}^t]+\eta_{R_i}^t \end{cases} \tag{3.18}$$

Similarly for the boundary points $i=0$ or $i=n$

$$\begin{cases} \eta_{J_i}^t & := \mathbb{1}_{\{X_i\in\Gamma_D\}}[(\beta(t)+\frac{\delta_{\omega_i}}{\varepsilon})h_i+\frac{\gamma\varepsilon}{JH_i}(1+J\zeta_i+\zeta_i^2)](\hat{u}_h-\hat{u}_D)|_{X_i}^2 \\ & \quad +\frac{1}{2}[(\beta(t)+\frac{\delta_{\omega_{i\pm1}}}{\varepsilon})h_{i\pm1}+\frac{\gamma\varepsilon}{JH_{i\pm1}}(1+J\zeta_{i\pm1}+\zeta_{i\pm1}^2)][[\hat{u}_h]]|_{X_{i\pm1}}^2 \\ \eta_{E_i}^t & := \mathbb{1}_{\{X_i\in\Gamma_N\}}\frac{\rho_i}{\sqrt{\varepsilon}}(\frac{\varepsilon}{J}\partial_X\hat{u}_h-\hat{u}_N)|_{X_i}^2+\frac{1}{2}\frac{\rho_{i\pm1}}{\sqrt{\varepsilon}}[[\frac{\varepsilon}{J}\partial_X\hat{u}_h]]|_{X_{i\pm1}}^2 \end{cases} \tag{3.19}$$

such that by **Theorem 2.9**

$$\forall t\in[0,T],\quad \kappa^2=(|||\hat{\theta}|||+|\hat{\theta}|_A)^2\lesssim\sum_{K\in\mathcal{T}_h}(1+\tfrac{1}{\gamma})\eta_i^t.$$

Notice that the operator $\mathcal{A}_h$ we built in **Lemma 2.10** preserves the smoothness in time and allows us to define $\hat{u}_h^r$ and $\hat{u}_h^c$ as space-time functions
$\hat{u}_h^r\in C^1(0,T;V_h)$ and $\hat{u}_h^c\in C^1(0,T;V_h^c)$

$$\begin{aligned} |||\hat{u}_h^r|||^2+|\hat{u}_h^r|_A^2 &\lesssim \sum_{K\in\mathcal{T}_h}[\frac{1}{\gamma}+1]\eta_{J_i}^t \\ \|\hat{u}_h^r\|_{H(t)}^2 &\lesssim \sum_{\Gamma_D\cup\{0,\dots,n-1\}} h_i[[\hat{u}_h]]|_{X_i}^2 \\ \|\frac{\partial\hat{u}_h^r}{\partial t}\|_{H(t)}^2 &\lesssim \sum_{\Gamma_D\cup\{0,\dots,n-1\}} h_i[[\frac{\partial\hat{u}_h}{\partial t}]]|_{X_i}^2 \end{aligned}$$

for all $t\in[0,T]$.

We already proved the first inequality, the last two follow since:
$\forall\hat{v}_h\in C^1(0,T;V_h),\quad \frac{\partial}{\partial t}(\mathcal{A}_h\hat{v}_h)=\mathcal{A}_h\frac{\partial\hat{v}_h}{\partial t}$
and applying the **Lemma 2.10** to the function $\frac{\partial\hat{u}_h}{\partial t}$.

Lemma 2.16. $\forall\hat{v}\in H_D^1(\Omega_r),\quad \int_{\Omega_r}J\frac{\partial\hat{e}}{\partial t}\hat{v}+A(t;\hat{\rho},\hat{v})=0$

Proof. The lemma is a direct consequence of the definition of $\hat{u}$ and $\hat{u}^s$.

□

To state the final global error estimate we need some criteria. Let

$$\begin{cases} \eta_1^t & \coloneqq \sum_i \eta_i^t \\ \eta_2^t & \coloneqq \sum_{\Gamma_D \cup \{0,\dots,n-1\}} h_i [[\frac{\partial \hat{u}_h}{\partial t}]]|_{X_i}^2 \\ \eta_3^t & \coloneqq \sum_{\Gamma_D \cup \{0,\dots,n-1\}} h_i [[\hat{u}_h]]|_{X_i}^2 \end{cases} \tag{3.20}$$

For $\hat{v} \in L^\infty(0,T;H^1(\mathcal{T}_h))$ and $v(t,x) \coloneqq \hat{v}(t,X)$ we define:

$$||v||_\#^2 \coloneqq ||v||_{L^\infty(0,T;L^2(\Omega))}^2 + \int_0^T |||\hat{v}|||_t^2 dt \tag{3.21}$$

This allows us to prove the final estimate.

Theorem 2.17. *Let $\hat{u} \in C(0,T;H_D^1(\Omega_r)) \cap C^1(0,T;H^{-1}(\Omega_r))$ be a solution of (3.2), $\hat{u}_h \in C^1(0,T;V_h)$ a solution of (3.5), η_1^t, η_2^t and η_3^t be defined in (3.20), $||\cdot||_\#^2$ be the norm defined in (3.21) and $e \coloneqq (\hat{u} - \hat{u}_h)(t, \chi(t,X))$ then*

$$||e||_\#^2 \lesssim S(t)\{||e(0)||_{L^2(\Omega)}^2 + \textstyle\int_0^T \eta_1^t + T\int_0^T \eta_2^t + \max_{t\in[0,T]}(\eta_3^t)\}$$

with $S(t) = \exp(\|\partial_x \tilde{V}\|_\infty t)$.

Proof. Let $\hat{\theta}_c \coloneqq \hat{u}^s - \hat{u}_h^c \in C^1(0,T;H_D^1(\Omega_r))$ and $\hat{e}_c \coloneqq \hat{u} - \hat{u}_h^c \in C^1(0,T;H_D^1(\Omega_r))$. Taking **Lemma 2.16** with $\hat{e}_c$ we have

$$\textstyle\int_{\Omega_r} J\frac{\partial \hat{e}_c}{\partial t}\hat{e}_c + A(t;\hat{e}_c,\hat{e}_c) = \int_{\Omega_r} J\frac{\partial \hat{u}_h^r}{\partial t}\hat{e}_c + A(t;\hat{\theta}_c,\hat{e}_c)$$

Additionally the inequalities

$$\int_{\Omega_r} J\frac{\partial \hat{e}_c}{\partial t}\hat{e}_c = \frac{1}{2}\frac{d}{dt}\|e_c\|_{L^2(\Omega)}^2 - \int_{\Omega_r}\frac{\partial_x \tilde{V}}{2}J\hat{e}_c^2 \geq \frac{1}{2}\frac{d}{dt}\|e_c\|_{L^2(\Omega)}^2 - \frac{\|\partial_x\tilde{V}\|_\infty}{2}\|e_c\|_{L^2(\Omega)}^2$$

$$A(t;\hat{e}_c,\hat{e}_c) \geq |||\hat{e}_c|||_t^2$$

$$\int_{\Omega_r} J\frac{\partial \hat{u}_h^r}{\partial t}\hat{e}_c \leq \frac{T}{2}\|\frac{\partial \hat{u}_h^r}{\partial t}\|_{H(t)}^2 + \frac{1}{2T}\|e_c\|_{L^2(\Omega)}^2$$

$$A(t;\hat{\theta}_c,\hat{e}_c) \leq C\cdot(|||\hat{\theta}_c|||_t + |\hat{\theta}_c|_A)|||\hat{e}_c|||_t \leq \frac{C^2}{2}\cdot(|||\hat{\theta}_c|||_t + |\hat{\theta}_c|_A)^2 + \frac{|||\hat{e}_c|||_t^2}{2}$$

hold, therefore

$$\frac{d}{dt}\|e_c\|^2_{L^2(\Omega)} + (|||\hat{e}_c|||_t^2 - C^2 \cdot (|||\hat{\theta}_c|||_t + |\hat{\theta}_c|_A)^2 - T \cdot \|\frac{\partial \hat{u}_h^r}{\partial t}\|^2_{H(t)}) \\ \leq (\|\partial_x \tilde{V}\|_\infty + \frac{1}{T})||e_c||^2_{L^2(\Omega)}$$

and by Gronwall's Lemma

$$\|e_c\|^2_{\#} \lesssim S(t)\{\|e_c(0)\|^2_{L^2(\Omega)} + \int_0^T (|||\hat{\theta}_c|||_t + |\hat{\theta}_c|_A)^2 + T\int_0^T \|\tfrac{\partial \hat{u}_h^r}{\partial t}\|_{H(t)}\}$$

Then by definition of η_3^t

$$\|e\|^2_{\#} \lesssim S(t)\{\|e(0)\|^2_{L^2(\Omega)} + \int_0^T \eta_1^t + T\int_0^T \eta_2^t + \max_{t\in[0,T]}(\eta_3^t)\} \tag{3.22}$$

□

Note that η_3^t, appearing in (3.22), is the only estimator independent of the stopping time. The presence of this term, which is also present on static meshes, explains the fact that the jumps are a good estimator of the error and can be used for h or p-refinement (see [41], [42]). Since we are also interested in the effect of the moving mesh method on the error estimate, we can also notice the presence of the term $S(t)$, which we will see in section **3 - 3.1** will play an important role in the evolution of the error after a few time steps. The presence of this term can be linked to the volume of each cell, $S(t)$ being an upper and lower bound of the volume of each cell ($h(0)/S(t) < h(t) < h(0)S(t)$). The control of this quantity ensures no entanglement. Finally, we can note the presence of the spatial criterion η_1^t, which is integrated in time. The ability of this term to represent the error is studied in section **3 - 3.3**.

By carefully considering the generation and propagation of the error, we have been able to construct error criteria that go beyond classical error theory. Indeed, while gradient-based error criteria focus on the spatial variations of the computed solution (which we capture with η_R and η_E), we are also able to capture how the error propagates at the edges of the grid with η_J. This theoretical study for a relaxed advection velocity was made possible by the moving mesh framework we mobilised. In particular, we were able to see that the characteristics of the mesh motion also have an effect on the estimates.

3 Test cases

In this set of test cases we will first show that for short times, the moving mesh method is more accurate than Eulerian methods, which poorly resolve the large-scale trends in the flow velocity. The second test case will show that this moving mesh method is more accurate than the case where $J = 1$, that is the classical SL methods (see section **2 - 7**), because it better resolves the effect of the spatial variations of the characteristics on the fluxes. Finally the last test case exhibits the performance of the error criteria and tests if η_1^t catches the error. In addition, the last two test cases are test cases where the DG operator would not be coercive on a static mesh.

In the examples, the time discretisation for the PDE (3.1) is a Runge-Kutta method of order 3. This is chosen because of the optimality of the RKDG method (see [4]) when the DG method is of polynomial order 2 (chosen here). Since the RK3 in the RKDG method requires a midpoint evaluation of the DG operator, the flow map is discretised with a time step of $\frac{\Delta t}{2}$ using a Runge-Kutta method of order 4, and J is computed once the characteristics are obtained, using $J = \exp(\int_0^T \nabla \cdot \tilde{V})$. As the focus is on the moving mesh, we used the standard RK4 method, which leaves room for improvement regarding the computation of the characteristics.

In the examples, we will always work in the spatial domain $[0, 1]$.

3 - 1 Example 1: A comparison with static meshes

In this test case we want to focus on two features of the moving mesh method: its ability to resolve large trends in advection, and its effect on the error. As mentioned in section **2 - 3**, the velocity-based moving mesh method has a tendency for the mesh to tangle, but even smaller deformations can be subject to large imprecisions that can strongly affect the error. We will focus on the following: first the L^2-error of the moving mesh method is much smaller than that of the static mesh method for short times. Than how the error evolves with mesh movement, we than outline the existence of a stopping time where the static mesh method becomes more accurate and finally we discuss a balance between the remaining advection velocity and the steepness of the mesh velocity.

To do this, we will compare the moving mesh method with the same DG method on a static mesh. To check the ability of the moving mesh method to reduce advection-dominance by an order of magnitude, we will compare a toy experiment with the following two properties:

- $V(0) = 10 \cdot V(1)$ for the advection-dominance.
- $\partial_x V < 0$

Since $\partial_x V < 0$ we can solve this problem with the static mesh method and since $V(0) = 10 \cdot V(1)$ we can find a mesh motion such that $\int_{[0,1]} V - \tilde{V}$ is arbitrarily close to $V(1)$ (i.e. less than $\int_{[0,1]} V$). We want to emphasize that since $\partial_x V \leq 0$ is needed for static meshes, this condition implies $||V||_\infty = |V(0)|$ or $|V(1)|$ and since $\tilde{V}(0) = \tilde{V}(1) = 0$, there is $||V - \tilde{V}||_\infty \geq ||V||_\infty$. Thus, the study of the dependance of the error on $||V - \tilde{V}||_\infty$ is not possible here and and we cannot do a clear comparison with the statement from **Theorem 3.1**. Unlike here, the 2D case is prone to this study in section **4 - 2**.
To test whether variations in the mesh velocity have an effect on the error, we will also compare different approximations with mesh velocities $\tilde{V}_p$:

$b = 0.1$, $\varepsilon = \frac{1}{40}$, $V(t,x) = (1+b)\pi - \pi x$

$$\tilde{V}_p(t,x) = \pi(1-x)(1-\exp(-px))$$

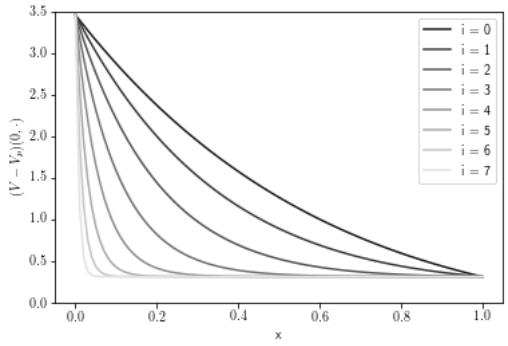

Figure 3.1: Modified advection velocity $(V - \tilde{V}_p)$ for values $p = 2^i$

The computation of the flow map makes the method computationally expensive, but has a complexity proportional to the number of cells, comparable to that of the RKDG method. Finally, the gain in accuracy that we have for short times justifies the use of a moving mesh method in certain cases. In particular we will see in section **3 - 3.2** that the use of a moving mesh method can be considered when using a SL method.

In this test case the solution is given by $u(t,x) = \exp\left(-t - \ln\left(\frac{1+b-x}{b}\right)/\pi\right)$ with time-step $\Delta t = 2 \cdot 10^{-4}$ for the RKDG method and $X_i = i \cdot 0.02$ for $i = 0, \ldots, 50$.

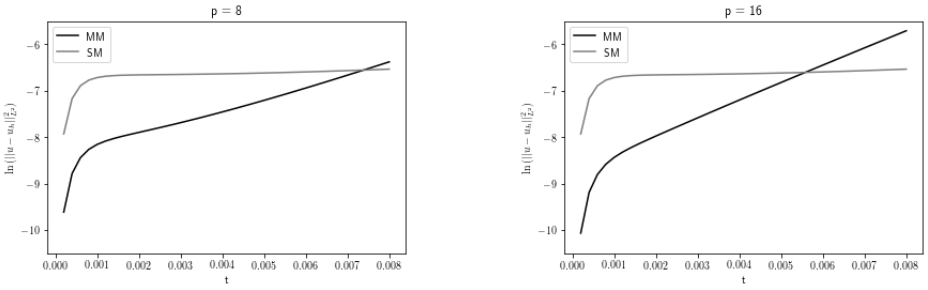

Figure 3.2: L^2-error for short times ($t = 0.008$ is 40 time steps)

We can see in Figure 3.2 that for short times the moving mesh method is more accurate than the static mesh method. After some time steps, the curves between moving and static mesh methods eventually cross. One sees that the initial difference in accuracy increases with p: $\ln\left(||u - u_h^{SM}||_{L^2}^2 / ||u - u_h^{MM}||_{L^2}^2\right) \approx 1.5$ for $p = 8$ and $\ln\left(||u - u_h^{SM}||_{L^2}^2 / ||u - u_h^{MM}||_{L^2}^2\right) \approx 2$ for $p = 16$. Simultaneously, the number of time steps required before the static mesh method becomes more accurate decreases with p: $n_t \approx 37$ for $p = 8$ and $n_t \approx 28$ for $p = 16$. The first effect can be explained because the average value of $V - \tilde{V}_p$ decreases when p increases and the second behaviour because the maximal value of $\partial_x \tilde{V}_p$ increases with p.

In Figure 3.3 we plot the value of $\ln\left(||u - u_h^{SM}||_{L^2}^2 / ||u - u_h^{MM}||_{L^2}^2\right)$ after one time step and then, the first time step where $||u - u_h^{SM}||_{L^2} < ||u - u_h^{MM}||_{L^2}$ for cases where $p = \lfloor 1.5^i \rfloor$ for $i = 1, \ldots, 22$.

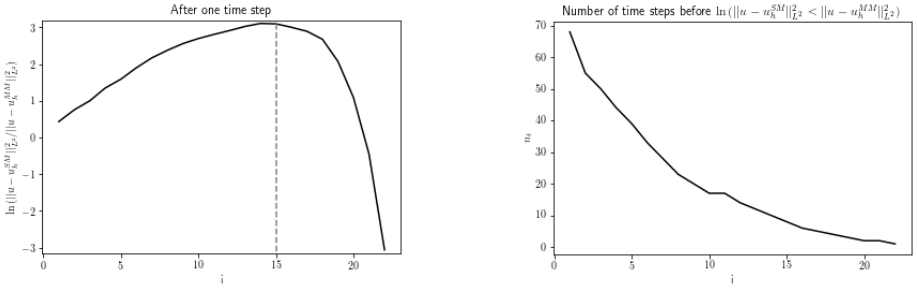

Figure 3.3: Plots of the L^2-error after one time step and number of time steps before which the static mesh methods becomes more accurate than the moving mesh method, $p = \lfloor 1.5^i \rfloor$

We can see that there is a minimal value ($i = 15$, $p = 437$) for the L^2-error after the first time step. It confirms a balance between the value of $|V - \tilde{V}_p|$ and $|\partial_x \tilde{V}_p|$ even after only one time step, for instance, when $p > 21$, the L^2-error after one time step is larger for the moving mesh method than for the static mesh method. Therefore, the steepness of the flow map has to be controlled.

We can also see that, even if the L^2-error is decreasing for $i = 1 \ldots, 15$, the first

time step where $||u - u_h^{SM}||_{L^2} < ||u - u_h^{MM}||_{L^2}$ is also decreasing. This means that the mesh's deformation plays a role in the development of the L^2-error after several time steps. In Figure 3.2 we can see that after a few time steps the error is increasing exponentially with a slope increasing with p. In Figure 3.4, we compute the slope of this exponential regime by computing:

$$s(p) = \frac{\ln\left(||(u-u_h^{MM})(n_t(p)\cdot\Delta t,\cdot)||_{L^2}^2 - \ln\left(||(u-u_h^{MM})(3\cdot\Delta t,\cdot)||_{L^2}^2\right)\right.}{(n_t(p)-3)\Delta t} \approx 0.62 \cdot p + 48 \text{ with } r^2 \approx 0.998$$

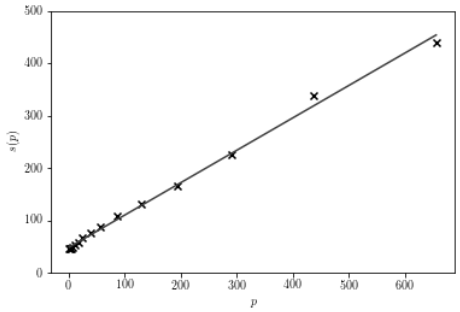

Figure 3.4: Slope of the exponential regime governing the L^2-error for increasing values of $||\partial_x \tilde{V}_p||_\infty = p$

We can notice that $||\partial_x \tilde{V}_p||_\infty = p$, which is in accordance to the presence of $S(t)$ in **Theorem 2.17** and latter **Theorem 3.1** which involve a term proportional to $\exp\left(||\partial_x \tilde{V}_p||_\infty \cdot t\right)$ in the error analysis.
This example first confirms that the moving mesh method was more accurate than the static mesh method in terms of the L^2-norm for short times. It also shows the existence of a balance between the local values of $|V - \tilde{V}|$ and $|\partial_x \tilde{V}|$. Finally we noticed that there is a regime where we approximately had

$$\frac{d}{dt} \ln\left(||(u - u_h^{MM})(t,\cdot)||_{L^2}^2\right) \propto t||\partial_x \tilde{V}||_\infty.$$

Figure 3.2 encourages us to use this moving mesh method for short times while Figure 3.3 orients us to the existence of an optimal mesh velocity and associated stopping time (the steeper the mesh velocity, the shorter the stopping time).

3 - 2 Example 2: A comparison with a classical semi-Lagrangian method

In the case of the comparison of our method with a classical SL method, since we are not interested here in the reconstruction, we only need to make the comparison

on one time step. As classical SL methods consider the same problem as (3.1) with $J = 1$ (see section **2 - 7**), there will be no difference in the flow map (the characteristics will be the same) and the difference will be in the DG operator. The computation of J is of course expensive, but it is still of the same order of complexity as the Runge-Kutta method for the flow map. Computing and inverting the mass matrix ($\int_K J\hat{u}_h\hat{v}_h$) has a cost proportional to the number of cells, because it is block diagonal (where the number of blocks is the number of cells and the size of the block is the number of degrees of freedom in each cell). The difference between the moving mesh and the SL method can be seen when J becomes large. For short times, this occurs when the variations of the mesh velocity are large. this motivates the following construction:

$$\beta = 15,\ c = 0.4,\ y(x) = \tfrac{x-0.5}{(c+x)(1+c-x)}$$
$$H(t,x) = -\tfrac{3}{2}\cdot\tfrac{\tanh(\beta y(x))}{y'(x)}(1+\ln(t+1)),\ H_M(t) = \max(H(t,x)),$$

$$\tilde{V}(t,x) = 2H_M(t) + H(t,x) - (x-\tfrac{1}{2}) - \cos(\pi x)^7[2H_M(t) + H(t,0) + \tfrac{1}{2}]$$

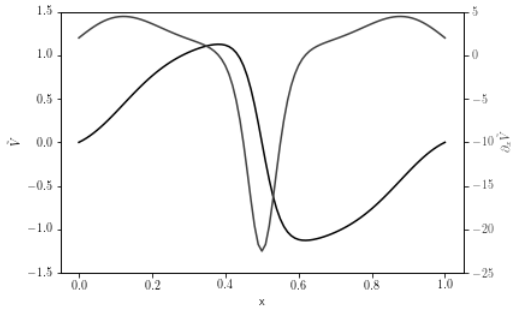

Figure 3.5: Mesh velocity $\tilde{V}(0,\cdot)$ and its gradient $\partial_x\tilde{V}(0,\cdot)$ on $x \in [0,1]$

In order to study an advection-dominated regime after moving the mesh, let $V(t,x) = \tilde{V}(t,x) + 2 + \cos(\pi x)$.
First we show the evolution of the energy-error of the approximate solution after one time step for different values of the time step. In this test case, the solution is $u(t,x) = \exp(2t-x)$ with $\varepsilon = 0.1$ and spatial grid points $X_i = i \cdot 0.04$ for $i = 0,\ldots,25$. The time step is chosen of size $\Delta t = \frac{1}{n_t}$ for $n_t \in [\![300,500]\!]$ and compare the two relative errors when the time step becomes short ($n_t \in [\![300,1400]\!]$). In Figure 3.6 the relative energy-error of the approximate solution after one time step is more accurate for the moving mesh method than for the classical SL methods for $n_t \in [\![300,500]\!]$. This difference decreases for shorter time steps,

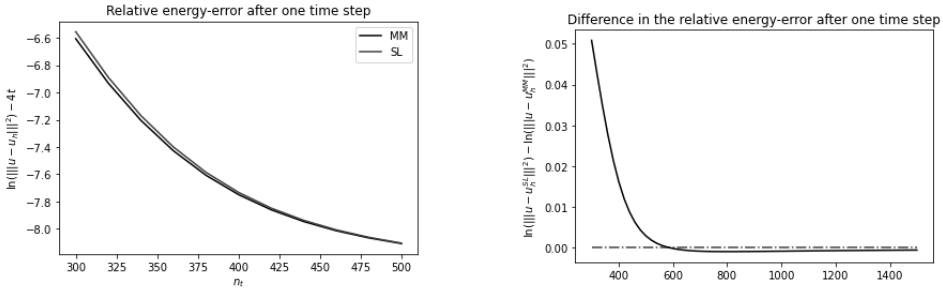

Figure 3.6: Evolution of the relative energy-error after one time step for different time step sizes for the SL and the moving mesh method, $n_t \in [300, 500]$ (right), evolution of the difference of energy-error between the SL and the moving mesh method after one time step for different time step sizes, $n_t > 350$ (left)

probably because the shorter the time step, the closer J will be to 1. Although the gain in accuracy is very small, the computational cost is negligible, so it can be an interesting tool for designing SL methods. As we plot it on Figure 3.6, for very short time steps ($n_t > 600$), the gain of this method becomes so negligible that it is outweighed by the inconsistency and the loss of accuracy that we have when computing the mass matrix: whereas the SL mass matrix involves computing integrals of polynomials which can be done accurately with the right quadrature, in our case, J is not polynomial and computing the mass matrix adds some imprecision. We can also see that this difference decreases when the time step becomes shorter also because J will be closer to 1.

To explain this very small gain, notice that in 1D, for advection-dominated cases, since as we can see in the definition of O_h (3.6), the advective flux is the same for classical SL and for moving mesh methods, there is only a small difference between the approximations. In Figure 3.6, the gain of the moving mesh method predominantly a consequence of the modification in the mass matrix. We will see in Chapter 4 that for the 2D case, the difference becomes more significant.

To then design a SL method, it is important to understand the idea of this method: the moving mesh strategy directed us towards an advection and a diffusion modified by the features of the flow map. It is only after this that we have defined the fluxes and the advection and diffusion operators. Using this strategy can help us to design all kinds of SL methods (with, for example, a different time integration for the advection and diffusion operators, such as IMEX schemes). The argument presented (and which we will explore further in section **4 - 5.2**) is that to make the fluxes of a DG method more accurate, one must take into account the deformation of the outward normal vector implied by the SL formulation.

3 - 3 Example 3: Testing the error criteria with strong deformations

As a final set of examples, we will focus on the fact that we gain with this method an analysis of the *a posteriori* error estimation. Apart from the fact that it makes a SL method more accurate, it has also helped us to build tools for analysing the spatial error. In this setup we still define the function H and the velocity $\tilde{V}$ in the same way as in section **3 - 3.2** with the difference that $\beta = 20$ and $c = 0.1$. Whereas in the second example we wanted a large zone where the mesh velocity is steep, here we want a very localised zone where the mesh velocity is steep, which can be seen in Figure 3.7.

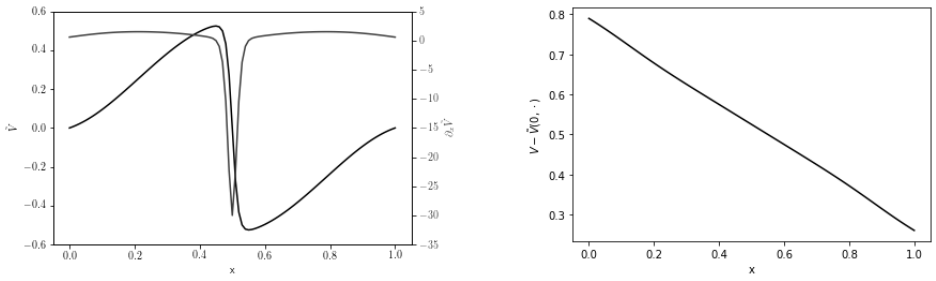

Figure 3.7: Velocity $\tilde{V}(0,\cdot)$, $\partial_x\tilde{V}(0,\cdot)$ and velocity $(V-\tilde{V})(0,\cdot)$ on $x \in [0,1]$

Here there are a couple of different test cases. On one hand, we want to see how the error criteria approximate the different errors when the remaining advection velocity $V - \tilde{V}$ is still dominant and on the other hand when it is closer to ε. To compare these two cases, we do not use the velocities V and $\tilde{V}$ as previously defined, but the advection velocity will be $V_{\text{eff}} = pV$ and the grid velocity will be $\tilde{V}_{\text{eff}} = p\tilde{V}$ with $p = 0.5$ or 10, in addition the Peclet number of the mesh is constant, namely $h = \frac{1}{50} = 2\varepsilon$, $P_e = \frac{h}{\varepsilon} = 2$ and the time step is taken constant $\Delta t = 10^{-4}$. We look at several solutions u to outline different properties of the error criteria.

(a) Solution $u(t,x) = \sin(2\pi x) + \frac{\cos(20\pi x)}{10}$, $p = 10$: In this situation the error criteria are dominated by the term η_J and in particular by the term $\delta[\![\hat{u}_h]\!]^2/\varepsilon$. Indeed, while the L^2-norm of the solution is the same at $x \approx 0.2$ and $x \approx 0.8$, the local L^2-error around $x \approx 0.2$ is twice as large as the L^2-error around $x \approx 0.8$. This behaviour is predicted by the error criterion and in particular by the multiplier δ. We can see in Figure 3.8 that the error criteria approximate the L^2-error adequately. This behaviour is maintained over time. In this situation, since the L^2-error is 0 where the mesh is most deformed, we cannot check whether the error criteria are still efficient when the mesh is very deformed.

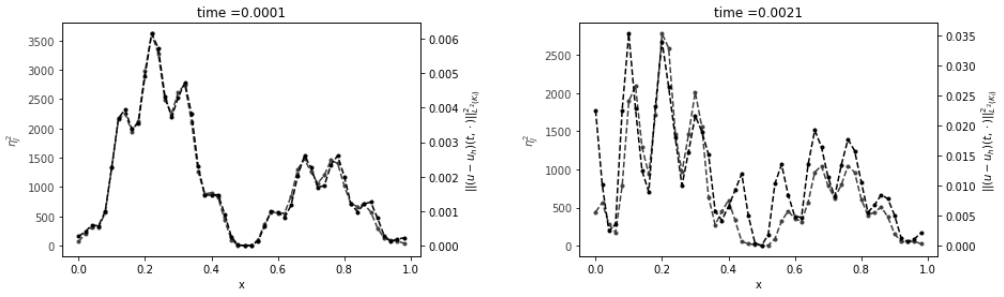

Figure 3.8: Comparison of the criterion η_J^t and the L^2-error after one and 51 time steps in case (a)

(b) Solution $u(t,x) = x(1-x)$**,** $p = 10$**:** Again the error criteria are dominated by the term η_J and in particular by the term $\delta[\![\hat{u}_h]\!]^2/\varepsilon$. In Figure 3.9, since the error is large in the central cells, we can see that the total L^2-error in the central cell decreases as the size of the cell decreases. The η_J criterion also follows this movement, but when the deformation of the mesh is strong, we can see that this decrease in the central cell is slower for the criterion than for the L^2-error. This confirms that the error criterion is reliable, but loses efficiency under strong deformation.

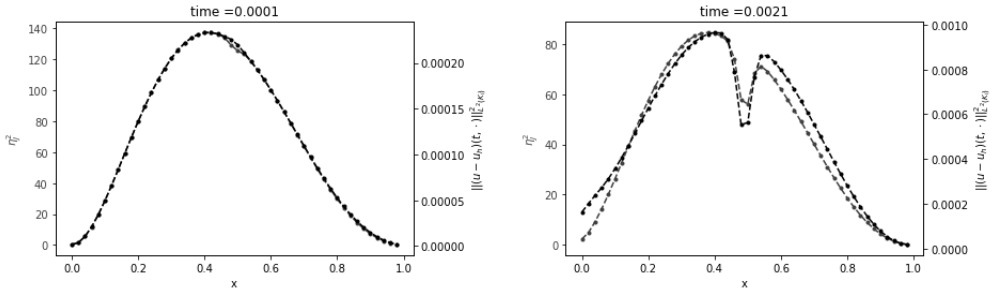

Figure 3.9: Comparison of the criterion η_J^t and the L^2-error after one and 51 time steps in case (b)

(c) Solution $u(t,x) = \sin(2\pi x) + \frac{\cos(20\pi x)}{10}$**,** $p = 0.5$**:** In contrast to the first situation, here the phenomenon is dominated by diffusion and the error criteria are no longer dominated by η_J. In Figure 3.10, the energy-error is as adequately approximated by the error criterion η after one time step as after 51 time steps. Similar to situation (a), since the energy-error is 0 where the mesh is most deformed, we cannot check if the error criteria are still efficient when the mesh is very deformed.

(d) Solution $u(t,x) = \sin(2\pi x)$**,** $p = 0.5$**:** Again the phenomenon is dominated by diffusion and the error criteria are dominated by η. In Figure 3.10 the energy error is as appropriately approximated by the error criterion η after one time step as after 51 time steps. Here the local energy-error of the solution is

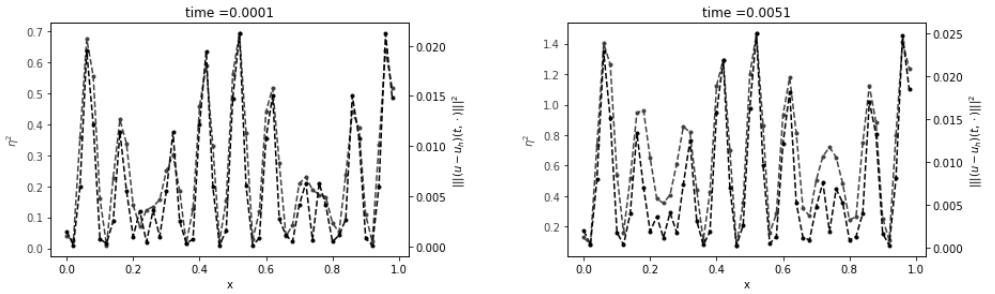

Figure 3.10: Comparison of the criterion η^t and the energy-error after one and 51 time steps in case (c)

maximal at the centre and we can see that the error decreases as the central cell becomes small (after 51 time steps). This is slightly predicted by the η criterion, but we clearly lose efficiency due to mesh deformation. The criterion is still reliable.

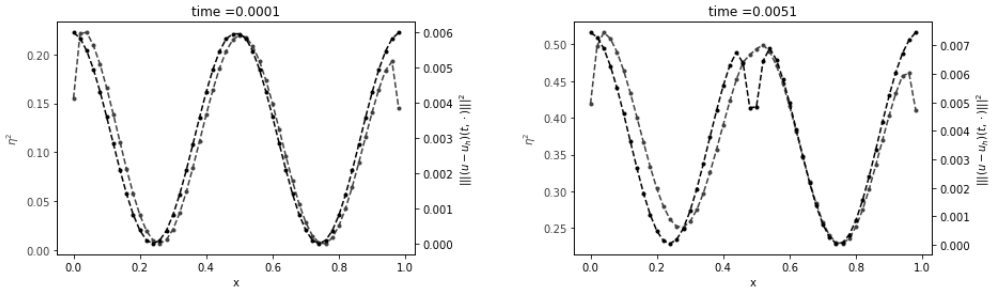

Figure 3.11: Comparison of the criterion η^t and the energy-error after one and 51 time steps in case (d)

From these four test cases one sees the behaviour of the error and the criteria:

- When the remaining advection velocity is still dominant, the η criterion is dominated by its η_J contribution and the criterion is close to the L^2-error.
- In situation (a) the non-robustness of the criteria is important to still catch the L^2-norm when the problem is strongly advection-dominated.
- When the remaining advection velocity becomes small, the η criterion is able to adequately approximate the energy-error.
- When the grid becomes very deformed, the criteria are able to show a small effect of deformation, in particular when a cell becomes small and so its local L^2-error becomes small, the criterion also shrinks but slower. In the end in both situations (b) and (d) the criteria remain reliable but are less efficient.

In this chapter we formulated a velocity-based moving mesh DG method for the unsteady advection-diffusion equation. From this formulation we derived *a posteriori* error criteria that are reliable. Finally, the test cases show that:

- By suitably parameterising the mesh velocity, we find an optimal velocity that reduces the L^2-norm as much as possible for short times. This optimal mesh velocity results from a balance between the remaining advection velocity $V - \tilde{V}$ and the variations of the advection velocity $\partial_x \tilde{V}$.
- This moving mesh method, in particular the definition of fluxes, can be used to make SL methods more accurate. Instead of having the advected gradient to approximate the DG operator in a SL method, we can make the calculation of J more accurate and see a SL method as a moving mesh method (see section **2 - 7**).
- This error criterion is capable of reliably represent the L^2-error or the energy-error (depending on the situation of remaining advection-dominance). When the deformation becomes large, it becomes less efficient.
- The non-robustness is important because it is involved in the representation of the error in cases of strong advection-dominance. The presence of the term δ/ε in the criterion η_J is something that we find again in the *a priori* error estimation from **Theorem 3.1**.

In the second chapter we complete the study by formulating a moving mesh DG method for the unsteady advection-diffusion equation in 2D. We extend the conclusions of this section. In particular section **4 - 3** is devoted to the existence of a balance between $V - \tilde{V}$ and $\nabla \cdot \tilde{V}$.

Chapter 4

The interior penalty discretisation for the 2D unsteady advection-diffusion equation on a moving mesh

After Chapter 3, we apply the previous method and criteria in 2D. Although the *a posteriori* available data are not exactly the same, the tools developed in the previous chapter can be generalised to the 2D case.

The aim is to solve both the large trends of a advection-dominated flow, the discontinuities of the flow (internal layers) and the interactions with diffusion (for instance boundary layers). To resolve large trends, we use a moving mesh strategy, the problem being that a strictly advection velocity-based moving mesh strategy causes entanglement in the mesh (section **2 - 3**). We therefore move towards a SL, which can be reinterpreted as a certain form of mesh movement with occasional reconstruction (section **2 - 7**). Unfortunately, a SL method does not solve the fluxes very well for cases of strong mesh deformation. It is therefore necessary to give a framework for error analysis, and this is what we propose to do by prescribing a mesh velocity that will capture the large but not too steep trends, which will leave the discontinuities to be resolved by the spatial discretisation method.

For these discontinuities, we refer to [20] and use a remainder-based refinement strategy to resolve both the discontinuities from the remaining advection velocity $V - \tilde{V}$ and the boundary layers occurring in advection-dominated flows. This study has to be adapted to the case of moving mesh because it introduces an

error term $e^{\|\nabla\tilde{V}\|_\infty T}$, which is large when either T or $\|\nabla\tilde{V}\|_\infty$ are large.
An additional feature of the error criteria that we develop is non-robustness in the sense that the criteria depend on the local value of $||V-\tilde{V}||^2$. This is important both because we are interested in cases where the remaining advection velocity has spatial variations, and also because we develop criteria to parameterise the mesh velocity.
In the DG framework, instead of continuously estimating an interpolation of the solution and inducing the gradient (like for SL methods), the approximate solution will be a discontinuous polynomial on a regular mesh and only the features of the equation will be estimated by the characteristics. The regularity of the approximate solution allows us to use the well-established results that exist for polynomials on triangular and polygonal meshes (for instance the results of [2], [18], [22], [23], [43]).

The aim of this 2D study is to fill a gap between SL methods and error estimation based AMR. Following the strategy developed in [28] and taking into account the reasoning of section **2 - 7**, we interpret a SL method as a velocity-based moving mesh method with occasional mesh reconstructions. Finally the fact that the mesh velocity is considered as parameterised in the *a priori* and *a posteriori* studies, helps to outline some principles in the choice of the mesh velocity.
In section **4 - 1**, the first step of the analysis is to exhibit a DG discretisation for the steady-state problem (4.1). Inspired by the litterature ([43], [45], [46], [47]), we state some approximation theorems and develop *a posteriori* error estimates. Existing analysis are either done with a discontinuous but piecewise polynomial or with a continuous diffusion tensor a. In this case, since the diffusion tensor under consideration is to be equal to $JF^{-1}F^{-T}$, it will be treated as continuous in the analysis (which is the case with $\tilde{V}$ smooth enough). The method that we will use is not consistent but according to [43], this can be controlled to still prove convergence if $\tilde{V}$ is smooth enough (see **Remark 3.3**).
In section **4 - 2** the DG method on a moving mesh is presented, section **4 - 3** uses some of the previous lemmas and also other material to study an *a priori* error estimate that outlines the importance of the two quantities $\frac{||V-\tilde{V}||^2}{\varepsilon}$ and $\frac{||\nabla\cdot\tilde{V}||}{2}$.
Finally in section **4 - 4** we integrate the error criteria from section **4 - 3** to show their signifiance for the unsteady case.
Section **4 - 5** consists of four test cases comparing the accuracy of static meshes

and moving meshes, then comparing moving meshes with SL methods, in situations where $\tilde{V}$ has either large vorticity or divergence, evaluating its response to a boundary layer problem and finally investigating the accuracy of the error criteria in cases where the deformation of the mesh is strong. We will there be able to comment on a flux comparison between SL and moving mesh methods and outline the importance of adapting the error criteria to the specific moving mesh situation. Finally we see the importance of non-robustness in the error criteria.

1 The interior penalty discretisation formulation for the steady-state advection-diffusion equation

Our choice here is to develop the tools of the spatial semi-discretisation by studying the steady-state problem (4.1). We take here an arbitrary advection velocity $W \in W^{1,\infty}(\Omega)$ that is to be equal to $JF^{-1}(V - \tilde{V})$ with the notations introduced in section **2 - 6**. For the tensor vector in the formulation (2.3) we can see that $a = \varepsilon JF^{-1}F^{-T}$ and therefore a is symmetric, definite and positive, continuous and not piecewise polynomial, with determinant equal to ε^2. With this stated, we can use [43], chapter 5, to help our study. Finally, because the study has to be applied for the lagrangian variable, the approximations are given with norms weighted by a positively bounded and continuous function J on Ω, that is to be equal to $J(t, X)$ with the notations from section **2 - 6**.

With this framework, we can define a DG approximation of the problem (4.1), give some properties of the DG operator and finally derive an *a posteriori* error estimation.

We consider a steady-state advection-diffusion equation:

$$\begin{aligned} &W \cdot \nabla u - \nabla \cdot \{a(x)\nabla u\} = f && \Omega \\ &u = 0 && \Gamma_D \\ &a\nabla u \cdot \mathbf{n} = u_N && \Gamma_N \end{aligned} \tag{4.1}$$

in a bounded convex $\Omega \subset \mathbb{R}^2$, having a Lipschitz boundary Γ consisting of two disjoint connected parts Γ_D and Γ_N. We assume that the data satisfy the following conditions:

(B1) $f \in L^2(\Omega),\ u_N \in L^2(\Gamma_N), W \in W^{1,\infty}(\Omega)^2$.

(B2) $a \in [\mathcal{C}^0(\Omega)]^{2,2}$ is a symmetric definite positive matrix and $\det a = \varepsilon^2$ constant with $\varepsilon \ll |W|_\infty$.

(B3) $-\nabla \cdot W > b > 0$ on Ω and $||\nabla \cdot W|| \leq c_* b$

(B4) The Dirichlet boundary Γ_D has positive $(d-1)$-dimensional measure and includes the inflow boundary $\{x \in \Gamma \,|\, W \cdot \mathbf{n}(x) < 0\}$.

Assumption (B2) means that we are interested in the advection-dominated regime, it also implies that a has a square root that we will write $\sqrt{a}$.

Remark 1.1. *Denoting the group of orthogonal matrices of $\mathcal{M}^{2,2}$ by $O(2)$ $\sqrt{a}$ is built as follows*

$$\exists \lambda_1, \lambda_2 > 0,\ \exists O \in O(2)\ a = O^T\, diag(\lambda_1, \lambda_2) O$$

$$\sqrt{a} \coloneqq O^T\, diag(\sqrt{\lambda_1}, \sqrt{\lambda_2}) O$$

Let $G \in [\mathcal{C}^0(\Omega)]^{2,2}$ such that $a = \varepsilon G G^T$ with $\det(G) = 1$.

1 - 1 Notation and weak form

For any bounded open subset ω of Ω with Lipschitz boundary γ, we denote by $H^k(\omega)$, $k \in \mathbb{N}$, $L^2(\omega) = H^0(\omega)$, and $L^2(\gamma)$ the usual Sobolev and Lebesgue spaces equipped with the standard norms $||\cdot||_{k;\omega} = ||\cdot||_{H^k(\omega)}$ and $||\cdot||_{0;\gamma} = ||\cdot||_{L^2(\gamma)}$ as well as the standard seminorm $|\cdot|_{H^1(\omega)} = ||\nabla \cdot||_{0,\omega}$. Similarly, $(\cdot,\cdot)_\omega$ and $(\cdot,\cdot)_\gamma$ denote the scalar products of $L^2(\omega)$ and $L^2(\gamma)$, respectively. If $\omega = \Omega$, the index Ω is omitted.

Let $J : \Omega \to \mathbb{R}_+^*$ be bounded in $L^2(\Omega)$. Let the weighted seminorm and norm:

$$|v|_{U_\omega}^2 \coloneqq \int_\omega (\nabla v)^T G G^T \nabla v \text{ and } ||v||_{H_\omega}^2 \coloneqq \int_\omega J v^2$$
$$0 < \beta < -\tfrac{\nabla \cdot W}{J}$$

Additionally let

$$H_D^1(\Omega) \coloneqq \{v \in H^1(\Omega) \colon v = 0 \text{ on } \Gamma_D\} \text{ and } H_0^1(\Omega) \coloneqq \{v \in H^1(\Omega) \colon v = 0 \text{ on } \Gamma\}$$

For $u, v \in H^1(\Omega)$ we define the following

$$\begin{aligned} A(u,v) &\coloneqq \int_\Omega a \nabla u \cdot \nabla v + v W \cdot \nabla u \\ l(v) &\coloneqq \int_\Omega f v + \int_{\Gamma_N} u_N v \end{aligned}$$

We can now formulate the definition of the weak form of (4.1).

$$\text{Find } u \in H_D^1(\Omega) \text{ s.t. } \forall v \in H_D^1(\Omega)\ \ A(u,v) = l(v) \tag{4.2}$$

1 - 2 Bilinear forms and function spaces for the semi-discretisation

To discretise (4.2), we consider regular and shape-regular meshes $\mathcal{T}_h = \{K\}$ that partition the computational domain Ω into open triangles. For simplicity we assume that Ω is a polyhedron that is covered exactly by $\mathcal{T}_h$. We assume the following:

(i) The elements of $\mathcal{T}_h$ satisfy the minimal angle condition. Specifically, there is a constant $\theta_0 > 0$ such that $\frac{h_K}{r_K} < \theta_0$ where h_K and r_K denote, respectively, the diameters of the circumscribed and inscribed balls to K.

(ii) $\mathcal{T}_h$ is locally quasi-uniform; that is, if two elements K_1 and K_2 are adjacent in the sense that $\mu_{d-1}(\partial K_1 \cap \partial K_2) > 0$ then $\operatorname{diam}(K_1) \approx \operatorname{diam}(K_2)$.
Here μ_{d-1} denotes the $(d-1)$-dimensional Lebesgue measure. Let h_E be the size of an edge E.
Given the discontinuous nature of the piecewise polynomial functions, let

$$
\begin{aligned}
\mathcal{E}^{\text{int}} &= \{e = \partial K_1 \cap \partial K_2 \,:\, \mu_{d-1}(\partial K_1 \cap \partial K_2) > 0\} \\
\mathcal{E}^{\text{ext}} &= \{e = \partial K \cap \Gamma \,:\, \mu_{d-1}(\partial K \cap \Gamma) > 0\} \\
\mathcal{E}_N^{\text{ext}} &= \{e = \partial K \cap \Gamma_N \,:\, \mu_{d-1}(\partial K \cap \Gamma_N) > 0\} \\
\mathcal{E}_D^{\text{ext}} &= \{e = \partial K \cap \Gamma_D \,:\, \mu_{d-1}(\partial K \cap \Gamma_D) > 0\} \\
\mathcal{E} &= \mathcal{E}^{\text{ext}}(\mathcal{T}_h) \cup \mathcal{E}^{\text{int}}(\mathcal{T}_h) \\
\mathcal{E}_N &= \mathcal{E}_N^{\text{ext}}(\mathcal{T}_h) \cup \mathcal{E}^{\text{int}}(\mathcal{T}_h) \\
\mathcal{E}_D &= \mathcal{E}_D^{\text{ext}}(\mathcal{T}_h) \cup \mathcal{E}^{\text{int}}(\mathcal{T}_h)
\end{aligned}
$$

set of edges.
We write $\mathbf{n}_K$ the outward unit normal vector on the boundary ∂K of an element K and for a set of points Y: $\omega_Y = \bigcup_{K \cap Y \neq \varnothing} K$. ω_K are the subsets of Ω_r on which we maximize or average the features (W, a, G) to be used in the error estimate. Let the inflow and outflow boundaries of $\partial\Omega$

$$\Gamma_{\text{in}}^t \coloneqq \{x \in \Gamma \colon W \cdot \mathbf{n} < 0\}, \text{ and } \Gamma_{\text{out}}^t \coloneqq \{x \in \Gamma \colon W \cdot \mathbf{n} \geq 0\}$$

Similarly, the inflow and outflow boundaries of an element K are defined by

$$\partial K_{\text{in}}^t \coloneqq \{x \in \partial K \colon W \cdot \mathbf{n}_K < 0\},\ \partial K_{\text{out}}^t \coloneqq \{x \in \partial K \colon W \cdot \mathbf{n}_K \geq 0\}.$$

The broken Sobolev spaces associated with the mesh $\mathcal{T}_h$

$$H^k(\mathcal{T}_h) = \{\varphi \in L^2(\Omega_r) \colon \forall K \in \mathcal{T}_h \quad \varphi|_K \in H^k(K)\}$$

And

$$V_h \coloneqq \{\varphi \in H^1(\mathcal{T}_h) \colon \forall K \in \mathcal{T}_h \quad \varphi|_K \in \mathcal{S}_p(K)\}$$

with $\mathcal{S}_p$ the space of polynomials of degree $\leq p$.
Finally $U_h \coloneqq V_h + H^1_D(\Omega_r)$ and $V_h^c \coloneqq V_h \cap H^1_D(\Omega_r)$.

The jumps and averages of functions in $H^{1/2}(\mathcal{T}_h)$ are defined as follows. Let the edge $E \in \mathcal{E}^{\text{int}}$ be shared by two neighboring elements K and K^e. For $v \in H^{1/2}(\mathcal{T}_h)$, $v|_E$ its trace on E taken from inside K, and $v^e|_E$ the one taken inside K^e. The average and jump of v across the edge E are then defined as

$$\{\{v\}\} = \tfrac{1}{2}(v|_E + v^e|_E), \qquad [\![v]\!] = v|_E \mathbf{n}_K + v^e|_E \mathbf{n}_{K^e}$$

For a vector field $\mathbf{q} \in H^{1/2}(\mathcal{T}_h)^d$ there is

$$\{\{\mathbf{q}\}\} = \tfrac{1}{2}(\mathbf{q}|_E + \mathbf{q}^e|_E), \qquad [\![\mathbf{q}]\!] = \mathbf{q}|_E \cdot \mathbf{n}_K + \mathbf{q}^e|_E \cdot \mathbf{n}_{K^e}$$

For $E \in \mathcal{E}^{\text{ext}}$

$$\{\{\mathbf{q}\}\} = \mathbf{q}|_E, \qquad [\![v]\!] = v|_E \mathbf{n}_r$$

We consider the DG method that is based on an upwind discretisation for the convective term and on a (non-)symmetric interior penalty discretisation for the Laplacian

$$\text{Find } u_h \in V_h \text{ s.t. } \forall v_h \in V_h \;\; A_h(u_h, v_h) = l_h(v_h) \tag{4.3}$$

With A_h given by

$$\begin{aligned} A_h(u,v) \coloneqq \sum_{K\in\mathcal{T}_h} \int_K a\nabla u\cdot\nabla v + vW\cdot\nabla u - \int_{\partial K^t_{\text{in}}} W\cdot[\![u]\!]v + \sum_{E\in\mathcal{E}_D} \varepsilon \int_E \frac{\gamma}{h_E}[\![u]\!]\cdot[\![v]\!] \\ - \varepsilon \sum_{E\in\mathcal{E}_D} \int_E \{\{\Pi_{L^2}(G^T\nabla u)\}\}\cdot G^T[\![v]\!] + \theta\{\{\Pi_{L^2}(G^T\nabla v)\}\}\cdot G^T[\![u]\!] \end{aligned} \tag{4.4}$$

Π_{L^2} denotes the elementwise orthogonal L^2-projection onto the finite element space $(V_h)^2$ and $\gamma = \alpha|G^T\mathbf{n}|^2$ the interior penalty parameter with $\alpha > 0$ a scalar depending on the polynomial degree. $\theta \in \{-1, 1\}$, the method is called symmetric interior penalty when $\theta = 1$ and nonsymmetric interior penalty when $\theta = -1$.

Notice that by integration by part

$$A_h(u,v) \coloneqq \sum_{K\in\mathcal{T}_h}\int_K a\nabla u\cdot\nabla v - uW\cdot\nabla v - uv\nabla\cdot W + \int_{\partial K^t_{\text{out}}} W\cdot[\![v]\!]u$$
$$-\varepsilon\sum_{E\in\mathcal{E}_D}\int_E \{\{\Pi_{L^2}(G^T\nabla u)\}\}\cdot G^T[\![v]\!] + \theta\{\{\Pi_{L^2}(G^T\nabla v)\}\}\cdot G^T[\![u]\!] - \frac{\gamma}{h_E}[\![u]\!]\cdot[\![v]\!] \tag{4.5}$$

And $l_h(v) \coloneqq \sum_{K\in\mathcal{T}_h}\int_K fv + \sum_{E\in\mathcal{E}_N^{\text{ext}}}\int_E u_N v$

Finally, for $u, v \in H^1(\mathcal{T}_h)$

$$\begin{aligned}
D_h(u,v) &\coloneqq \sum_{K\in\mathcal{T}_h}\int_K a\nabla u\cdot\nabla v - uv\nabla\cdot W\\
O_h(u,v) &\coloneqq -\sum_{K\in\mathcal{T}_h}\int_K uW\cdot\nabla v + \sum_{K\in\mathcal{T}_h}\int_{\partial K^t_{\text{out}}} W\cdot[\![v]\!]u\\
J_h(u,v) &\coloneqq \sum_{E\in\mathcal{E}_D}\int_E \frac{\gamma}{h_E}[\![u]\!]\cdot[\![v]\!]\\
\tilde{A}_h(u,v) &\coloneqq D_h(u,v) + O_h(u,v) + \varepsilon J_h(u,v)\\
\tilde{K}_h(u,v) &\coloneqq \varepsilon\sum_{E\in\mathcal{E}_D}\int_E \{\{\Pi_{L^2}(G^T\nabla u)\}\}\cdot G^T[\![v]\!] + \theta\{\{\Pi_{L^2}(G^T\nabla v)\}\}\cdot G^T[\![u]\!]
\end{aligned} \tag{4.6, 4.7}$$

1 - 3 Some properties of the bilinear operator

We will give here some properties on the operator A_h that will be useful to demonstrate the stability and convergence of the method. Since these properties hold both in one and two dimensions, we gave the same lemmas and properties for the 1D case in Chapter 3 without proving them, we do it here.

In what follows the symbol $\lesssim$ indicates an inequality involving a positive constant depending of the mesh regularity, the polynomial degree and c_* defined in assumption (B3).

By (3.41) in [10] there exist inverse and trace inequalities for the eulerian framework.

$$||v_h||_{\partial K} \lesssim h_K^{-\frac{1}{2}}||v_h||_K \tag{4.8}$$

$$||\nabla v_h||_K \lesssim h_K^{-1}||v_h||_K \tag{4.9}$$

we call $C_T > 0$ the constant appearing in (4.8) and $C_I > 0$ the constant appearing in (4.9).

To analyse the spatial error, we introduce the following quantities: $W \in W^{1,\infty}(\Omega)$ motivates the definition of $\delta_\omega = ||(J^{\frac{1}{2}}G)^{-1}W||^2_{L^\infty(\omega)}$, $J_1^\omega = \frac{\int_\omega J}{|\omega|}$, $a_1^\omega = \frac{\int_\omega ||a||}{|\omega|}$ and $a_\infty^\omega = ||a||_{L^\infty(\omega)} = \sup_\omega ||a||$, with $||a||$ the larger eigenvalue of a. Also $\gamma_\infty^\omega = \frac{a_\infty^\omega}{\varepsilon}$, $\gamma_1^\omega = \frac{a_1^\omega}{\varepsilon}$ and:

$$\forall v \in H^1(\mathcal{T}_h),\ |||v|||^2 \coloneqq \sum_{K\in\mathcal{T}_h} [\varepsilon |v|^2_{U_K} + \beta ||v||^2_{H_K}] + \varepsilon J_h(v,v) \tag{4.10}$$

$$\forall \mathbf{q} \in H^0(\Omega)^d,\ |\mathbf{q}|_* \coloneqq \sup_{v\in H^1_0(\Omega)-\{0\}} \frac{\int_\Omega J^{\frac{1}{2}}\mathbf{q}\cdot G^T\nabla v}{|||v|||} \tag{4.11}$$

$$\forall v \in H^1(\mathcal{T}_h),\ |v|_A^2 \coloneqq |(J^{\frac{1}{2}}G)^{-1}Wv|_*^2 + \sum_{E\in\mathcal{E}_D} (\beta + \frac{\delta_{\omega_E}}{\varepsilon}) h_E J_1^{\omega_E} \int_E [\![v]\!]^2 \tag{4.12}$$

Remark 1.2. *We often use that in two dimensions since* $\det(G) = 1$*, then* $\max_{|n|=1}(|G^Tn|^2) = (\min_{|n|=1}(|G^Tn|^2))^{-1}$ *thus*

$$\gamma_\infty^\omega = \max_\omega(\max_{|n|=1}(|G^Tn|^2)) = (\min_\omega(\min_{|n|=1}(|G^Tn|^2)))^{-1}.$$

The first norm is the energy-norm associated with the DG discretisation of the advection–diffusion problem (4.1). In [20] the seminorm $|\cdot|_*$ is linked to the Helmholtz decomposition, in particular, q is called divergence-free when this quantity is 0, in this case, the seminorm $|\cdot|_*$ is a weighted version of the one in [20]. The third norm measures the error of the transport behaviour.

Lemma 1.3. *(Coercivity) For* α *large enough (depending on the value of the scalar* C_T *in the inverse trace inequality) then* A_h *is* $|||\cdot|||$*-coercive. For all* $v_h \in U_h$

$$|||v_h|||^2 \lesssim A_h(v_h, v_h) \tag{4.13}$$

Proof. Let $v_h \in V_h$, by noticing that $A_h = \frac{1}{2}(\ (4.4)\ +\ (4.5)\ )$:

$$
\begin{aligned}
A_h(v_h, v_h) = &\sum_{K\in\mathcal{T}_h}\int_K a\nabla v_h\cdot\nabla v_h - \frac{1}{2}v_h^2\nabla\cdot W \\
&+\frac{1}{2}(\int_{\partial K^t_{\text{out}}} W\cdot[\![v_h]\!]v_h - \int_{\partial K^t_{\text{in}}} W\cdot[\![v_h]\!]v_h) \\
&-\varepsilon\sum_{E\in\mathcal{E}_D}(1+\theta)\int_E\{\{\Pi_{L^2}(G^T\nabla v_h)\}\}\cdot G^T[\![v_h]\!] + \int_E\frac{\gamma}{h_E}[\![v_h]\!]^2 \\
&=\sum_{K\in\mathcal{T}_h}\int_K a\nabla v_h\cdot\nabla v_h - \frac{1}{2}v_h^2\nabla\cdot W + \frac{1}{2}\sum_{E\in\mathcal{E}}\int_E|W\cdot\mathbf{n}|[\![v_h]\!]^2 \\
&-\varepsilon\sum_{E\in\mathcal{E}_D}(1+\theta)\int_E\{\{\Pi_{L^2}(G^T\nabla v_h)\}\}\cdot G^T[\![v_h]\!] + \int_E\frac{\gamma}{h_E}[\![v_h]\!]^2
\end{aligned}
$$

We can see that if $\theta = -1$, we have $A_h(v_h, v_h) \geq \frac{1}{2}|||v_h|||^2$ with no condition on α.

$$
\begin{aligned}
\varepsilon\sum_{E\in\mathcal{E}_D}\int_E\{\{\Pi_{L^2}(G^T\nabla v_h)\}\}\cdot G^T[\![v_h]\!] &\leq \varepsilon\sum_{E\in\mathcal{E}_D}\frac{c}{2}|\int_E\frac{\gamma}{h_E}[\![v_h]\!]^2| \\
&+\varepsilon\sum_{E\in\mathcal{E}^{\text{int}}}\frac{h_E}{c\alpha}\frac{1}{4}(|\int_E\{\Pi_{L^2}(G^T\nabla v_h)|_K\}^2| + |\int_E\{\Pi_{L^2}(G^T\nabla v_h)|_{K^e}\}^2|) \\
&+\varepsilon\sum_{E\in\mathcal{E}_D^{\text{ext}}}\frac{h_E}{c\alpha}\frac{1}{2}|\int_E\{\Pi_{L^2}(G^T\nabla v_h)|_K\}^2| \\
&\leq \frac{c}{2}\varepsilon J_h(v_h, v_h) + \sum_{K\in\mathcal{T}_h}\frac{C_T}{2c\alpha}\varepsilon||\Pi_{L^2}(G^T\nabla v_h)||^2_K \\
&\leq \frac{c}{2}\varepsilon J_h(v_h, v_h) + \sum_{K\in\mathcal{T}_h}\frac{C_T}{2c\alpha}\varepsilon||G^T\nabla v_h||^2_K \\
&\leq \frac{c}{2}\varepsilon J_h(v_h, v_h) + \sum_{K\in\mathcal{T}_h}\frac{C_T}{2c\alpha}|v_h|^2_{U_K}
\end{aligned}
$$

for $c > 0$ an arbitrarily small constant.
Thus, if $\theta = 1$, for $c = \frac{1}{2}$ and $\alpha = 2C_T$:

$$
A_h(v_h, v_h) \geq \sum_{K\in\mathcal{T}_h}[\varepsilon(1-\frac{C_T}{c\alpha})|v_h|^2_{U_K} + \frac{1}{2}||v_h||^2_{H_K} + (1-c)\varepsilon J_h(v_h, v_h)] \geq \frac{1}{2}|||v_h|||^2
$$

□

Remark 1.4. *(a)To ensure coercivity, $\alpha > C_T$, which explains why α depends on the polynomial degree: C_T is related to the inverse trace inequality* (4.8) *which is described in [23] as depending on the polynomial degree and the shape regularity of the mesh. For the stability of the time discretisation scheme, it is also important to keep α as small as possible, so that the condition number of the operator is minimised.*

(b) The projection used in the expression of $\tilde{K}_h$ ensures that the operator is coercive and so the problem is stable.

The following lemma shows that the projection that is used in $\tilde{K}_h$ makes us lose consistency but this brings in two important properties discussed in **Remark 1.6**.

Lemma 1.5. *(Inconsistency) Let $u \in H^1(\Omega_r)$ be an analytical solution of* (4.1) *and u_h solve* (4.3)*. Then*

$$\forall v_h \in V_h,\ A_h(u - u_h, v_h) = \varepsilon \sum_{E \in \mathcal{E}_D} \int_E \{\{G^T \nabla u - \Pi_{L^2}(G^T \nabla u)\}\} \cdot G^T [\![v_h]\!] \quad (4.14)$$

Proof. Let $v_h \in V_h$, first notice that:

$$\begin{aligned}
A_h(u, v_h) =& \sum_{K \in \mathcal{T}_h} \int_K a\nabla u \cdot \nabla v_h + v_h W \cdot \nabla u \\
&- \varepsilon \sum_{E \in \mathcal{E}_D} \int_E \{\{\Pi_{L^2}(G^T \nabla u)\}\} \cdot G^T [\![v_h]\!] \\
=& \sum_{K \in \mathcal{T}_h} \int_K (W \cdot \nabla u - \nabla \cdot \{a\nabla u\}) v_h + \int_{\partial K} a\nabla u \cdot \mathbf{n} v_h \\
&- \varepsilon \sum_{E \in \mathcal{E}_D} \int_E \{\{\Pi_{L^2}(G^T \nabla u)\}\} \cdot G^T [\![v_h]\!] \\
=& \sum_{K \in \mathcal{T}_h} \int_K f v_h + \int_{\Gamma_N} u_N v_h + \sum_{E \in \mathcal{E}_D} \int_E a\nabla u \cdot [\![v_h]\!] \\
&- \varepsilon \sum_{E \in \mathcal{E}_D} \int_E \{\{\Pi_{L^2}(G^T \nabla u)\}\} \cdot G^T [\![v_h]\!] \\
=& A_h(u_h, v_h) + \varepsilon \sum_{E \in \mathcal{E}_D} \int_E \{\{G^T \nabla u - \Pi_{L^2}(G^T \nabla u)\}\} \cdot G^T [\![v_h]\!]
\end{aligned}$$

Which gives (4.14). □

Remark 1.6. *(a) On the one hand this DG formulation is inconsistent with* (4.1)*. On the other hand, we observe that weaker regularity assumptions on the analytical solution to* (4.1) *are required here: we shall merely assume that* $u \in H^1(\Omega)$*, since no additional regularity of* u *is required to ensure the existence of traces of* $\Pi_{L^2}(G^T \nabla u)$ *in the definition of the method. In addition the formulation is coercive (thus stable) independently of the smoothness of* G*.*

(b) In the case where a *is piecewise constant, this becomes equivalent for polynomial trial and test functions to the consistent formulation (for instance the one from [20]).*

(c) This formulation is inconsistent but we bound the inconsistency in ***Lemma 3.2*** (4.40) *when the solution and* G *are regular enough. We study a discontinuous* G *in* ***Remark 3.3*** *for the 2D case and see that for a very deformed mesh, the inconsistency increases. This is coherent with the fact that, for strong deformations, when the flux is precisely approximated, the formulation is not coercive and when the formulation is stable, the method is inconsistent.*

The following two lemmas (continuity and inf-sup condition) show well-posedness and stability, they will be useful for the development of *a posteriori* error estimates.

Lemma 1.7. *(Continuity) For* $v \in H^1_D(\Omega)$*,* $w_1, w_2 \in U_h$

$$|D_h(w_1, w_2)| \leq |||w_1||| \cdot |||w_2||| \tag{4.15}$$

$$|J_h(w_1, w_2)| \leq |||w_1||| \cdot |||w_2||| \tag{4.16}$$

$$|O_h(w_1, v)| \leq |(J^{\frac{1}{2}}G)^{-1} W w_1|_* \cdot |||v||| \tag{4.17}$$

Proof. (4.15) and (4.16) comes from Cauchy-Schwarz and the fact that $\beta > 0$.

$$\begin{aligned} |O_h(w_1, v)| &\leq |\sum_{K \in \mathcal{T}_h} \int_K w_1 W \cdot \nabla v| \\ &\leq |||v||| \frac{|\int_\Omega J^{\frac{1}{2}} w_1 (J^{\frac{1}{2}}G)^{-1} W \cdot G^T \nabla v|}{|||v|||} \\ &\leq |(J^{\frac{1}{2}}G)^{-1} W w_1|_* \cdot |||v||| \end{aligned}$$

□

Lemma 1.8. *(Inf-Sup)*

$$\inf_{v\in H^1_D(\Omega)-\{0\}}\sup_{w\in H^1_D(\Omega)-\{0\}}\frac{\tilde{A}_h(v,w)}{(|||v|||+|(J^{\frac{1}{2}}G)^{-1}Ww_1|_*)\cdot|||w|||}\geq C>0$$

Proof. Let $v\in H^1_D(\Omega)-\{0\}$ and $\theta\in]0;1[$. Then by definition of the *-norm $\exists w_\theta\in H^1_0(\Omega)$ s.t. $|||w_\theta|||=1$ and

$$O_h(v,w_\theta)=-\int_\Omega J(J^{\frac{1}{2}}G)^{-1}Wv\cdot G^T\nabla w_\theta\geq\theta|(J^{\frac{1}{2}}G)^{-1}Wv|_*$$

$$\tilde{A}_h(v,w_\theta)\geq -C_1|||v|||\cdot|||w_\theta|||+\theta|(J^{\frac{1}{2}}G)^{-1}Wv|_*=\theta|(J^{\frac{1}{2}}G)^{-1}Wv|_*-C_1|||v|||$$

for a constant $C_1>0$. Let us then define

$$v_\theta=v+\frac{|||v|||}{1+C_1}w_\theta$$

s.t. $|||v_\theta|||\leq|||v|||(1+\frac{1}{1+C_1})$ and $v_\theta\in H^1_D(\Omega)$.

Thus

$$\begin{aligned}\tilde{A}_h(v,v_\theta)=A(v,v_\theta)&=A(v,v)+|||v|||\frac{A(v,w_\theta)}{1+C_1}\\&\geq|||v|||\cdot[|||v|||+\frac{\theta|(J^{\frac{1}{2}}G)^{-1}Wv|_*-C_1|||v|||}{1+C_1}]\end{aligned}$$

Finally

$$\sup_{w\in H^1_D(\Omega)-\{0\}}\frac{\tilde{A}_h(v,w)}{|||w|||}\geq\frac{\tilde{A}_h(v,v_\theta)}{|||v_\theta|||}\geq\frac{\theta|(J^{\frac{1}{2}}G)^{-1}Wv|_*+|||v|||}{2C_1}$$

□

Remark 1.9. *$C_1=O(c_*)$ with c_* defined in assumption (B3).*

1 - 4 A residual-based error estimator

In this section we want to build reliable error criteria for the steady-state weak formulation (4.2). We first present the error criteria:
Let $J^\omega_{\min}=\min_\omega(J)$ and $\rho_S=\min(h_S(\frac{\gamma^{\omega_S}_\infty}{\varepsilon})^{\frac{1}{2}},(\beta J^{\omega_S}_{\min})^{-\frac{1}{2}})$, $S=E$ or K.

$$\text{Let} \begin{cases} \eta_{J_K}^2 & \coloneqq \frac{1}{2} \sum\limits_{E \in \mathcal{E}^{\text{int}} \cap K} [(\beta + \frac{\delta_{\omega_E}}{\varepsilon}) h_E J_1^{\omega_E} + a_1^{\omega_E} \frac{\alpha}{h_E}] \gamma_\infty^{\omega_E} \int_E [\![G^T u_h]\!]^2 \\ & \quad + \sum\limits_{E \in \mathcal{E}_D^{\text{ext}} \cap K} [(\beta + \frac{\delta_{\omega_E}}{\varepsilon}) h_E J_1^{\omega_E} + a_1^{\omega_E} \frac{\alpha}{h_E}] \gamma_\infty^{\omega_E} \int_E [\![G^T u_h]\!]^2 \\ \eta_{E_K}^2 & \coloneqq \frac{1}{2} \sum\limits_{E \in \mathcal{E}^{\text{int}} \cap K} \sqrt{\frac{\gamma_\infty^{\omega_E}}{\varepsilon}} \rho_E \int_E [\![a \nabla u_h]\!]^2 \\ & \quad + \sum\limits_{E \in \mathcal{E}_N^{\text{ext}} \cap K} \sqrt{\frac{\gamma_\infty^{\omega_E}}{\varepsilon}} \rho_E \int_E (u_N - a \nabla u_h \cdot \mathbf{n})^2 \\ \eta_{R_K}^2 & \coloneqq \rho_K^2 ||f + \nabla \cdot \{a \nabla u_h\} - W \cdot \nabla u_h||_{L^2(K)}^2 \end{cases} .$$

$$\eta_K^2 \coloneqq \eta_{J_K}^2 + \eta_{E_K}^2 + \eta_{R_K}^2 \tag{4.18}$$

We show that these local error criteria give a reliable estimation $\sum\limits_K \eta_K$.

Theorem 1.10. *Let $u \in H_D^1(\Omega_r)$ and $\hat{u}_h \in V_h$ be solutions of* (4.2)*, respectively* (4.3) *and η_K be defined in* (4.18) *then*

$$|||\hat{u} - \hat{u}_h||| + |\hat{u} - \hat{u}_h|_A \lesssim (\sum_K \eta_K)^{\frac{1}{2}}$$

1 - 5 Proof of Theorem 1.10

The topic of this section is to prove the reliability of the error estimate. Based on the continuity and inf-sup conditions given in the previous part, we will derive *a posteriori* weighted-error estimators for the piecewise polynomial solution of (4.3). The first lemmas of this section give an upper bound for each contribution of the operator $\tilde{A}_h$, the last argument uses the inf-sup condition and an upper bound for the operator $\tilde{K}_h$.

The outline of the proof for the stationary case is as follow: separate our solution into a continuous and a discontinuous part (**Lemma 1.12**), give a bound to the discontinuous part (**Lemma 1.14**), derive a bound for the bilinear forms as an estimate multiplied by the energy-norm of the continuous function (**Lemma 1.11**, **Lemma 1.16**) and conclude with **Lemma 1.8**.

First we give the upper bound on the operator $\tilde{K}_h$ for test functions in V_h^c.

Lemma 1.11.

$$\forall v \in V_h \; \forall w \in V_h^c$$
$$|\tilde{K}_h(v,w)| \lesssim \alpha^{-\frac{1}{2}} \Big(\sum_{E \in \mathcal{E}_D} a_1^{\omega_E} \gamma_\infty^{\omega_E} \int_E \frac{\varepsilon\gamma}{h_E} [\![v]\!]^2 \Big)^{\frac{1}{2}} \cdot \Big(\sum_{K \in \mathcal{T}_h} \frac{\varepsilon}{a_1^{\omega_K} \gamma_\infty^{\omega_K}} ||G^T \nabla w||^2_{L^2(K)} \Big)^{\frac{1}{2}}.$$

Proof. $\tilde{K}_h(\hat{v},\hat{w}) = -\sum\limits_{E \in \mathcal{E}_D} \varepsilon \int_E \{\{\Pi_{L^2}(G^T \nabla w)\}\} \cdot G^T [\![v]\!]$
And by Cauchy-Schwarz

$$\begin{aligned}
|\tilde{K}_h(v,w)| &\leq \Big(\sum_{E \in \mathcal{E}_D} a_1^{\omega_E} \gamma_\infty^{\omega_E} \int_E \frac{\varepsilon\gamma}{h_E} [\![v]\!]^2 \Big)^{\frac{1}{2}} \\
&\quad \Big(\sum_{E \in \mathcal{E}_D} \int_E \frac{\varepsilon h_E}{2\alpha a_1^{\omega_E} \gamma_\infty^{\omega_E}} ((\Pi_{L^2}(G^T \nabla w)|_K)^2 + (\Pi_{L^2}(G^T \nabla w)|_{K^e})^2) \Big)^{\frac{1}{2}} \\
&\lesssim \alpha^{-\frac{1}{2}} \Big(\sum_{E \in \mathcal{E}_D} a_1^{\omega_E} \gamma_\infty^{\omega_E} \int_E \frac{\varepsilon\gamma}{h_E} [\![v]\!]^2 \Big)^{\frac{1}{2}} \Big(\sum_{K \in \mathcal{T}_h} \frac{\varepsilon}{a_1^{\omega_K} \gamma_\infty^{\omega_K}} ||\Pi_{L^2}(G^T \nabla w)||^2_{L^2(K)} \Big)^{\frac{1}{2}} \\
&\lesssim \alpha^{-\frac{1}{2}} \Big(\sum_{E \in \mathcal{E}_D} a_1^{\omega_E} \gamma_\infty^{\omega_E} \int_E \frac{\varepsilon\gamma}{h_E} [\![v]\!]^2 \Big)^{\frac{1}{2}} \Big(\sum_{K \in \mathcal{T}_h} \frac{\varepsilon}{a_1^{\omega_K} \gamma_\infty^{\omega_K}} ||G^T \nabla w||^2_{L^2(K)} \Big)^{\frac{1}{2}}
\end{aligned}$$

□

We will now study an approximation of elements of V_h by elements of V_h^c in case of conforming meshes. A similar theorem for the eulerian problem is stated in **Theorem 2.2** in [22].

Lemma 1.12. *Let $\mathcal{T}_h$ be a conforming mesh. Then there exists an approximation operator $\mathcal{A}_h \colon V_h \to V_h^c$ satisfying:*

$$\forall v_h \in V_h \begin{cases} \sum\limits_{K \in \mathcal{T}_h} ||v_h - \mathcal{A}_h v_h||^2_{H_K} & \lesssim \sum\limits_{E \in \mathcal{E}_D} h_E J_1^{\omega_E} \int_E [\![v_h]\!]^2 \\ \sum\limits_{K \in \mathcal{T}_h} |v_h - \mathcal{A}_h v_h|^2_{U_K} & \lesssim \sum\limits_{E \in \mathcal{E}_D} h_E^{-1} \gamma_1^{\omega_E} \int_E [\![v_h]\!]^2 \end{cases}$$

Proof. We build the approximation with lagrangian nodes and use the property of polynomials to conclude.
For each $K \in \mathcal{T}_h$, $\mathcal{N}_K \coloneqq \{x_K^{(j)} : j = 1, \dots, m\}$ the set of distinct nodes of K with nodes on both ends. Let $\{\phi_K^{(j)} : j = 1, \dots, m\}$ be a local basis of functions satisfying $\phi_K^{(i)}(x_K^{(j)}) = \delta_{ij}$.
Let $\mathcal{N} \coloneqq \bigcup\limits_{K \in \mathcal{T}_h} \mathcal{N}_K$ be the set of nodes and

$$\mathcal{N}_D \coloneqq \{\nu \in \mathcal{N} : \ \nu \in E \in \mathcal{E}_D^{\text{ext}}\}$$
$$\mathcal{N}_N \coloneqq \{\nu \in \mathcal{N} : \ \nu \in E \in \mathcal{E}_N^{\text{ext}}\}$$
$$\mathcal{N}_i \coloneqq \{\nu \in \mathcal{N} - \mathcal{N}_D : \ |\omega_\nu| = 1\}$$
$$\mathcal{N}_v \coloneqq \mathcal{N} - (\mathcal{N}_i \cup \mathcal{N}_D)$$

Additionally define $\omega_\nu \coloneqq \{K \in \mathcal{T}_h : \ \nu \in K\}$ for each $\nu \in \mathcal{N}$.

We have that for each $\nu \in \mathcal{N}$, $|\omega_\nu|$ is bounded by a constant depending only on θ_0.

Finally, let $\overset{o}{\mathcal{N}}$ be the collection of distinct Lagrange nodes ν needed to build an element of V_h^c. In this case (conforming mesh) we have $\overset{o}{\mathcal{N}} = \mathcal{N}$. To each $\nu \in \overset{o}{\mathcal{N}}$ we associate a basis function $\phi^{(\nu)}$:

$$\operatorname{supp} \phi^{(\nu)} \subset \bigcup_{K \in \omega_\nu} K, \ \phi^{(\nu)}|_K = \phi_K^{(j)}, \ x_K^{(j)} = \nu.$$

Write $v_h \in V_h$ as $v_h = \sum_{K \in \mathcal{T}_h} \sum_{j=1}^{m} \alpha_K^{(j)} \phi_K^{(j)}$ and define

$$\mathcal{A}_h v_h \coloneqq \sum_{\nu \in \overset{o}{\mathcal{N}}} \beta^{(\nu)} \phi^{(\nu)}, \text{ where } \beta^{(\nu)} \coloneqq \begin{cases} 0 & \text{if } \nu \in \mathcal{N}_D \\ \frac{1}{|\omega_\nu|} \sum_{x_K^{(j)} = \nu} \alpha_K^{(j)} & \text{if } \nu \in \overset{o}{\mathcal{N}} - \mathcal{N}_D \end{cases}$$

We define now $\beta_K^{(j)} \coloneqq \beta^{(\nu)}$ if $x_K^{(j)} = \nu$.

We have $||\phi_K^{(j)}||_{L^\infty(K)}^2 \lesssim 1$ and $||\nabla \phi_K^{(j)}||_{L^\infty(K)}^2 \lesssim h_K^{-2}$.

Thus:

$$\begin{aligned}
\sum_{K\in\mathcal{T}_h} |v_h - \mathcal{A}_h v_h|^2_{U_K} &\leq \sum_{K\in\mathcal{T}_h} \gamma_1^K \; h_K^2 \; |\nabla(v_h - \mathcal{A}_h v_h)|^2_{L^\infty(K)} \\
&\lesssim \sum_{K\in\mathcal{T}_h} \gamma_1^K \sum_{j=1}^{m} |\alpha_K^{(j)} - \beta_K^{(j)}|^2 \\
&\lesssim \sum_{\nu\in\mathcal{N}} \gamma_1^{\omega_\nu} \sum_{x_K^{(j)}=\nu} |\alpha_K^{(j)} - \beta^{(\nu)}|^2 \\
&\lesssim \sum_{\nu\in\mathcal{N}_v} \gamma_1^{\omega_\nu} \sum_{x_K^{(j)}=\nu} |\alpha_K^{(j)} - \beta^{(\nu)}|^2 + \sum_{\nu\in\mathcal{N}_D} \gamma_1^{\omega_\nu} \sum_{x_K^{(j)}=\nu} |\alpha_K^{(j)}|^2 \\
\sum_{K\in\mathcal{T}_h} ||v_h - \mathcal{A}_h v_h||^2_{H_K} &\leq \sum_{K\in\mathcal{T}_h} J_1^K h_K^2 \; |v_h - \mathcal{A}_h v_h|^2_{L^\infty(K)} \\
&\lesssim \sum_{K\in\mathcal{T}_h} J_1^K h_K^2 \sum_{j=1}^{m} |\alpha_K^{(j)} - \beta_K^{(j)}|^2 \\
&\lesssim \sum_{\nu\in\mathcal{N}} J_1^{\omega_\nu} h_\nu^2 \sum_{x_K^{(j)}=\nu} |\alpha_K^{(j)} - \beta^{(\nu)}|^2 \qquad (h_\nu = \max_{\omega_\nu}(h_K)) \\
&\lesssim \sum_{\nu\in\mathcal{N}_v} J_1^{\omega_\nu} h_\nu^2 \sum_{x_K^{(j)}=\nu} |\alpha_K^{(j)} - \beta^{(\nu)}|^2 + \sum_{\nu\in\mathcal{N}_D} J_1^{\omega_\nu} h_\nu^2 \sum_{x_K^{(j)}=\nu} |\alpha_K^{(j)}|^2
\end{aligned}$$

where we used $\alpha_K^{(j)} = \beta^{(\nu)}$ for $\nu \in \mathcal{N}_i$ in the fourth and last lines.

Now let $\kappa_i(\cdot)$ defined for the nodes ν, the edges E as well as any subset or collection of subsets of Ω_r depending also on some integer i and such that it is increasing in terms of element and inclusion (*i.e.* if $a \in b$ then $\kappa_i(a) \leq \kappa_i(b)$ and if $a \subset b$, then $\kappa_i(a) \leq \kappa_i(b)$).

$A_i \coloneqq \sum_{\nu\in\mathcal{N}_v} \kappa_i(\nu) \sum_{x_K^{(j)}=\nu} |\alpha_K^{(j)} - \beta^{(\nu)}|^2.$

Let $\omega_\nu = \{K_1, \ldots, K_{|\omega_\nu|}\}$ with $\mu_{d-1}(K_l \cap K_{l+1}) > 0$ then there is a constant depending only on $|\omega_\nu|$ and so θ_0 such that

$$\sum_{x_K^{(j)}=\nu} |\alpha_K^{(j)} - \beta^{(\nu)}|^2 \leq c \sum_{l=1}^{|\omega_\nu|-1} |\alpha_{K_l}^{(j_l)} - \alpha_{K_{l+1}}^{(j_{l+1})}|^2.$$

Then $A_i \lesssim \sum_{\nu\in\mathcal{N}_v} \kappa_i(\nu) \sum_{l=1}^{|\omega_\nu|-1} |\alpha_{K_l}^{(j_l)} - \alpha_{K_{l+1}}^{(j_{l+1})}|^2$

Let $B_i \coloneqq \sum_{\nu\in\mathcal{N}_D} \kappa_i(\nu) \sum_{x_K^{(j)}=\nu} |\alpha_K^{(j)}|^2.$

If we work in $\nu \in \mathcal{N}_D$, in the case $|\omega_\nu| > 1$, with the same kind of argument we have

$$\sum_{x_K^{(j)}=\nu} |\alpha_K^{(j)}|^2 \lesssim \sum_{l=1}^{|\omega_\nu|-1} |\alpha_{K_l}^{(j_l)} - \alpha_{K_{l+1}}^{(j_{l+1})}|^2 + |\alpha_{K_{|\omega_\nu|}}^{(j_{|\omega_\nu|})}|^2$$

where we can ensure $K_{|\omega_\nu|}$ such that $\mu_{d-1}(K_{|\omega_\nu|} \cap \Gamma_D) \neq 0$.

Writing $\omega_\nu^D \coloneqq \{K \in \omega_\nu : \mu_{d-1}(K \cap \Gamma_D) \neq 0\}$, it means that for each $\nu \in \mathcal{N}_D$, for each $K \in \omega_\nu^D$, the value $\alpha_K^{(j)}$ for $x_K^{(j)} = \nu$ is the jump over an edge of Γ_D.

Thus $B_i \lesssim \sum_{\nu \in \mathcal{N}_D} \kappa_i(\nu)(\underbrace{\sum_{l=1}^{|\omega_\nu|-1} |\alpha_{K_l}^{(j_l)} - \alpha_{K_{l+1}}^{(j_{l+1})}|^2}_{=0 \text{ if } |\omega_\nu|=1} + \sum_{\{(j,K):\, K \in \omega_\nu^D, x_K^{(j)}=\nu\}} |\alpha_K^{(j)}|^2)$

Finally

$$\sum_{K \in \mathcal{T}_h} |v_h - \mathcal{A}_h v_h|_{U_K}^2 \lesssim \sum_{E \in \mathcal{E}^{\text{int}}} \sum_{\nu \in E} \gamma_1^{\omega_\nu} \, |\alpha_{K^+}^{(j_+)} - \alpha_{K^-}^{(j_-)}|^2 + \sum_{\nu \in \mathcal{N}_D} \sum_{\{(j,K):\, K \in \omega_\nu^D, x_K^{(j)}=\nu\}} \gamma_1^{\omega_\nu} \, |\alpha_K^{(j)}|^2$$

And

$$\sum_{K \in \mathcal{T}_h} ||v_h - \mathcal{A}_h v_h||_{H_K}^2 \lesssim \sum_{E \in \mathcal{E}^{\text{int}}} \sum_{\nu \in E} h_\nu^2 J_1^{\omega_\nu} |\alpha_{K^+}^{(j^+)} - \alpha_{K^-}^{(j^-)}|^2 + \sum_{\nu \in \mathcal{N}_D} h_\nu^2 J_1^{\omega_\nu} \sum_{\{(j,K):\, K \in \omega_\nu^D, x_K^{(j)}=\nu\}} |\alpha_K^{(j)}|^2$$

As for any $E \in \mathcal{E}^{\text{int}}$:

$$\sum_{\nu \in E} \kappa_i(\nu) |\alpha_{K^+}^{(j_\nu^+)} - \alpha_{K^-}^{(j_\nu^-)}|^2 \lesssim \kappa_i(E) |[\![v_h]\!]|_{L^\infty(E)}^2 \lesssim \frac{\kappa_i(E)}{h_E} \int_E [\![v_h]\!]^2$$

$$\sum_{\nu \in \mathcal{N}_D} \kappa_i(\nu) \sum_{\{(j,K):\, K \in \omega_\nu^D, x_K^{(j)}=\nu\}} |\alpha_K^{(j)}|^2 = \sum_{E \in \mathcal{E}_D^{\text{ext}}} \sum_{\nu \in E} \kappa_i(\nu) |\alpha_{K_E}^{(j_\nu)}|^2 \lesssim \sum_{E \in \mathcal{E}_D^{\text{ext}}} \kappa_i(E) \int_E [\![v_h]\!]^2$$

Then

$$\begin{cases} \sum_{K\in\mathcal{T}_h} |v_h - \mathcal{A}_h v_h|^2_{U_K} & \lesssim \sum_{E\in\mathcal{E}_D} h_E^{-1}\,\gamma_1^{\omega_E} \int_E [\![v_h]\!]^2 \\ \sum_{K\in\mathcal{T}_h} ||v_h - \mathcal{A}_h v_h||^2_{H_K} & \lesssim \sum_{E\in\mathcal{E}_D} h_E J_1^{\omega_E} \int_E [\![v_h]\!]^2 \end{cases}$$

□

Remark 1.13. *Note that this operator, that we will use again for the study of the unsteady problem, $\mathcal{A}_h$ is a linear operator only depending on the mesh and not on the features, it is therefore independent of time when the features are dependent of the mesh deformation.*

Let's now project u_h via $\mathcal{A}_h$:

$$u_h = u_h^c + u_h^r \text{ with } u_h^c = \mathcal{A}_h u_h \tag{4.19}$$

Here, u_h^c is a continuous projection of u_h and u_h^r catches the jumps. With this we will find a bound for

$$\kappa \coloneqq |||u - u_h||| + |u - u_h|_A \tag{4.20}$$

By definition and triangular inequality

$$\kappa \leq |||\hat{u}^s - \hat{u}_h^c||| + |\hat{u}^s - \hat{u}_h^c|_A + |||\hat{u}_h^r||| + |\hat{u}_h^r|_A.$$

We then bound κ with these error estimators. We first bound the jump term by applying **Lemma 1.12** to u_h^r.

Lemma 1.14. $|||u_h^r||| + |u_h^r|_A \lesssim (\sum_{K\in\mathcal{T}_h} [\frac{1}{\alpha} + 1]\eta^2_{J_K})^{\frac{1}{2}}$.

Proof. Knowing that $[\![u_h^r]\!] = [\![u_h]\!]$ on $\mathcal{E}_D$:

$$\begin{aligned} |||u_h^r|||^2 + |u_h^r|_A^2 \leq & \sum_{K\in\mathcal{T}_h} [\varepsilon |u_h^r|^2_{U_K} + \beta ||u_h^r||^2_{H_K}] + |(J^{\frac{1}{2}}G)^{-1} W u_h^r|^2_* \\ & + \sum_{E\in\mathcal{E}_D} [(\beta + \frac{\delta^2_{\omega_E}}{\varepsilon}) h_E J_1^{\omega_E} \gamma_\infty^{\omega_E} + \frac{\varepsilon\alpha}{h_E}] \int_E [\![G^T u_h]\!]^2 \end{aligned}$$

By **Lemma 1.12**

$$\begin{cases} \sum_{K\in\mathcal{T}_h} \varepsilon |u_h^r|^2_{U_K} & \lesssim \alpha^{-1} \sum_{E\in\mathcal{E}_D} a_1^{\omega_E} \frac{\alpha}{h_E} \int_E [\![u_h^r]\!]^2 \\ \sum_{K\in\mathcal{T}_h} \beta ||u_h^r||^2_{H_K} & \lesssim \sum_{E\in\mathcal{E}_D} \beta h_E J_1^{\omega_E} \int_E [\![u_h^r]\!]^2 \end{cases}$$

$$
\begin{aligned}
|(J^{\frac{1}{2}}G)^{-1}Wu_h^r|_*^2 &\leq \sup_{v\in H_0^1(\Omega_r)\colon |||\hat{v}|||=1} (||(J^{\frac{1}{2}}G)^{-1}Wu_h^r||_H^2 \cdot |v|_U^2) \leq \frac{1}{\varepsilon}||(J^{\frac{1}{2}}G)^{-1}Wu_h^r||_H^2 \\
&\leq \frac{1}{\varepsilon}\sum_{K\in\mathcal{T}_h}\delta_K||u_h^r||_{H_K}^2 \lesssim \sum_{E\in\mathcal{E}_D}\frac{h_E\delta_{\omega_E}}{\varepsilon}\int_E[\![u_h^r]\!]^2 \\
&\lesssim \sum_{K\in\mathcal{T}_h}\eta_{J_K}^2
\end{aligned}
$$

□

Finally, we want to use the inf-sup condition to bound the continuous part of κ, namely $|||\hat{u}^s - \hat{u}_h^c||| + |\hat{u}^s - \hat{u}_h^c|_A$. To do so we present a lemma of approximation of function of $H_D^1(\Omega_r)$ by continuous, piecewise polynomials. This is done for static meshes in [19] with Clement-type interpolant.

We denote $\mathcal{N}_h$ the vertices of the mesh and $\mathcal{N}_N$ the ones not lying on the Dirichlet boundary and define a nodal basis function λ_y for $y \in \mathcal{N}_N$

$$\lambda_{y|K} \in \mathcal{P}_1(K)\ \forall K \in \mathcal{T}_h,\ \lambda_y(z) = 0\ \forall z \in \mathcal{N}_h - \{y\}.$$

And

$$
\begin{aligned}
\mathcal{I}_h\colon L^1(\Omega) &\to \{\varphi \in C(\Omega)\colon \varphi|_K \in S_1(K), \varphi = 0 \text{ on } \Gamma_D\} \\
v &\mapsto \sum_{y\in\mathcal{N}_N}\frac{\int_{\omega_y} v}{|\omega_y|}\lambda_y.
\end{aligned}
$$

with $|\omega_y|$ the Lebesgue measure of the set ω_y in Ω.

Lemma 1.15. *For all $v \in H_D^1(\Omega_r)$, there is $\varepsilon|\mathcal{I}_h v|_{U_K}^2 \lesssim a_1^{\omega_K}\gamma_\infty^{\omega_K}|v|_{U_K}^2$ and*

$$
\begin{cases}
\sum_{K\in\mathcal{T}_h}\rho_K^{-2}||v - \mathcal{I}_h v||_{L^2(K)}^2 & \lesssim |||v|||^2 \\
\sum_{E\in\mathcal{E}}\sqrt{\frac{\varepsilon}{\gamma_\infty^{\omega_E}}}\rho_E^{-1}\int_E(v - \mathcal{I}_h v)^2 & \lesssim |||v|||^2
\end{cases}
$$

Proof. Since $\mathcal{I}_h v$ is piecewise affine, we can write $\nabla\mathcal{I}_h v = n_v^K$. [19], **Lemma 5.1** says that $|K| \cdot ||n_v^K||^2 \lesssim ||\nabla v||_{L^2(\omega_K)}^2$. We have the following inequality

$$\varepsilon|\mathcal{I}_h v|_{U_K}^2 = \int_K a n_v^K \cdot n_v^K \leq a_1^K|K| \cdot ||n_v^K||^2 \lesssim a_1^K||\nabla v||_{L^2(\omega_K)}^2 \lesssim a_1^{\omega_K}\gamma_\infty^{\omega_K}|v|_{U_K}^2$$

Lemma 3.1 in [17] gives

$$\begin{cases} \beta J_{\min}^{\omega_K} \int_K (v - \mathcal{I}_h v)^2 & \lesssim \beta J_{\min}^{\omega_K} ||v||^2_{L^2(\omega_K)} \lesssim \beta ||v||^2_{H_{\omega_K}} \\ \frac{\varepsilon}{h_K^2 \gamma_\infty^{\omega_K}} \int_K (v - \mathcal{I}_h v)^2 & \lesssim \frac{\varepsilon}{\gamma_\infty^{\omega_K}} ||\nabla v||^2_{L^2(\omega_K)} \lesssim \varepsilon |v|^2_{U_{\omega_K}} \end{cases}$$

Which gives the second inequality. The last inequality comes from the technique in **Lemma 3.2** in [17]. □

Using the inf-sup condition and the previous lemmas, we can now bound the continuous part of κ, namely $|||u - u_h^c||| + |u - u_h^c|_A$.

Lemma 1.16. $|||u - u_h^c||| + |u - u_h^c|_A \lesssim (\sum_{K \in \mathcal{T}_h} (1 + \frac{1}{\alpha}) \eta_K^2)^{\frac{1}{2}}$ *with* u_h^c *defined in* (4.19).

Proof. We will first bound

$$T(v) \coloneqq l(v - \mathcal{I}_h v) - \tilde{A}_h(u_h, v - \mathcal{I}_h v) \text{ for } v \in H_D^1(\Omega_r).$$

$T = T_1 + T_2 + T_3$ with

$$\begin{cases} T_1(v) & \coloneqq \sum_{K \in \mathcal{T}_h} \int_K (f + \nabla \cdot \{a \nabla u_h\} - W \cdot \nabla u_h)(v - \mathcal{I}_h v) \\ T_2(v) & \coloneqq -\varepsilon \sum_{K \in \mathcal{T}_h} \int_{\partial K} (G^T \nabla u_h \cdot G^T \mathbf{n}_K)(v - \mathcal{I}_h v) \\ T_3(v) & \coloneqq - \sum_{K \in \mathcal{T}_h} \int_{\partial K_{\text{in}}^t - \Gamma_r} W \cdot [\![u_h]\!](v - \mathcal{I}_h v) \end{cases}$$

Since

$$\begin{aligned} |T_1| &\leq (\sum_{K \in \mathcal{T}_h} \eta_{R_K}^2)^{\frac{1}{2}} (\sum_{K \in \mathcal{T}_h} \rho_K^{-2} ||v - \mathcal{I}_h v||^2_{L^2(K)})^{\frac{1}{2}} \\ &\lesssim (\sum_{K \in \mathcal{T}_h} \eta_{R_K}^2)^{\frac{1}{2}} |||v||| \\ |T_2| &= |\varepsilon \sum_{K \in \mathcal{T}_h} \int_{\partial K} (G^T \nabla u_h \cdot G^T \mathbf{n}_K)(v - \mathcal{I}_h v)| \\ &\lesssim (\sum_{K \in \mathcal{T}_h} \eta_{E_K}^2)^{\frac{1}{2}} |||v||| \\ |T_3| &= |\sum_{K \in \mathcal{T}_h} \int_{\partial K_{\text{in}}^t - \Gamma_r} W \cdot [\![u_h]\!](v - \mathcal{I}_h v)| \\ &\lesssim (\sum_{K \in \mathcal{T}_h} \eta_{J_K}^2)^{\frac{1}{2}} |||v||| \end{aligned}$$

Therefore for all $v \in H_D^1(\Omega_r)$

$$\begin{aligned}\tilde{A}_h(u-u_h^c,v) &= l(v)-\tilde{A}_h(u_h^c,v)\\ &= l(v)-\tilde{A}_h(u_h,v)+\tilde{A}_h(u_h^r,v)\end{aligned}$$

And $l(\mathcal{I}_h v)=A_h(u_h,\mathcal{I}_h v)=\tilde{A}_h(u_h,\mathcal{I}_h v)+\tilde{K}_h(u_h,\mathcal{I}_h v)$
Then $\tilde{A}_h(u-u_h^c,v)=T(v)+\tilde{A}_h(u_h^r,v)+\tilde{K}_h(u_h,\mathcal{I}_h v)$

$$\begin{aligned}|\tilde{A}_h(u-u_h^c,v)| \lesssim \{&(\sum_{K\in\mathcal{T}_h}\eta_{R_K}^2)^{\frac{1}{2}}+(\sum_{K\in\mathcal{T}_h}\eta_{E_K}^2)^{\frac{1}{2}}+(\sum_{K\in\mathcal{T}_h}\eta_{J_K}^2)^{\frac{1}{2}}\\ &+(\sum_{K\in\mathcal{T}_h}[\frac{1}{\alpha}+1]\eta_{J_K}^2)^{\frac{1}{2}}+(\sum_{K\in\mathcal{T}_h}\frac{1}{\alpha}\eta_{J_K}^2)^{\frac{1}{2}}\}|||v|||\end{aligned}$$

And by noticing that $|u-u_h^c|_A=|(J^{\frac{1}{2}}G)^{-1}W(u-u_h^c)|_*$:

$$|||u-u_h^c|||+|u-u_h^c|_A \lesssim \sup_{v\in H_D^1(\Omega_r)-\{0\}}\frac{\tilde{A}_h(u-u_h^c,v)}{|||v|||}$$

□

Lemma 1.17. $\kappa^2 \lesssim \sum_{K\in\mathcal{T}_h}(1+\frac{1}{\alpha})\eta_K^2$ *with* κ *defined in* (4.20).

Proof. This result comes directly from **Lemma 1.14** and **Lemma 1.16**. □

2 The semi-discrete interior penalty discretisation formulation for the unsteady advection-diffusion equation

We now use the discretisation from section **4 - 2** in order to semi-discretise 2.3. This semi-discretisation is the basis for the *a priori* study from section **4 - 3** and finally the result from **Theorem 1.10** is used to develop an *a posteriori* error criterion in section **4 - 4**.
We notice that formulation (2.3) can be written as (4.1): $a(t,X)=\varepsilon JF^{-1}F^{-T}$ and $W(t,X)=JF^{-1}(V-\tilde{V})$ and we can thus use the analysis done for the steady-state problem with $J=J(t,X)$ and $G=J^{\frac{1}{2}}F^{-1}$, notice that $\det(G)=1$ in 2D.

2 - 1 Notation and weak form

Let $\omega_r \subset \Omega_r$ (we recall that $\Omega_r = \Omega$), we define the following:

$$||\hat{v}||^2_{H_{\omega_r}(t)} \coloneqq \int_{\omega_r} \hat{v}^2 J(t,\cdot),\ |\hat{v}|^2_{U_{\omega_r}(t)} \coloneqq \int_{\omega_r} (\nabla_X \hat{v})^T F(t,\cdot)^{-1} F(t,\cdot)^{-T} (\nabla_X \hat{v}) J(t,\cdot)$$

If $\omega_r = \Omega_r$, the index Ω_r is omitted.
Denoting $v(t,\chi(t,X)) \coloneqq \hat{v}(X)$, $\omega(t) \coloneqq \chi(t,\omega_r)$,

$$||v||_{0;\omega} = ||\hat{v}||_{H_{\omega_r}(t)} \text{ and } |v|_{H^1(\omega)} = |\hat{v}|_{U_{\omega_r}(t)}.$$

Remark 2.1. *This property shows that the approximation constructed are given with respect to the reference variable X. By denoting e the approximation error, the bounds on $\|\hat{e}\|_{H(t)}$ and $|\hat{e}|_{U(t)}$ represent L^2- and H^1-bounds on e.*

We define the spaces $L^p(0,T;X)$ (withs X a Banach space) that consist of mesurable functions $v\colon [0,T] \to X$ for which:

$$||v||^p_{L^p(0,T;X)} \coloneqq (\int_0^T ||v(t)||^p_X \mathrm{d}t) < +\infty \text{ for } 1 \leq p < +\infty$$
$$||v||_{L^\infty(0,T;X)} \coloneqq \operatorname*{ess\,sup}_{0\leq t\leq T} ||v(t)||_X < +\infty \text{ for } p = +\infty$$

Set

$$H^1_D(\Omega_r) \coloneqq \{\hat{v} \in H^1(\Omega_r)\colon \hat{v} = 0 \text{ on } \Gamma_D\} \text{ and}$$
$$H^1_0(\Omega_r) \coloneqq \{\hat{v} \in H^1(\Omega_r)\colon \hat{v} = 0 \text{ on } \Gamma\}$$

For $\hat{u}, \hat{v} \in H^1(\Omega_r)$ we define the following:

$$A(\hat{u},\hat{v}) \coloneqq \int_{\Omega_r} J[\varepsilon(F^{-T}\nabla_X \hat{u}) \cdot (F^{-T}\nabla_X \hat{v}) + (V - \tilde{V}) \cdot (F^{-T}\nabla_X \hat{u})\hat{v}]$$

$$l(\hat{v}) \coloneqq \int_{\Omega_r} J\hat{f}\hat{v} + \int_{\Gamma_N} \hat{u}_N \hat{v} |F^{-T}\mathbf{n}_r|$$

This gives us the weak form. The weak formulation of (2) is:

$$\text{Find } \hat{u} \in L^2(0,T;H^1_D(\Omega_r)) \cap C^1(0,T;H^{-1}(\Omega_r))$$
$$\text{s.t. } \forall t \in [0,T],\ \forall \hat{v} \in H^1_D(\Omega_r) \quad \int_{\Omega_r} J\frac{\partial \hat{u}}{\partial t}\hat{v} = l(\hat{v}) - A(\hat{u},\hat{v}) \quad (4.21)$$

By integration by part

$$A(\hat{u},\hat{v}) \coloneqq \int_{\Omega_r} J[\varepsilon(F^{-T}\nabla_X\hat{u})\cdot(F^{-T}\nabla_X\hat{v}) - \hat{u}(V-\tilde{V})\cdot(F^{-T}\nabla_X\hat{v}) - \nabla\cdot(V-\tilde{V})\hat{u}\hat{v}] + \int_{\Gamma_N} J(V-\tilde{V})\cdot(F^{-T}\mathbf{n}_r)\hat{u}\hat{v}$$

2 - 2 Bilinear forms and function spaces for the semi-discretisation

To discretise (4.21), we consider regular and shape-regular meshes $\mathcal{T}_h = \{K\}$ that partition the computational domain Ω_r into open triangles and has the same properties as for the steady-state problem. We consider this mesh to be static and steady. We define the same way as in section **4 - 1.2** the sets of edges $\mathcal{E}^{\text{int}}$, $\mathcal{E}^{\text{ext}}$, $\mathcal{E}^{\text{ext}}_N$, $\mathcal{E}^{\text{ext}}_D$, $\mathcal{E}$, $\mathcal{E}_N$ and $\mathcal{E}_D$, the outward normal vectors $\mathbf{n}_K$, the inflow and outflow boundaries Γ^t_{in} and Γ^t_{out} of the domain and ∂K^t_{in} and $\partial K^t_{\text{out}}$ of each triangle, the broken Sobolev spaces $H^k(\mathcal{T}_h)$, the polynomial spaces V_h and V^c_h, the functional space U_h, the average and jump $\{\{\hat{v}\}\}$ and $[\![\hat{v}]\!]$ of a scalar and $\{\{\mathbf{q}\}\}$ and $[\![\mathbf{q}]\!]$ of a vector. Additionally we define $A_h(\cdot,\cdot)$ as

$$A_h(\hat{u},\hat{v}) \coloneqq \sum_{K\in\mathcal{T}_h}\int_K J[\varepsilon(F^{-T}\nabla_X\hat{u})\cdot(F^{-T}\nabla_X\hat{v}) + (V-\tilde{V})\cdot(F^{-T}\nabla_X\hat{u})\hat{v}]$$
$$-\sum_{E\in\mathcal{E}_D}\int_E J^{\frac{1}{2}}\varepsilon(\{\{\Pi_{L^2}(J^{\frac{1}{2}}F^{-T}\nabla_X\hat{u})\}\}\cdot F^{-T}[\![\hat{v}]\!] + \theta\{\{\Pi_{L^2}(J^{\frac{1}{2}}F^{-T}\nabla_X\hat{v})\}\}\cdot F^{-T}[\![\hat{u}]\!])$$
$$+\frac{\alpha\varepsilon}{h_E}\int_E JF^{-T}[\![\hat{u}]\!]\cdot F^{-T}[\![\hat{v}]\!] - \sum_{K\in\mathcal{T}_h}\int_{\partial K^t_{\text{in}}} J(V-\tilde{V})\cdot(F^{-T}[\![\hat{u}]\!])\hat{v}$$

With $\alpha > 0$ the interior penalty parameter. And let $\theta \in \{-1,1\}$.

We consider the DG method that is based on an upwind discretisation for the convective term and a (non-)symmetric interior penalty discretisation for the Laplacian, i.e.

Find $\hat{u}_h \in C^1(0,T;V_h)$ s.t. $\forall t \in [0,T]$, $\forall \hat{v}_h \in V_h$

$$\int_{\Omega_r} J\frac{\partial \hat{u}_h}{\partial t}\hat{v}_h = l(\hat{v}_h) - A_h(\hat{u}_h,\hat{v}_h)$$

where $\hat{u}_h(0,\cdot) \in V_h$ is a projection of $\hat{u}_0(\cdot)$ onto V_h. (4.22)

The operator $\mathcal{A}_h \colon V_h \to V_h^c$ defined in **Lemma 1.12**, β, δ_ω and the time dependent norms and seminorms $|||\cdot|||$, $|\cdot|_*$ and $|\cdot|_A$ similarly to (4.10), (4.11) and (4.12) respectively.
Let $\hat{u}^s \colon [0,T] \to H_D^1(\Omega_r)$ and $\hat{u}_h^s \colon [0,T] \to V_h$ for each t such that

$$\begin{cases} \forall \hat{v} \in H_D^1(\Omega_r) & l(\hat{v}) - \int_{\Omega_r} J\frac{\partial \hat{u}_h}{\partial t}\hat{v} - A(t;\hat{u}^s(t),\hat{v}) = 0 \\ \forall \hat{v}_h \in V_h & l(\hat{v}_h) - \int_{\Omega_r} J\frac{\partial \hat{u}_h}{\partial t}\hat{v}_h - A_h(t;\hat{u}_h^s(t),\hat{v}_h) = 0 \end{cases} \tag{4.23}$$

Notice that $\hat{u}^s(t)$ (resp. $\hat{u}_h^s(t)$) is the solution of (4.21) (resp. (4.22)) with right-hand side $J(\hat{f} - \frac{\partial \hat{u}_h}{\partial t})$.

Remark 2.2. *From **Remark 1.13** we conclude that the operator $\mathcal{A}_h$ is preserving the smoothness in time, thereby defining $\hat{u}_h^r$ and $\hat{u}_h^c$ as space-time functions: $\hat{u}_h^r \in C^1(0,T;V_h)$ and $\hat{u}_h^c \in C^1(0,T;V_h^c)$.*

Denoting $\gamma = \alpha J|F^{-T}\mathbf{n}|^2$ on any edge E, we also define:

$$J_h(t;\hat{u},\hat{v}) = \sum_{E\in\mathcal{E}_D} \int_E \frac{\gamma}{h_E}[\![\hat{u}]\!]\cdot[\![\hat{v}]\!].$$

3 An *a priori* error estimate for the semi-discrete formulation

Before considering a full *a posteriori* error criterion for the unsteady problem, we present here an *a priori* approach. In **Remark 3.3** (b) we describe the convergence of the method depending on the regularity of the flow map and the solution, linking this study to [43]. Unlike [43], where **Theorem 46** gives a convergence rate when $J^{\frac{1}{2}}F^{-T}\nabla_X\hat{u} \in H^l(\Omega_r)$, we quantify here the dependence of an *a priori* error estimate on the derivatives of the mesh velocity and thus the estimate depending on the derivatives of J and F is insufficient. Therefore, we first develop the *a priori* approach from **Theorem 3.1** to highlight a balance between $||V-\tilde{V}||^2/\varepsilon$ and $||\nabla\cdot\tilde{V}||$, and then give the approximation **Properties**

3.2 to explicitly expose the dependence in the different derivatives of the mesh velocity. This section is concluded with **Remark 3.3** for a situation where the deformation map is not smooth.

As stated in Chapter 3, even if this study is only done for the 2D case, since the theorems that we use as well as the data that we can access are the same in the two cases, this *a priori* study also holds for 1D.

This *a priori* error estimation can help us to choose a mesh velocity. In the test cases from sections **3 - 3.1** and **4 - 5.1** we prolong this theoretical statement by highlighting a balance between $||V - \tilde{V}||^2/\varepsilon$ and $||\nabla \cdot \tilde{V}||$,

In this section we suppose higher regularity the strong solution of (2.3), namely $\hat{u} \in H^2(\Omega_r)$. For the analysis we need to define the following projections:

$\Pi_{L^2} : (H^0(\mathcal{T}_h))^2 \to V_h^2$ the L^2-projection.

$P_h(t) : H^0(\mathcal{T}_h) \to V_h$ the weighted projections s.t.

$$\forall \hat{v} \in H^0(\mathcal{T}_h),\ \int_K J(t,\cdot)(\hat{v} - P_h\hat{v})\hat{v}_h = 0\ \forall \hat{v}_h \in V_h.$$

In the following lemma we call

$$\hat{e} = (\hat{u} - P_h\hat{u}) + (P_h\hat{u} - \hat{u}_h) = \hat{e}_p + \hat{e}_h \tag{4.24}$$

$$\hat{E}_p = J^{\frac{1}{2}} F^{-T} \nabla_X \hat{u} - \Pi_{L^2}(J^{\frac{1}{2}} F^{-T} \nabla_X \hat{u}) \tag{4.25}$$

$$\hat{N} : [0,T] \times H^1(\mathcal{T}_h) \to \mathbf{R}, \text{the seminorm s.t. } \hat{N}(t,\hat{v})^2 = |\hat{v}|^2_{U(t)} + 2J_h(t;\hat{v},\hat{v}) \tag{4.26}$$

$$\hat{B} : H^{1/2}(\mathcal{T}_h) \to \mathbf{R}, \text{the seminorm s.t. } \hat{B}(\hat{v})^2 = \frac{\sum_{\mathcal{E}_D} h_E \int_E \{\{\hat{v}\}\}^2}{C_T} \tag{4.27}$$

Notice that $\hat{E}_p \in H^1(\mathcal{T}_h)$ and define $N(t,\cdot)$ and $B(t,\cdot)$ as the corresponding time dependant seminorm s.t. $N(t,v) = \hat{N}(t,\hat{v})$ and $B(t,v) = \hat{B}(\hat{v})$ and e_p and E_p are the corresponding functions in the eulerian variable.

Recalling that $\dot{J} = J(\nabla \cdot \tilde{V})$, $\dot{F} = (\nabla \tilde{V})F$ (implying $\dot{F^{-1}} = -F^{-1}(\nabla \tilde{V})$) yields

$\forall \hat{v} \in H^1(T_h)$

$$\frac{d}{\mathrm{d}t}||\hat{v}||^2_{H_K(t)} = \int_K \hat{v}^2 J(\nabla \cdot \tilde{V})$$
$$\frac{d}{\mathrm{d}t}\int_E J\hat{v}^2 = \int_E \hat{v}^2 J(\nabla \cdot \tilde{V})$$
$$\frac{d}{\mathrm{d}t}||\hat{v}||^2_{U_K(t)} = \int_K J(F^{-T}\nabla_X \hat{v})^T(\nabla \cdot \tilde{V} - \nabla\tilde{V} - (\nabla\tilde{V})^T)F^{-T}\nabla_X \hat{v}$$
$$\frac{d}{\mathrm{d}t}\int_E \gamma[\![\hat{v}]\!]^2 = \int_E \alpha J(F^{-T}\mathbf{n})^T(\nabla \cdot \tilde{V} - \nabla\tilde{V} - (\nabla\tilde{V})^T)F^{-T}\mathbf{n}[\![\hat{v}]\!]^2$$

for $C_0(t) \coloneqq \frac{1}{2}||\nabla \cdot \tilde{V}||_{L^1(0,t;L^\infty(\Omega))}$ and $C_1(t) \coloneqq C_0(t) + ||\frac{\nabla\tilde{V}+(\nabla\tilde{V})^T}{2}||_{L^1(0,t;L^\infty(\Omega))}$. Using Gronwall's inequality we have:

$$||\hat{v}||_{H(0)}e^{-C_0(t)} \leq ||\hat{v}||_{H(t)} \leq ||\hat{v}||_{H(0)}e^{C_0(t)} \tag{4.28}$$
$$\int_E \hat{v}^2 e^{-2C_0(t)} \leq \int_E J\hat{v}^2 \leq \int_E \hat{v}^2 e^{2C_0(t)} \tag{4.29}$$
$$||\hat{v}||_{U(0)}e^{-C_1(t)} \leq ||\hat{v}||_{U(t)} \leq ||\hat{v}||_{U(0)}e^{C_1(t)} \tag{4.30}$$
$$J_h(0;\hat{v},\hat{v})e^{-2C_1(t)} \leq J_h(t;\hat{v},\hat{v}) \leq J_h(0;\hat{v},\hat{v})e^{2C_1(t)} \tag{4.31}$$

We can now state the *a priori* error estimate.

Theorem 3.1. *Let $T > 0$ and $\hat{u}_h$ be the solution of* (4.22)*, $\hat{e}_p$ and $\hat{E}_p$ be respectively defined in* (4.24) *and* (4.25) *and $N(t,\cdot)$ and $B(t,\cdot)$ be the seminorms respectively defined in* (4.26) *and* (4.27)*.*

For SIPG

$$||e||^2_{L^\infty(0,T;L^2(\Omega))} + \frac{\varepsilon}{4}||e||^2_{L^2(0,T;N(t,\cdot))} \leq C_S(||e(0)||^2_{L^2(\Omega)} + 2||e_p||^2_{L^\infty(0,T;L^2(\Omega))} + 30\varepsilon||e_p||^2_{L^2(0,T;N(t,\cdot))} + \frac{97}{8}\varepsilon||E_p||^2_{L^2(0,T;B(t,\cdot))}) \tag{4.32}$$

with $C_S = \exp[\frac{8+12e^{4C_0^\Omega(T)}}{\varepsilon}||V - \tilde{V}||^2_{L^2(0,T;L^\infty(\Omega))} + \frac{1}{2}||\nabla \cdot \tilde{V}||_{L^1(0,T;L^\infty(\Omega))}]$ *holds.*

For NIPG

$$||e||^2_{L^\infty(0,T;L^2(\Omega))} + \frac{\varepsilon}{2}||e||^2_{L^2(0,T;N(\cdot))} \leq C_N(||e(0)||^2_{L^2(\Omega)} + 2||e_p||^2_{L^\infty(0,T;L^2(\Omega))} + 4\varepsilon||e_p||^2_{L^2(0,T;N(t,\cdot))} + \frac{17}{8}\varepsilon||E_p||^2_{L^2(0,T;B(t,\cdot))}) \quad (4.33)$$

with $C_N = \exp[\frac{1+2e^{4C_0^\Omega(T)}}{\varepsilon}||V-\tilde{V}||^2_{L^2(0,T;L^\infty(\Omega))} + \frac{1}{2}||\nabla\cdot\tilde{V}||_{L^1(0,T;L^\infty(\Omega))}]$ *holds.*

Proof. In the beginning of the proof we work with the generic form of interior penalty methods, namely $\theta \in \{-1, 1\}$.
We have the following inequalities

$$\begin{aligned}
\int_{\Omega_r} J\frac{\partial\hat{e}}{\partial t}\hat{e} &= \frac{1}{2}\frac{\mathrm{d}}{\mathrm{d}t}||e||^2_{L^2(\Omega)} - \int_{\Omega_r}\frac{\nabla\cdot\tilde{V}}{2}J\hat{e}_c^2 \\
&\geq \frac{1}{2}\frac{\mathrm{d}}{\mathrm{d}t}||e||^2_{L^2(\Omega)} - \frac{||\nabla\cdot\tilde{V}||_\infty}{2}||e||^2_{L^2(\Omega)} \\
\int_{\Omega_r} J\frac{\partial\hat{e}_p}{\partial t}\hat{e}_p &= \frac{1}{2}\frac{\mathrm{d}}{\mathrm{d}t}||e_p||^2_{L^2(\Omega)} - \int_{\Omega_r}\frac{\nabla\cdot\tilde{V}}{2}J\hat{e}_c^2 \\
&\leq \frac{1}{2}\frac{\mathrm{d}}{\mathrm{d}t}||e_p||^2_{L^2(\Omega)} + \frac{||\nabla\cdot\tilde{V}||_\infty}{2}||e_p||^2_{L^2(\Omega)}
\end{aligned}$$

and the identity

$$\begin{aligned}
\int_{\Omega_r} J\frac{\partial\hat{e}}{\partial t}\hat{e} + A_h(\hat{e},\hat{e}) &= \int_{\Omega_r} J\frac{\partial\hat{e}}{\partial t}\hat{e}_p + \int_{\Omega_r} J\frac{\partial\hat{e}}{\partial t}\hat{e}_h + A_h(\hat{e},\hat{e}_p) + A_h(\hat{e},\hat{e}_h) \\
&= \int_{\Omega_r} J\frac{\partial\hat{e}_p}{\partial t}\hat{e}_p + \underbrace{\int_{\Omega_r} J\frac{\partial\hat{e}_h}{\partial t}\hat{e}_p}_{0} + A_h(\hat{e},\hat{e}_p) \\
&\quad + \underbrace{\int_{\Omega_r} J\frac{\partial\hat{e}}{\partial t}\hat{e}_h + A_h(\hat{e},\hat{e}_h)}_{\varepsilon\sum_{\mathcal{E}_D}\int_E\{\{\hat{E}_p\}\}\cdot J^{\frac{1}{2}}F^{-T}[\![\hat{e}_h]\!]}
\end{aligned}$$

Notice that $[\![\hat{e}]\!] = [\![\hat{u}_h]\!]$.
We will also use the following bounds

$$\forall\hat{v}\in H^1(\mathcal{T}_h)\ \sum_{E\in\mathcal{E}_D} h_E\int_E\{\{\Pi_{L^2}(J^{\frac{1}{2}}F^{-T}\nabla_X\hat{v})\}\}^2 \leq C_T||\hat{v}||^2_{U(t)} \quad (4.34)$$

$$\forall \hat{v} \in V_h \sum_{E \in \mathcal{E}_D} h_E \int_E J\hat{v}^2 \leq C_T e^{4C_0^\Omega} ||\hat{v}||^2_{H(t)} \tag{4.35}$$

$$\forall \hat{v}, \hat{w} \in H^1(\mathcal{T}_h)\ \forall c > 0\ J_h(\hat{v}, \hat{w}) \leq \frac{c}{2} J_h(t; \hat{v}, \hat{v}) + \frac{1}{2c} J_h(t; \hat{w}, \hat{w}) \tag{4.36}$$

with C_T defined by (4.8). (4.34) is already proven in the proof of **Lemma 1.3**, (4.36) is a consequence of the trace inequality (4.8) and (4.28) and (4.36) by Cauchy-Schwarz and Young's inequality. Estimating

$$\begin{aligned}
I &= \frac{1}{2}(\frac{\mathrm{d}}{\mathrm{d}t}||e||^2_{L^2(\Omega)} - \frac{\mathrm{d}}{\mathrm{d}t}||e_p||^2_{L^2(\Omega)}) + \varepsilon|\hat{e}|^2_{U(t)} + \varepsilon J_h(t; \hat{e}, \hat{e}) \\
&\leq \sum_{K \in \mathcal{T}_h} -\int_K J\hat{e}(V - \tilde{V}) \cdot F^{-T} \nabla_X \hat{e} - JF^{-T} \nabla_X \hat{e} \cdot F^{-T} \nabla_X \hat{e}_p + J\hat{e}_p (V - \tilde{V}) \cdot F^{-T} \nabla_X \hat{e} \\
&\qquad + \int_{\partial K^t_{\mathrm{in}}} J(V - \tilde{V}) \cdot F^{-T} [\![\hat{e}]\!] \hat{e}_h + \varepsilon J_h(t; \hat{e}, \hat{e}_p) \\
&\quad + \tilde{K_h}(\hat{e}, \hat{e}_h) + \sum_{\mathcal{E}_D} \int_E \{\{\hat{E}_p\}\} \cdot J^{\frac{1}{2}} F^{-T} [\![\hat{e}_h]\!] + \frac{||\nabla \cdot \tilde{V}||_\infty}{2} (||e||^2_{L^2(\Omega)} + ||e_p||^2_{L^2(\Omega)})
\end{aligned}$$

Using $\hat{e}_h = \hat{e} - \hat{e}_p$

$$\begin{aligned}
I &\leq \frac{\alpha_1}{2}\varepsilon|\hat{e}|^2_{U(t)} + \frac{||V - \tilde{V}||^2_\infty}{\varepsilon} \frac{1}{2\alpha_1} ||e||^2_{L^2(\Omega)} + \frac{\alpha_2}{2}\varepsilon|\hat{e}|^2_{U(t)} + \frac{1}{2\alpha_2}\varepsilon|\hat{e}_p|^2_{U(t)} + \frac{\alpha_3}{2}\varepsilon|\hat{e}|^2_{U(t)} \\
&\quad + \frac{||V - \tilde{V}||^2_\infty}{\varepsilon} \frac{1}{2\alpha_3} ||e_p||^2_{L^2(\Omega)} + \frac{\alpha_4}{2}\varepsilon J_h(t; \hat{e}, \hat{e}) + \frac{1}{2\alpha_4} \frac{||V - \tilde{V}||^2_\infty}{\varepsilon\alpha} \sum_{E \in \mathcal{E}_D} h_E \int_E J e_h^2 \\
&\quad + \frac{\alpha_5}{2}\varepsilon J_h(t; \hat{e}, \hat{e}) + \frac{1}{2\alpha_5}\varepsilon J_h(t; \hat{e}_p, \hat{e}_p) + \frac{\alpha_6}{2}(1 + \theta)\frac{\varepsilon C_T}{\alpha}|\hat{e}|^2_{U(t)} + \frac{(1 + \theta)}{2\alpha_6}\varepsilon J_h(t; \hat{e}, \hat{e}) \\
&\quad + \frac{\alpha_7}{2}(1 + \theta)\frac{\varepsilon C_T}{\alpha}|\hat{e}|^2_{U(t)} + \frac{(1 + \theta)}{2\alpha_7}\varepsilon J_h(t; \hat{e}_p, \hat{e}_p) + \frac{\alpha_8}{2}\varepsilon J_h(t; \hat{e}, \hat{e}) + \frac{1}{2\alpha_8}\frac{\varepsilon C_T}{\alpha}|\hat{e}_p|^2_{U(t)} \\
&\quad + \frac{\varepsilon}{2\alpha_9}\frac{C_T}{\alpha}\hat{B}(\hat{E}_p)^2 + \frac{\alpha_9}{2}\varepsilon J_h(t; \hat{e}, \hat{e}) + \frac{\varepsilon}{2\alpha_{10}}\frac{C_T}{\alpha}\hat{B}(\hat{E}_p)^2 + \frac{\alpha_{10}}{2}\alpha_\varepsilon J_h(t; \hat{e}_p, \hat{e}_p) \\
&\quad + \frac{||\nabla \cdot \tilde{V}||_\infty}{2}(||e||^2_{L^2(\Omega)} + ||e_p||^2_{L^2(\Omega)})
\end{aligned}$$

And bounded via $\alpha > 2C_T$

$$I \leq [\frac{\alpha_1}{2} + \frac{\alpha_2}{2} + \frac{\alpha_3}{2} + \frac{\alpha_6}{4}(1+\theta) + \frac{\alpha_7}{4}(1+\theta)]\varepsilon|\hat{e}|^2_{U(t)} + [\frac{1}{2\alpha_2} + \frac{1}{4\alpha_8}]\varepsilon|\hat{e}_p|^2_{U(t)}$$
$$+ [\frac{\alpha_4}{2} + \frac{\alpha_5}{2} + \frac{(1+\theta)}{2\alpha_6} + \frac{\alpha_8}{2} + \frac{\alpha_9}{2}]\varepsilon J_h(t;\hat{e},\hat{e})$$
$$+ [\frac{1}{2\alpha_5} + \frac{(1+\theta)}{2\alpha_7} + \frac{\alpha_{10}}{2}]\varepsilon J_h(t;\hat{e}_p,\hat{e}_p) + \frac{e^{4C_0^\Omega}}{4\alpha_4}\frac{||V-\tilde{V}||^2_\infty}{\varepsilon}||\hat{e}_h||^2_{H(t)}$$
$$+ \frac{\varepsilon}{4}[\alpha_9^{-1} + \alpha_{10}^{-1}]\hat{B}(\hat{E}_p)^2 + \frac{||V-\tilde{V}||^2_\infty}{\varepsilon}\frac{1}{2\alpha_3}||e_p||^2_{L^2(\Omega)} + \frac{||V-\tilde{V}||^2_\infty}{\varepsilon}\frac{1}{2\alpha_1}||e||^2_{L^2(\Omega)}$$
$$+ \frac{||\nabla\cdot\tilde{V}||_\infty}{2}(||e||^2_{L^2(\Omega)} + ||e_p||^2_{L^2(\Omega)}) \quad (4.37)$$

This is true for both SIPG and NIPG. In the following we distinguish between the two methods.

For SIPG: Using and setting $\alpha_6 = \frac{3}{2}$, $\alpha_1 = \alpha_2 = \alpha_3 = \alpha_7 = \frac{1}{16}$, $\alpha_4 = \alpha_5 = \alpha_8 = \alpha_9 = \frac{1}{24}$, $\alpha_{10} = 4$ implies

$$\frac{1}{2}(\frac{\mathrm{d}}{\mathrm{d}t}||e||^2_{L^2(\Omega)} - \frac{\mathrm{d}}{\mathrm{d}t}||e_p||^2_{L^2(\Omega)}) + \frac{\varepsilon}{8}(N(t,e)^2 - 120N(t,e_p)^2) - \frac{97}{16}\varepsilon\hat{B}(\hat{E}_p)$$
$$\leq ([8 + 12e^{4C_0^\Omega}]\frac{||V-\tilde{V}||^2_\infty}{\varepsilon} + \frac{||\nabla\cdot\tilde{V}||_\infty}{2})(||e||^2_{L^2(\Omega)} + ||e_p||^2_{L^2(\Omega)})$$

For NIPG: α_6 and α_7 do not matter because $1 + \theta = 0$.
Using and setting $\alpha_1 = \alpha_2 = \alpha_3 = \frac{1}{2}$, $\alpha_4 = \alpha_5 = \alpha_8 = \alpha_9 = \frac{1}{4}$, $\alpha_{10} = 4$ implies

$$\frac{1}{2}(\frac{\mathrm{d}}{\mathrm{d}t}||e||^2_{L^2(\Omega)} - \frac{\mathrm{d}}{\mathrm{d}t}||e_p||^2_{L^2(\Omega)}) + \frac{\varepsilon}{4}(N(t,e)^2 - 8N(t,e_p)^2) - \frac{17}{16}\varepsilon\hat{B}(\hat{E}_p)$$
$$\leq ([1 + 2e^{4C_0^\Omega}]\frac{||V-\tilde{V}||^2_\infty}{\varepsilon} + \frac{||\nabla\cdot\tilde{V}||_\infty}{2})(||e||^2_{L^2(\Omega)} + ||e_p||^2_{L^2(\Omega)})$$

and we conclude with Grönwall's inequality in the form
$\frac{d}{dt}(a-\alpha) + (b-\beta) \leq C(t)(a+\alpha)$ for nonnegative quantities implies

$$a(T) + \int_0^T \mu(s,T)b(s)ds \leq \mu(0,T)a(0) + 2\mu(0,T)\max_{0\leq s\leq T}\alpha(s) + \int_0^T \mu(s,T)\beta(s)ds$$

with $\mu(s,t) = \exp(\int_s^t C(y)dy)$.

□

In both cases here, since $e^{4C_0^\Omega}$ stays close to 1 for short times, one sees the multiplier (C_S for SIPG and C_N for NIPG) driven exponentially by $||V-\tilde{V}|^2/\varepsilon$ and $||\nabla\cdot\tilde{V}||$. This directs our study towards a balance between these terms. The following approximation properties yield the necessary tools to interpret the a

priori error estimate by providing upper bounds on the terms on the right hand side of (4.33) and (4.32).

Properties 3.2. *(Approximation in $H^2(\Omega_r)$) Let $T > 0$, $p \geq 1$ and $\hat{u}_h$ be the solution of (4.22), $\hat{e}_p$ and $\hat{E}_p$ defined by (4.24) and (4.25) respectively and $N(t,\cdot)$ and $B(t,\cdot)$ be the seminorms defined by (4.26) and (4.27) respectively. Let $h = \max_{E\in\mathcal{E}} h_E$ and suppose that $J^{\frac{1}{2}}F^{-T} \in H^2(\mathcal{T}_h)^{2\times 2}$ then:*

$$N(t, e_p) \lesssim e^{2C_0(t)+C_1(t)} h|\hat{u}|_{H^2(\Omega_r)} \tag{4.38}$$

$$||e_p||_{L^2(\Omega_r)} \lesssim e^{C_0(t)} h^2 |\hat{u}|_{H^2(\Omega_r)} \tag{4.39}$$

$$B(t, E_p) \lesssim e^{C_1(t)} h|\hat{u}|_{H^2(\Omega_r)} + ||\hat{u}||_{L^2(\Omega_r)} |J^{\frac{1}{2}}F^{-T}|_{H^2(\Omega_r)} \tag{4.40}$$

Proof. **Proof of** (4.38)**:** See [1] **Lemma 2.24** states that

$$|\hat{u} - P_h(0)\hat{u}|_{U(0)} \lesssim h|\hat{u}|_{H^2(\Omega_r)}$$

and **Lemma 2.25** provides

$$J_h(0; \hat{u} - P_h(0)\hat{u}, \hat{u} - P_h(0)\hat{u}) \lesssim h^2 |\hat{u}|^2_{H^2(\Omega_r)}$$

thus along with (4.30) and (4.31)

$$\hat{N}(t; \hat{u} - P_h(0)\hat{u}) \lesssim e^{C_1(t)} \hat{N}(0; \hat{u} - P_h(0)\hat{u}) \lesssim e^{C_1(t)} h|\hat{u}|_{H^2(\Omega_r)}$$

Also by (4.9)

$$\begin{aligned}
|P_h(0)\hat{u} - P_h(t)\hat{u}|_{U(0)} &\leq \frac{C_I}{h} ||P_h(t)\hat{u} - P_h(0)\hat{u}||_{H(0)} \\
&\leq \frac{C_I}{h} (||P_h(t)\hat{u} - \hat{u}||_{H(0)} + ||P_h(0)\hat{u} - \hat{u}||_{H(0)}) \\
&\leq \frac{C_I e^{C_0(t)}}{h} (||P_h(t)\hat{u} - \hat{u}||_{H(t)} + ||P_h(0)\hat{u} - \hat{u}||_{H(t)}) \\
&\leq 2\frac{C_I e^{C_0(t)}}{h} ||P_h(0)\hat{u} - \hat{u}||_{H(t)} \\
&\leq 2\frac{C_I e^{2C_0(t)}}{h} ||P_h(0)\hat{u} - \hat{u}||_{H(0)}
\end{aligned}$$

and by (4.8)

$$J_h(0; P_h(0)\hat{u} - P_h(t)\hat{u}, P_h(0)\hat{u} - P_h(t)\hat{u}) \leq 2\frac{C_T}{h^2} ||P_h(t)\hat{u} - P_h(0)\hat{u}||^2_{H(0)}$$

Therefore

$$\begin{aligned} N(t,e_p) &\leq \hat{N}(t,\hat{u}-P_h(0)\hat{u}) + \hat{N}(t,P_h(t)\hat{u}-P_h(0)\hat{u}) \\ &\lesssim e^{C_1(t)}h|\hat{u}|_{H^2(\Omega_r)} + e^{C_1(t)}\hat{N}(0,P_h(t)\hat{u}-P_h(0)\hat{u}) \\ &\lesssim e^{C_1(t)}h|\hat{u}|_{H^2(\Omega_r)} + \frac{e^{2C_0(t)+C_1(t)}}{h}||P_h(t)\hat{u}-P_h(0)\hat{u}||_{H(0)} \\ &\lesssim e^{2C_0(t)+C_1(t)}h|\hat{u}|_{H^2(\Omega_r)} \end{aligned}$$

Proof of (4.39)**:**

$$\begin{aligned} ||\hat{e}_p||_{H(t)} &\leq ||\hat{u}-P_h(0)\hat{u}||_{H(t)} \\ &\leq e^{C_0(t)}||\hat{u}-P_h(0)\hat{u}||_{H(0)} \\ &\lesssim e^{C_0(t)}h^2|\hat{u}|_{H^2(\Omega_r)} \end{aligned}$$

Proof of (4.40)**:** Let $\Pi^2_{L^2}\colon (H^0(\mathcal{T}_h))^{2\times 2} \to V_h^{2\times 2}$ and $\Pi_1\colon H^0(\mathcal{T}_h) \to \{\hat{v} \in H^0(\mathcal{T}_h) \mid \hat{v} \in \mathcal{S}_1(K)\}$ the L^2-projection on the DG space with polynomial degree one. Then

$$\begin{aligned} \hat{E}_p = \underbrace{J^{\frac{1}{2}}F^{-T}\nabla_X(\hat{u}-\Pi_1\hat{u})}_{A_1} + \underbrace{(J^{\frac{1}{2}}F^{-T}-\Pi^2_{L^2}(J^{\frac{1}{2}}F^{-T}))\nabla_X\Pi_1\hat{u}}_{A_2} \\ + \underbrace{\Pi^2_{L^2}(J^{\frac{1}{2}}F^{-T})\nabla_X\Pi_1\hat{u} - \Pi_{L^2}(J^{\frac{1}{2}}F^{-T}\nabla_X\hat{u})}_{A_3} \end{aligned}$$

By **Lemma 2.25** in [1]: $\hat{B}(A_1) \leq e^{C_1(t)}\hat{B}(\nabla_X(\hat{u}-\Pi_1\hat{u})) \lesssim e^{C_1(t)}h|\hat{u}|_{H^2(\Omega_r)}$. Additionally $\nabla_X\Pi_1\hat{u}$ is constant over every triangle, for $\rho_K > 0$ and $||\pi_K|| = 1$, write $\nabla_X\Pi_1\hat{u} = \rho_K\pi_K$, implying

$$||\nabla_X\Pi_1\hat{u}||^2_{L^2(K)} \approx \rho_K^2 h_K^2 \lesssim \frac{||\Pi_1\hat{u}||^2_{L^2(K)}}{h_K^2} \lesssim \frac{||\hat{u}||^2_{L^2(K)}}{h_K^2}$$

By **Lemma 2.25** [1]:

$$\begin{aligned}\hat{B}(A_2)^2 &= \frac{\sum_{\mathcal{E}_D} h_E \int_E \{\{(J^{\frac{1}{2}}F^{-T} - \Pi^2_{L^2}(J^{\frac{1}{2}}F^{-T}))\nabla_X \Pi_1 \hat{u}\}\}^2}{C_T} \\ &\lesssim \sum_K \frac{||\hat{u}||^2_{L^2(K)}}{h_K^3} \int_{\partial K} ((J^{\frac{1}{2}}F^{-T} - \Pi^2_{L^2}(J^{\frac{1}{2}}F^{-T}))\pi_K)^2 \\ &\lesssim \sum_K ||\hat{u}||^2_{L^2(K)} |J^{\frac{1}{2}}F^{-T}|^2_{H^2(K)}\end{aligned}$$

We have on each triangle K

$$\begin{aligned}&\int_K (\Pi^2_{L^2}(J^{\frac{1}{2}}F^{-T})\rho_K\pi_K - \Pi_{L^2}(J^{\frac{1}{2}}F^{-T}\nabla_X\hat{u}))^2 \\ &\quad\leq \int_K (\Pi^2_{L^2}(J^{\frac{1}{2}}F^{-T})\rho_K\pi_K) \cdot (\Pi^2_{L^2}(J^{\frac{1}{2}}F^{-T})\rho_K\pi_K - \Pi_{L^2}(J^{\frac{1}{2}}F^{-T}\nabla_X\hat{u})) \\ &\quad- \Pi_{L^2}(J^{\frac{1}{2}}F^{-T}\nabla_X\hat{u}) \cdot (\Pi^2_{L^2}(J^{\frac{1}{2}}F^{-T})\rho_K\pi_K - \Pi_{L^2}(J^{\frac{1}{2}}F^{-T}\nabla_X\hat{u})) \\ &\quad\leq \int_K (J^{\frac{1}{2}}F^{-T}\rho_K\pi_K) \cdot (\Pi^2_{L^2}(J^{\frac{1}{2}}F^{-T})\rho_K\pi_K - \Pi_{L^2}(J^{\frac{1}{2}}F^{-T}\nabla_X\hat{u})) \\ &\quad- (J^{\frac{1}{2}}F^{-T}\nabla_X\hat{u}) \cdot (\Pi^2_{L^2}(J^{\frac{1}{2}}F^{-T})\rho_K\pi_K - \Pi_{L^2}(J^{\frac{1}{2}}F^{-T}\nabla_X\hat{u})) \\ &\quad\leq \int_K (J^{\frac{1}{2}}F^{-T}\rho_K\pi_K - J^{\frac{1}{2}}F^{-T}\nabla_X\hat{u})(\Pi^2_{L^2}(J^{\frac{1}{2}}F^{-T})\rho_K\pi_K - \Pi_{L^2}(J^{\frac{1}{2}}F^{-T}\nabla_X\hat{u})) \\ &\quad\leq \frac{1}{2}\int_K (J^{\frac{1}{2}}F^{-T}\nabla_X(\Pi_1\hat{u} - \hat{u}))^2 + \frac{1}{2}\int_K (\Pi^2_{L^2}(J^{\frac{1}{2}}F^{-T})\rho_K\pi_K - \Pi_{L^2}(J^{\frac{1}{2}}F^{-T}\nabla_X\hat{u}))^2\end{aligned}$$

Thus

$$\int_K (\Pi^2_{L^2}(J^{\frac{1}{2}}F^{-T})\rho_K\pi_K - \Pi_{L^2}(J^{\frac{1}{2}}F^{-T}\nabla_X\hat{u}))^2 \leq \int_K (J^{\frac{1}{2}}F^{-T}\nabla_X(\Pi_1\hat{u} - \hat{u}))^2$$

and

$$\begin{aligned}\hat{B}(A_3)^2 &= \frac{\sum_{\mathcal{E}_D} h_E \int_E \{\{\Pi^2_{L^2}(J^{\frac{1}{2}}F^{-T})\nabla_X\Pi_1\hat{u} - \Pi_{L^2}(J^{\frac{1}{2}}F^{-T}\nabla_X\hat{u})\}\}^2}{C_T} \\ &\lesssim \sum_K \int_K (\Pi^2_{L^2}(J^{\frac{1}{2}}F^{-T})\rho_K\pi_K - \Pi_{L^2}(J^{\frac{1}{2}}F^{-T}\nabla_X\hat{u}))^2 \\ &\lesssim \sum_K \int_K (J^{\frac{1}{2}}F^{-T}\nabla_X(\Pi_1\hat{u} - \hat{u}))^2 \lesssim e^{2C_1(t)}|\Pi_1\hat{u} - \hat{u}|^2_{U(0)} \\ &\lesssim e^{2C_1(t)}h^2|\hat{u}|^2_{H^2(\Omega_r)}\end{aligned}$$

□

Remark 3.3. *In* (4.40)*, we bound the inconsistency when the deformation of the mesh is sufficiently smooth. In the following example, we outline that when this regularity is broken, and the flux is not well represented by the projection anymore, the inconsistency can become arbitrarily big compared to* $|\hat{u}|_{H^2}$*. This shows that this formulation is specific to the case where* $J^{\frac{1}{2}}F^{-T}$ *is continuous.*

(a) The situation exhibits the case where $\tilde{V} \in W^{1,\infty}(\Omega) \setminus C^1(\Omega)$ *and conclude that the term* $B(E_p)$ *cannot be bounded from above by the previous techniques. In order to show this, let two triangles* T_1 *and* T_2 *on the interior of the domain* Ω_r*,* E *the edge between the two triangles,* $\boldsymbol{n}_1$ *(respectively* $\boldsymbol{n}_2$*) the outward normal vectors to* T_1 *(respectively* T_2*). Suppose that the solution* $\hat{u}$ *is such that* $\nabla_X \hat{u} = \boldsymbol{n}_1$*, let* A*, the summit of* T_2*, such that* $A \notin T_1$*,* P_A *the orthogonal projection of* A *on* E*. The line between* A *and* P_A *divides* T_2 *into two triangles* $T_2^{(1)}$ *and* $T_2^{(2)}$ *and:*

$\tilde{V} \in W^{1,\infty}(\Omega) \setminus C^1(\Omega)$ *such that*

$$\tilde{V} = \begin{cases} (0,0)^T & \text{on } T_1 \\ -(\boldsymbol{n}_1 \cdot (x - P_A))\boldsymbol{n}_1 & \text{on } T_2^{(1)} \\ -(\boldsymbol{n}_1 \cdot (x - P_A))\boldsymbol{n}_1 - (\boldsymbol{n}_1^{\perp} \cdot (x - P_A))\boldsymbol{n}_1^{\perp} & \text{on } T_2^{(2)} \\ (0,0)^T & \text{on } \partial\Omega_r \end{cases}$$

with $\boldsymbol{n}_1^{\perp}$ *being the normal vector orthogonal to* $\boldsymbol{n}$ *rotated in the counterclockwise direction. By this definition* $\tilde{V}$ *is continuous,* $\forall t > 0$ $\chi(t, T_2 - T_1) \subset T_2 - T_1$ *and thus* $\forall X \in T_2$, $\forall t > 0$,

$$\tilde{V}(t, x(t, X)) = \begin{cases} -(\boldsymbol{n}_1 \cdot (x - P_A))\boldsymbol{n}_1 & \text{on } T_2^{(1)} \\ -(\boldsymbol{n}_1 \cdot (x - P_A))\boldsymbol{n}_1 - (\boldsymbol{n}_1^{\perp} \cdot (x - P_A))\boldsymbol{n}_1^{\perp} & \text{on } T_2^{(2)} \end{cases}.$$

The value of $\tilde{V}$ *is not specified outside* $T_1 \cup T_2$ *but we can build* $\tilde{V}$ *piecewise linear such that* $\tilde{V} = (0,0)^T$ *on each neighbouring summit of* A*. Since* $\tilde{V}$ *is piecewise linear in space and* $\tilde{V} = (0,0)^T$ *on* E*, then* J *and* F *are piecewise constant on* T_1*,* $T_2^{(1)}$ *and* $T_2^{(2)}$*, with* $J^{\frac{1}{2}}F^{-T} \notin H^1(T_2)^{2\times 2}$ *but* $J^{\frac{1}{2}}F^{-T} \in (H^2(T_2^{(1)}) \cap H^2(T_2^{(2)}))^{2\times 2}$*, given by*

$$J^{\frac{1}{2}}F^{-T} = \begin{cases} Id & \text{on } T_1 \\ M_1 = \exp[\begin{pmatrix} x_1^2 - \frac{1}{2} & x_1 x_2 \\ x_1 x_2 & x_2^2 - \frac{1}{2} \end{pmatrix} t] & \text{on } T_2^{(1)} \\ Id & \text{on } T_2^{(2)} \end{cases}$$

with $\boldsymbol{n}_1 = (x_1, x_2)^T$*. Defining* O *as the matrix with columns* $(\boldsymbol{n}_1, \boldsymbol{n}_1^{\perp})$*, it symmetric, orthogonal and fulfills:*

$$\begin{pmatrix} x_1^2 - \frac{1}{2} & x_1 x_2 \\ x_1 x_2 & x_2^2 - \frac{1}{2} \end{pmatrix} = O \begin{pmatrix} \frac{1}{2} & 0 \\ 0 & -\frac{1}{2} \end{pmatrix} O^T, \text{ then } M_1 = O \begin{pmatrix} e^{\frac{t}{2}} & 0 \\ 0 & e^{-\frac{t}{2}} \end{pmatrix} O^T$$

Writing $P = \Pi_{L^2}(\mathbb{1}_{X\in T_2^{(1)}})|_{T_2}$ *there is*

$$M_p = \Pi_{L^2}(J^{\frac{1}{2}}F^{-T})|_{T_2} = Id + (M_1 - Id)P$$

$$\begin{aligned}
\hat{B}(\hat{E}_p)^2 &\geq \frac{h_E \int_E \{\{J^{\frac{1}{2}}F^{-T}\nabla_X \hat{u} - \Pi_{L^2}(J^{\frac{1}{2}}F^{-T}\nabla_X \hat{u})\}\}^2}{C_T} \\
&\geq \frac{h_E[\int_{E\cap T_2^{(2)}}((Id - M_p)\boldsymbol{n}_1)^2 + \int_{E\cap T_2^{(1)}}((M_1 - M_p)\boldsymbol{n}_1)^2]}{4C_T} \\
&\geq \frac{h_E((Id - M_1)\boldsymbol{n}_1)^2[\int_{E\cap T_2^{(2)}} P^2 + \int_{E\cap T_2^{(1)}}(1-P)^2]}{4C_T} \qquad (4.41) \\
&\geq h_E(1 - e^{\frac{t}{2}})^2 C \geq \frac{h_E C t^2}{4} \\
C &= \frac{\int_{E\cap T_2^{(2)}} P^2 + \int_{E\cap T_2^{(1)}}(1-P)^2}{4C_T} > 0
\end{aligned}$$

This term cannot be bounded from above by $|J^{\frac{1}{2}}F^{-T}|_{H^2(T_2^{(1)})}$, $|J^{\frac{1}{2}}F^{-T}|_{H^2(T_2^{(2)})}$ *or* $|\hat{u}|_{H^2}$ *since they are all* 0.

(b) The example shows that since the DG method involves the computation of fluxes at the edges of the mesh, the matrix F *must be regular enough to control the inconsistency. In this case, we can see that the irregularity of the mesh movement makes a polynomial projection incapable of approximating the flux. To overcome the problem, one can imagine a method that tries to take the real flux (see [47] for a method with a discontinuous and piecewise constant diffusion tensor). Since* J *and* F *are in general not piecewise constant, using such a method would make the operator non-coercive and the method unstable.*

(c) In this case $J^{\frac{1}{2}}F^{-T}\nabla_X \hat{u} \notin H^2(\Omega_r)$ *and the convergence theorem from [43] does not hold either.*

(d) Since $\tilde{V}(A) = -(A - P_A) \neq 0$, $\tilde{V}$ *is continuous and* $\tilde{V}$ *not piecewise constant, then* $J^{\frac{1}{2}}F^{-T}$ *is not piecewise constant on the neighbouring cells of* A *and* ***Remark 1.6*** *(b) does not hold: this formulation is not equivalent to any consistent formulation for polynomial trial and test functions.*

In this section, we develop an *a priori* error estimate that directs us towards the existence of a balance between the remaining advection velocity $V - \tilde{V}$ and the spatial variations of $\tilde{V}$. This balance, that appears in the 1D simulations (see in particular section **3 - 3.1**) will also be investigated in the test cases of this chapter in sections **4 - 5.1**.

This *a priori* result, augmented by the convergence study of **Chapter 5** in [43] and the *a posteriori* study of section **4 - 4** and the following test cases, can give us a fair understanding of this moving mesh method.

4 An *a posteriori* error estimate for the semi-discrete formulation

Finally here we will integrate the error criteria that we developped previously. To go from the stationary to the nonstationary problem, we write $\hat{u}^s(t,\cdot) \coloneqq \hat{u}^s(t)$ and $\hat{u}^s_h(t,\cdot) \coloneqq \hat{u}^s_h(t)$. Now for any $t \in [0,T]$ we have $\hat{u}_h(t,\cdot)$ the unique solution of the same problem as $\hat{u}^s_h(t)$ then $\hat{u}_h = \hat{u}^s_h$.
With $a = \varepsilon J F^{-1} F^{-T}$, we define $J^\omega_1 = \frac{\int_\omega J}{|\omega|}$, $a^\omega_1 = \frac{\int_\omega ||a||}{|\omega|}$ and $a^\omega_\infty = ||a||_{L^\infty(\omega)}$, where $||a||$ is the larger eigenvalue of a. Also $\gamma^\omega_\infty = \frac{a^\omega_\infty}{\varepsilon}$, $\gamma^\omega_1 = \frac{a^\omega_1}{\varepsilon}$, let $J^\omega_{\min} = \min_\omega(J)$ and $\rho_S = \min(h_S(\frac{\gamma^{\omega_S}_\infty}{\varepsilon})^{\frac{1}{2}}, (\beta J^{\omega_S}_{\min})^{-\frac{1}{2}})$, $S = E$ or K. These variables correspond to the one of the static case.

We can see here that the features are here quite different to the ones in the 1D case where $a = J^{-1}$. The other difference in 1D is the data we can access, whereas here, the volume of a cell $|K|$ is difficult to approximate geometrically, and so we prefer to use the indirect computation of $\int_\omega J$, in 1D, $\int_\omega J = h_K$, that leads to the **Lemma 2.12**.

$$\text{let } \begin{cases} {\eta^t_{J_K}}^2 & \coloneqq \frac{1}{2} \sum\limits_{E \in \mathcal{E}^{\text{int}} \cap K} [(\beta + \frac{\delta_{\omega_E}}{\varepsilon}) h_E J^{\omega_E}_1 + a^{\omega_E}_1 \frac{\alpha}{h_E}] \gamma^{\omega_E}_\infty \int_E J (F^{-T} [\![\hat{u}_h]\!])^2 \\ & \quad + \sum\limits_{E \in \mathcal{E}^{\text{ext}}_D \cap K} [(\beta + \frac{\delta_{\omega_E}}{\varepsilon}) h_E J^{\omega_E}_1 + a^{\omega_E}_1 \frac{\alpha}{h_E}] \gamma^{\omega_E}_\infty \int_E J (F^{-T} [\![\hat{u}_h]\!])^2 \\ {\eta^t_{E_K}}^2 & \coloneqq \frac{1}{2} \sum\limits_{E \in \mathcal{E}^{\text{int}} \cap K} \sqrt{\frac{\gamma^{\omega_E}_\infty}{\varepsilon}} \rho_E \int_E (\varepsilon J F^{-1} F^{-T} [\![\nabla_X \hat{u}_h]\!])^2 \\ & \quad + \sum\limits_{E \in \mathcal{E}^{\text{ext}}_N \cap K} \sqrt{\frac{\gamma^{\omega_E}_\infty}{\varepsilon}} \rho_E \int_E (\hat{u}_N - \varepsilon J F^{-1} F^{-T} \nabla_X \hat{u}_h \cdot \mathbf{n})^2 \\ {\eta^t_{R_K}}^2 & \coloneqq \rho^2_K || J \hat{f} - J \frac{\partial \hat{u}_h}{\partial t} + \nabla_X \cdot \{ a \nabla_X \hat{u}_h \} - J(V - \tilde{V}) \cdot F^{-T} \nabla_X \hat{u}_h ||^2_{L^2(K)} \end{cases}.$$

$$\eta^t_K{}^2 \coloneqq ({\eta^t_{J_K}}^2 + {\eta^t_{R_K}}^2 + {\eta^t_{E_K}}^2) \tag{4.42}$$

We define $\hat{e} \coloneqq \hat{u} - \hat{u}_h = \hat{\rho} + \hat{\theta}$ with $\hat{\rho} \coloneqq \hat{u} - \hat{u}^s$ and $\hat{\theta} \coloneqq \hat{u}^s - \hat{u}^s_h = \hat{u}^s - \hat{u}_h$.

Then by **Theorem 1.10**: $\forall t \in [0,T]$, $(|||\hat{\theta}||| + |\hat{\theta}|_A)^2 \lesssim \sum\limits_{K \in \mathcal{T}_h} (1 + \frac{1}{\gamma}) \eta^t_K{}^2$.

Lemma 4.1. *For all* $t \in [0,T]$

$$|||\hat{u}_h^r|||^2 + |\hat{u}_h^r|_A^2 \lesssim \sum_{K\in\mathcal{T}_h} [\frac{1}{\gamma}+1]{\eta_{J_K}^t}^2$$
$$||\hat{u}_h^r||_{H(t)}^2 \lesssim \sum_{E\in\mathcal{E}_D} h_E J_1^{\omega_E} \int_E [\![\hat{u}_h]\!]^2$$
$$||\frac{\partial \hat{u}_h^r}{\partial t}||_{H(t)}^2 \lesssim \sum_{E\in\mathcal{E}_D} h_E J_1^{\omega_E} \int_E [\![\frac{\partial \hat{u}_h}{\partial t}]\!]^2$$

Proof. We already proved for the first two inequalities ; the third one is concluded from **Remark 2.2** that implies: $\forall \hat{v}_h \in C^1(0,T;V_h)$, $\frac{\partial}{\partial t}(\mathcal{A}_h\hat{v}_h) = \mathcal{A}_h\frac{\partial \hat{v}_h}{\partial t}$, and applying the **Lemma 1.12** to the function $\frac{\partial \hat{u}_h}{\partial t}$. □

Lemma 4.2. $\forall \hat{v} \in H_D^1(\Omega_r)$, $\quad \int_{\Omega_r} J\frac{\partial \hat{e}}{\partial t}\hat{v} + A(t;\hat{\rho},\hat{v}) = 0$

Proof. The Lemma is a direct consequence of the definition of $\hat{u}$ and $\hat{u}^s$. □

To state the final global error estimate we need some criteria. Let

$$\begin{aligned} {\eta_1^t}^2 &\coloneqq \sum_{K\in\mathcal{T}_h} (1+\tfrac{1}{\gamma}){\eta_K^t}^2 \\ {\eta_2^t}^2 &\coloneqq \sum_{E\in\mathcal{E}_D} h_E J_1^{\omega_E} \textstyle\int_E [\![\frac{\partial \hat{u}_h}{\partial t}]\!]^2 \\ {\eta_3^t}^2 &\coloneqq \sum_{E\in\mathcal{E}_D} h_E J_1^{\omega_E} \textstyle\int_E [\![\hat{u}_h]\!]^2 \end{aligned} \quad . \tag{4.43}$$

For $\hat{v} \in L^\infty(0,T;H^1(\mathcal{T}_h))$ and $v(t,x) \coloneqq \hat{v}(t,X)$ we define:

$$||v||_\#^2 \coloneqq ||v||_{L^\infty(0,T;L^2(\Omega))}^2 + \int_0^T |||\hat{v}|||_t^2 \mathrm{d}t \tag{4.44}$$

This allows us to prove the final estimate.

Theorem 4.3. *Let* $\hat{u} \in C(0,T;H_D^1(\Omega_r)) \cap C^1(0,T;H^{-1}(\Omega_r))$ *be a solution of* (4.21)*,* $\hat{u}_h \in C^1(0,T;V_h)$ *a solution of* (4.22)*,* η_1^t*,* η_2^t *and* η_3^t *be defined in* (4.43)*,* $||\cdot||_\#^2$ *be the norm defined in* (4.44)*,* $e \coloneqq (\hat{u}-\hat{u}_h)(t,\chi(t,X))$ *then*

$$||e||_\#^2 \lesssim S_0(t)\{||e(0)||_{L^2(\Omega)}^2 + \textstyle\int_0^T {\eta_1^t}^2 + T\int_0^T {\eta_2^t}^2 + \max_{t\in[0,T]}({\eta_3^t}^2)\}$$

holds with $S_0(t) = \exp(2C_0(t))$

Proof. Let $\hat{\theta}_c \coloneqq \hat{u}^s - \hat{u}_h^c \in C^1(0,T;H_D^1(\Omega_r))$ and $\hat{e}_c \coloneqq \hat{u}-\hat{u}_h^c \in C^1(0,T;H_D^1(\Omega_r))$. Taking **Lemma 4.2** with $\hat{e}_c$ we have

$$\textstyle\int_{\Omega_r} J\frac{\partial \hat{e}_c}{\partial t}\hat{e}_c + A(t;\hat{e}_c,\hat{e}_c) = \int_{\Omega_r} J\frac{\partial \hat{u}_h^r}{\partial t}\hat{e}_c + A(t;\hat{\theta}_c,\hat{e}_c).$$

Additionally the following inequalities

$$\int_{\Omega_r} J\frac{\partial \hat{e}_c}{\partial t}\hat{e}_c = \frac{1}{2}\frac{\mathrm{d}}{\mathrm{d}t}||e_c||^2_{L^2(\Omega)} - \int_{\Omega_r}\frac{\nabla\cdot\tilde{V}}{2}J\hat{e}_c^2 \geq \frac{1}{2}\frac{\mathrm{d}}{\mathrm{d}t}||e_c||^2_{L^2(\Omega)} - \frac{||\nabla\cdot\tilde{V}||_\infty}{2}||e_c||^2_{L^2(\Omega)}$$

$$A(t;\hat{e}_c,\hat{e}_c) \geq |||\hat{e}_c|||_t^2$$

$$\int_{\Omega_r} J\frac{\partial \hat{u}_h^r}{\partial t}\hat{e}_c \leq \frac{T}{2}||\frac{\partial \hat{u}_h^r}{\partial t}||^2_{H(t)} + \frac{1}{2T}||e_c||^2_{L^2(\Omega)}$$

$$A(t;\hat{\theta}_c,\hat{e}_c) \leq C\cdot(|||\hat{\theta}_c|||_t + |\hat{\theta}_c|_A)|||\hat{e}_c|||_t \leq \frac{C^2}{2}\cdot(|||\hat{\theta}_c|||_t + |\hat{\theta}_c|_A)^2 + \frac{|||\hat{e}_c|||_t^2}{2}$$

hold. Therefore

$$\frac{\mathrm{d}}{\mathrm{d}t}||e_c||^2_{L^2(\Omega)} + (|||\hat{e}_c|||_t^2 - C^2\cdot(|||\hat{\theta}_c|||_t + |\hat{\theta}_c|_A)^2 - T\cdot||\tfrac{\partial \hat{u}_h^r}{\partial t}||^2_{H(t)}) \leq (||\nabla\cdot\tilde{V}||_\infty + \tfrac{1}{T})||e_c||^2_{L^2(\Omega)}$$

And by Gronwall's lemma

$$||e_c||^2_{\#} \lesssim S_0(t)\{||e_c(0)||^2_{L^2(\Omega)} + \textstyle\int_0^T(|||\hat{\theta}_c|||_t + |\hat{\theta}_c|_A)^2 + T\int_0^T||\tfrac{\partial \hat{u}_h^r}{\partial t}||_{H(t)}\}$$

Then by definition of η_3^t

$$||e||^2_{\#} \lesssim S_0(t)\{||e(0)||^2_{L^2(\Omega)} + \int_0^T \eta_1^{t\,2} + T\int_0^T \eta_2^{t\,2} + \max_{t\in[0,T]}(\eta_3^{t\,2})\} \tag{4.45}$$

□

Note that η_3^t, appearing in (4.45), is the only estimator independent of the stopping time. The presence of this term, which is also present on static meshes, explains the fact that the jumps are a good estimator of the error and can be used for h or p-refinement (see [41], [42]). Since we are also interested in the effect of the moving mesh method on the error estimate, we can also notice the presence of the term $S(t)$, which we will see in section **4 - 5.1** will play an important role in the evolution of the error after a few time steps. The presence of this term can be linked to the volume of each cell, $S(t)$ being an upper and lower bound of the volume of each cell ($h(0)/S(t) < h(t) < h(0)S(t)$). The control of this quantity ensures no entanglement. Finally, we can note the presence of the spatial criterion η_1^t, which is integrated in time. The ability of this term to represent the error is studied in section **4 - 5.4**.

By carefully considering the generation and propagation of the error, we have been able to construct error criteria that go beyond classical error theory. Indeed,

while gradient-based error criteria focus on the spatial variations of the computed solution (which we capture with η_R and η_E), we are also able to capture how the error propagates at the edges of the grid with η_J. This theoretical study for a relaxed advection velocity was made possible by the moving mesh framework we mobilised. In particular, we were able to see that the characteristics of the mesh motion have an effect on the estimates.

These integrated criteria, along with the *a priori* study from section **4 - 3** are two key elements to understand the effect of moving meshes on the development of the error: one can see that large deformations of the mesh ($S(t) \gg 1$) can be sources of error. Similarly, a steep deformation ($|J^{\frac{1}{2}}F^{-T}|_{H^2(\Omega_r)} \gg 1$) makes the approximation of the fluxes less accurate and therefore leads to a larger error.

5 Test cases

Unlike the 1D case, we are able to study separately the effect of strong vorticity and strong divergence of the mesh velocity, which gives more diversity to the test cases. Therefore, the first example studies the effect of the moving mesh method on the L^2-error, trying to discuss the conclusions of **Theorem 3.1**. With three test cases, we first outline the exponential dependence of the error on the contraction of the grid, then the exponential dependence of the error on the square of the remaining advection velocity, and finally the presence of a balance between these two effects. The second example is a comparison between the classical SL method and the moving mesh method for a case where the mesh is strongly deformed. The third example looks at the ability of this moving mesh method to cope with boundary layers and the capability of the criteria to detect them. Finally, the last test case shows the performance of the error criterion when the mesh is highly deformed.

In the examples, the time discretisation for the PDE (2.3) is a Runge-Kutta method of order 3. This is chosen because of the optimality of the RKDG method (see [4]) when the DG method is of polynomial order 2 (chosen here). Since the RK3 in the RKDG method requires a midpoint evaluation of the DG operator, the flow map is discretised with a time step of $\frac{\Delta t}{2}$ using a Runge-Kutta method of order 4, and F is computed once the characteristics are obtained by solving the ODE $\dot{F} = \nabla\tilde{V}\,F$. As the focus is on the moving mesh, we used the standard RK4 method, which leaves room for improvement regarding the computation of the characteristics.

When writing $h(x) = (x(1-x))^2$, let the velocities

$$\tilde{V}_d(t,x,y) = (h(y)h'(x), h(x)h'(y))^T \text{ and } \tilde{V}_v(t,x,y) = (h(y)h'(x), -h(x)h'(y))^T \tag{4.46}$$

In the examples, we always work in the spatial domain $[0,1]^2$. We work with polynomials of order 2 and choose the penalty parameter $\alpha = 40$ accordingly, it remains constant for every test cases and there is no distinction between interior and exterior edges.

5 - 1 Example 1: A comparison with static meshes

In first test case, we check the dependence of the L^2-error on the divergence of the mesh velocity, a second test case outlines the dependence of the L^2-error on the remaining advection speed, and a third test case concludes on the existence of a balance between the remaining advection speed and the mesh deformation. The test cases are ran with $\varepsilon = \frac{1}{70}$.
Recall that in the 1D test cases, we underlined the gain of moving mesh methods over static mesh ones and outlined the effect of the mesh deformation. We additionally exhibited the existence of a balance between the mesh deformation and the remaining advection velocity.

A test with divergence

We want to see what happens when the divergence of the mesh velocity increases. What we expect to see is that the L^2-error is largely dependent on this increasing divergence.
So we look at the problem $V(t,x,y) = \alpha\tilde{V}_d(t,x,y) = \tilde{V}(t,x,y)$ as defined in (4.46), which gives the opportunity to check whether, as predicted in **Theorem 3.1**, $||u - u_h||_{L^2} \propto \alpha$. To do this, we take the solution $u(t,x,y) = e^{-t}(\frac{h(x)-h(y)}{h(x)+h(y)})^2$ with Dirichlet boundary conditions.

In Figure 4.1 the error after one time step ($t = 2^{-13}$) is exponentially proportional to α for both NIPG and SIPG. This confirms the term $||\nabla \cdot \tilde{V}||$ from the constants C_S and C_N in the **Theorem 3.1**. In addition, they both have the same slope, which also confirms the fact that C_N and C_S have the same dependence on $||\nabla \cdot \tilde{V}||$.

A test with no divergence

We want to see what happens when the divergence of the mesh velocity is 0 everywhere. What we expect to see is that the L^2-error depends mostly on the

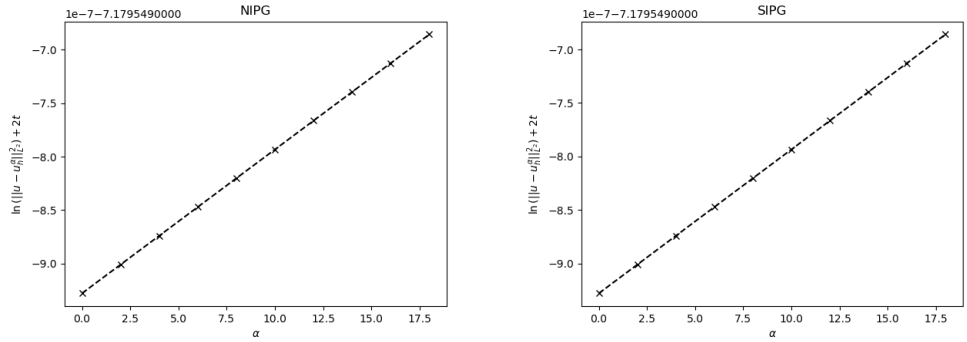

Figure 4.1: Evolution of the L^2-error after one time step when the velocity is $\alpha\tilde{V}_d$, for NIPG (left) and SIPG (right)

maximal value of the remaining advection speed.

Therefore we look at the problem $V(t,x,y) = 10\tilde{V}_v(t,x,y)$ as defined in (4.46), and the mesh velocity is $\tilde{V}(t,x,y) = \alpha\tilde{V}_v(t,x,y)$ with $\alpha = 0,\ldots,10$. The solution is $u(t,x) = e^{-t}h(x)h(y)$ with Dirichlet boundary conditions. Notice that $\alpha = 0$ is the static mesh case.

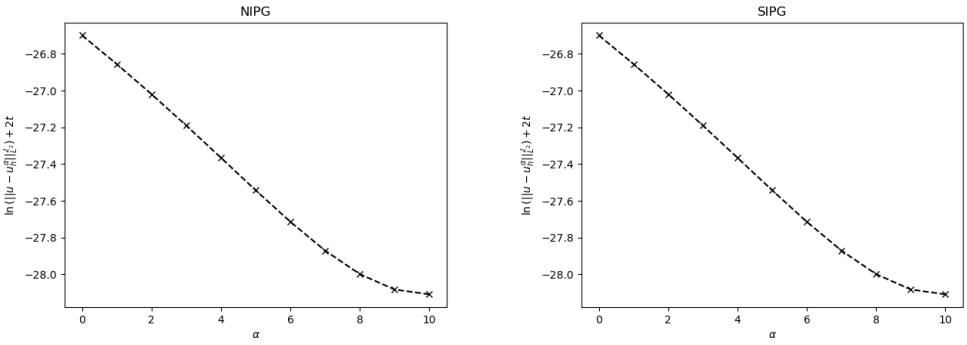

Figure 4.2: Evolution of the L^2-error after one time step when the velocity is $\alpha\tilde{V}_v$, for NIPG (left) and SIPG (right)

In Figure 4.2, the error after a time step decreases with the remaining advection velocity, for both NIPG and SIPG. According to **Theorem 3.1**, the plotted curve should be proportional to $(\alpha - 10)^2$. This is not what we have here, which means that the conclusion from **Theorem 3.1** can be optimised. One sees that the curves are almost the same, hence the values of C_N and C_S should be the same for short times.

A test case with balance

Following on from the test case in section **3 - 3.2**, here we outline the balance that exists in 2D between the modified advection and the divergence of the mesh velocity. A first comment to make is that the larger the $||\nabla \cdot \tilde{V}||_\infty$, the shorter the method will break the CFL condition and thus be unstable. But in addition to this effect, and similar to what we showed in section **3 - 3.2**, there is an optimal balance between reducing the advection velocity by moving the mesh and having a smooth mesh velocity.

We work here with $b = 0.1$, $V(t, x, y) = ((1 + b)\pi - \pi x, (1 + b)\pi - \pi y)^T$.

$$\tilde{V}_p(t, x, y) = (\pi(1 - x)(1 - \exp(-px)), \pi(1 - y)(1 - \exp(-py)))^T$$

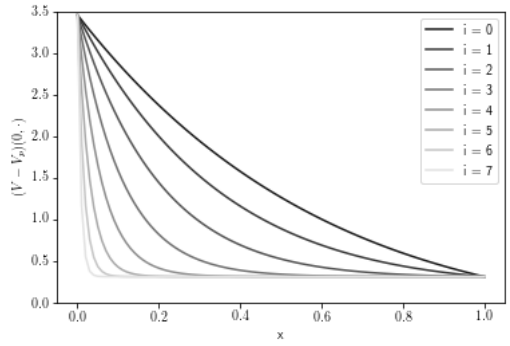

Figure 4.3: Modified advection velocity $(V - \tilde{V}_p) \cdot (1, 0)^T$ for values $p = 2^i$

The test case we use is very similar to that of section **3 - 3.2**, we test values of $p = 1.5^k$ with the solution $u(t, x, y) = \exp\left(-t - \ln\left(\frac{1+b-x}{b}\right)/\pi\right)$. It is discretised with 200 triangles.

One sees that even without an unstable solution there is a balance between the average value of $|V - \tilde{V}_p|$ and the steepness of the mesh motion $|\nabla \cdot \tilde{V}_p|$. For $t \approx 4.6\text{e} - 4$ this value is about $p = 300$. In contrast to the 1D case, the plots of the evolution of the error over time did not show any clear regimes that we could describe. For a further study of the equilibrium and the statement of a stopping time, we refer to section **3 - 3.2**.

This comparison with static meshes completes the theoretical study from **Theorem 3.1**: the L^2-error is confirmed to be exponentially dependant of the

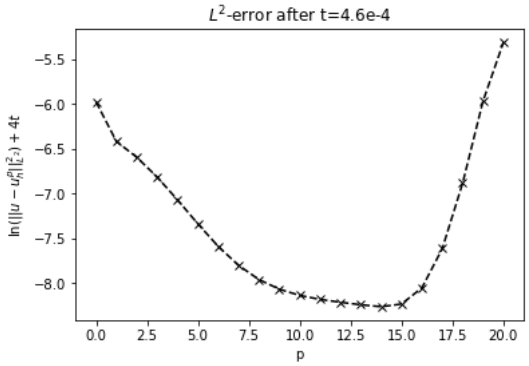

Figure 4.4: L^2-error after $t \approx 4.6\text{e}-4$

contraction of the mesh $||\nabla \cdot \tilde{V}||$. Yet the squared term was not found, it is shown to be increasingly dependent of the remaining advection speed $||V - \tilde{V}||$. Finally, the third test case could outline the need for a balance between $||\nabla \cdot \tilde{V}||$ and $||V - \tilde{V}||$.

5 - 2 Example 2: A comparison with classical semi-Lagrangian methods

In this section we discuss the difference between the classical SL framework and the moving mesh method. Therefore, starting from the reasoning of section **2 - 7**, we compare the moving mesh formulation with a DG formulation with $F = \text{Id}$ and $J = 1$. Our main focus is to outline the role of the accurate computation of numerical fluxes.
Recall that we showed in Chapter 3 that when there is a remaining advection velocity, the moving mesh method is more accurate than the SL method and that for very short time steps, the inconsistency dominates the gain for the fluxes. The 2D case is also the occasion to study a larger variety of mesh velocities.

We study this comparison with four test cases: we the cases where there is no remaining advection velocity and the cases where $V - \tilde{V} = 0$, and comment on the cases where the velocity $\tilde{V}$ is divergence-free and when it isn't. We take $\varepsilon = \frac{1}{100}$ and the diffusion operator is SIPG. For this we have the following cases for solutions and velocities:

- $V - \tilde{V} = 0$ and $\nabla \cdot \tilde{V} = 0$: $\tilde{V} = 50\tilde{V}_v = V$, $u(t,x) = e^{-t}h(x)h(y)$
- $V - \tilde{V} \neq 0$ and $\nabla \cdot \tilde{V} = 0$: $\tilde{V} = 50\tilde{V}_v = V - (1,1)^T$, $u(t,x) = e^{-t}h(x)h(y)$
- $V - \tilde{V} = 0$ and $\nabla \cdot \tilde{V} \neq 0$: $\tilde{V} = 50\tilde{V}_d = V$, $u(t,x) = e^{-t}(\frac{h(x)-h(y)}{h(x)+h(y)})^2$

- $V-\tilde{V} \neq 0$ and $\nabla \cdot \tilde{V} \neq 0$: $\tilde{V} = 50\tilde{V}_d = V-(1,1)^T$, $u(t,x) = e^{-t}(\frac{h(x)-h(y)}{h(x)+h(y)})^2$

The choice of cases where the mesh velocity is divergence-free comes from the fact that it removes the effect of the choice between the conservative and non-conservative formulation of the ALE.

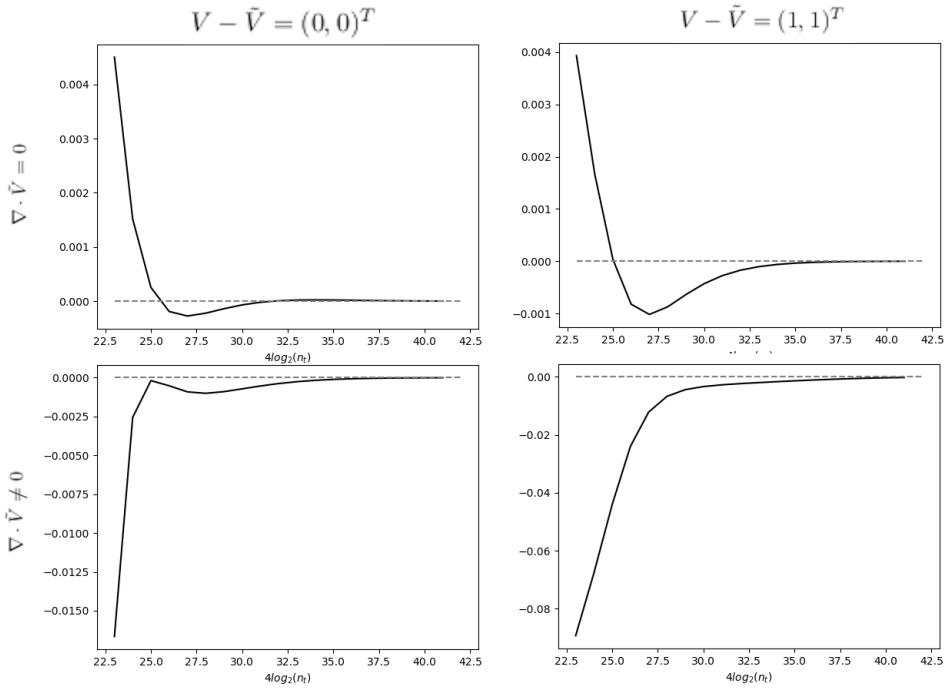

Figure 4.5: Value of $2\ln\frac{|||u-u_h^{MM}|||}{|||u-u_h^{SL}|||}$ for the four cases after one time step as the time step $\Delta t = \frac{1}{n_t}$ decreases

In Figure 4.5 are plotted the value of $2\ln\frac{|||u-u_h^{MM}|||}{|||u-u_h^{SL}|||}$ after a time step of decreasing size: $\Delta t = \frac{1}{n_t}$. In the first case, (namely, $V-\tilde{V}=0$ and $\nabla\cdot\tilde{V}=0$) for large time steps ($\Delta t \in [\frac{1}{90}, \frac{1}{55}]$) the SL method is more accurate than the moving mesh method, then there is a band ($\Delta t \in [\frac{1}{220}, \frac{1}{90}]$) where the moving mesh method is more accurate, and finally the difference tends to zero by positive values. Since we use $\alpha = 40$, we have that the condition number of the diffusion operator is 0.4, so for large time steps the method is not accurate. The fact that the moving mesh method produces the diffusion tensor with eigenvalues greater than ε^2 makes the condition number larger and the method less accurate for the largest time steps.

The fact that the difference tends to zero by positive values can be explained as follows: since the moving mesh method uses projections of the diffusion tensor

to compute the fluxes and is therefore inconsistent, when the time step is very short, we do not gain as much with the diffusion tensor in computing the fluxes, but we still lose consistency.

For the case where $\nabla \cdot \tilde{V} = 0$ and $V - \tilde{V} \neq 0$, the same effect holds for longer time steps with the difference that this problem of condition number also applies to the remaining advection velocity. But, the fact that the gain of the method is also important for the advection operator, where we can compute more precise fluxes ($F^{-T}\mathbf{n}$ instead of $\mathbf{n}$), implies that the gain for $\Delta t \in [\frac{1}{220}, \frac{1}{90}]$ is even larger than for the previous case. In addition, since the advection operator dominates ($|V - \tilde{V}| \gg \varepsilon$), the consistent advection operator dominates the inconsistent diffusion operator and the difference tends to zero by negative values when $\Delta t \to 0,\ \Delta t < \frac{1}{220}$. in section **3 - 3.2**, we expected the flux modification to play a more important role for the 2D simulation, than that of the 1D simulation, this is indeed our conclusion here.

When $\nabla \cdot \tilde{V} \neq 0$ we can see that the fact that our method is non-conservative makes the approximation better for all times and compensates for the loss of consistency effect (the method tends towards zero by negative values). And when $\nabla \cdot \tilde{V} \neq 0$ and $V - \tilde{V} \neq 0$, the two effects add up.

From this we can conclude that the use of modified fluxes for advection and diffusion is a substantial gain to the method. The inconsistency occurring in the diffusion operator is not a major loss and plays a negligible role that is dominant only for very short time steps, even when the advection completely vanishes. The use of the non-conservative formulation is a clear gain here.

5 - 3 Example 3: A test for boundary layers

In this test case we investigate the ability of this method to handle boundary layers. [20] shows that the residual-based error estimator is suitable for a boundary layer test case for the static mesh version, we investigate if this remains as the mesh moves. To do this, we consider the same kind of test case with a modification, the advection velocity will be $V(t,x,y) = (1,1)^T + 2^{16}\tilde{V}_v(t,x,y)$ on $\Omega = [0,1]^2$, u_0, f and u_D are induced from the solution

$$u(t,x,y) = (1 - e^{-t})[\tfrac{e^{(x-1)/\varepsilon)} - 1}{e^{-1/\varepsilon} - 1} + x - 1][\tfrac{e^{(y-1)/\varepsilon)} - 1}{e^{-1/\varepsilon} - 1} + y - 1]$$

It has a boundary layer of order $O(\varepsilon)$ and we will look at the approximation and the error criterion for short times in the case where the mesh moves at velocity $2^{16}\tilde{V}_1(t,x,y)$ and in the case where the mesh is static. The problem is discretised on a regular triangular mesh with 162 cells, the time step is $\Delta t = \frac{1}{1024}$

and $\varepsilon = \frac{1}{70}$ (the mesh Peclet number is approximately 0.13). The results of the energy-norm and the error criteria are plotted after one and twelve time steps. The velocity $\tilde{V}_1$ transports the flow on concentric curves with centre $(0.5, 0.5)$, which are plotted in Figure 4.6 with maximum angular velocity for the curve in black passing through point $(0.5, 0.5 + \frac{1}{2\sqrt{3}})$.

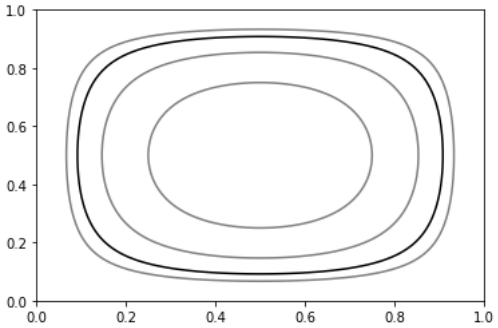

Figure 4.6: Curves on which the particles are advected by the velocity $\tilde{V}_v$

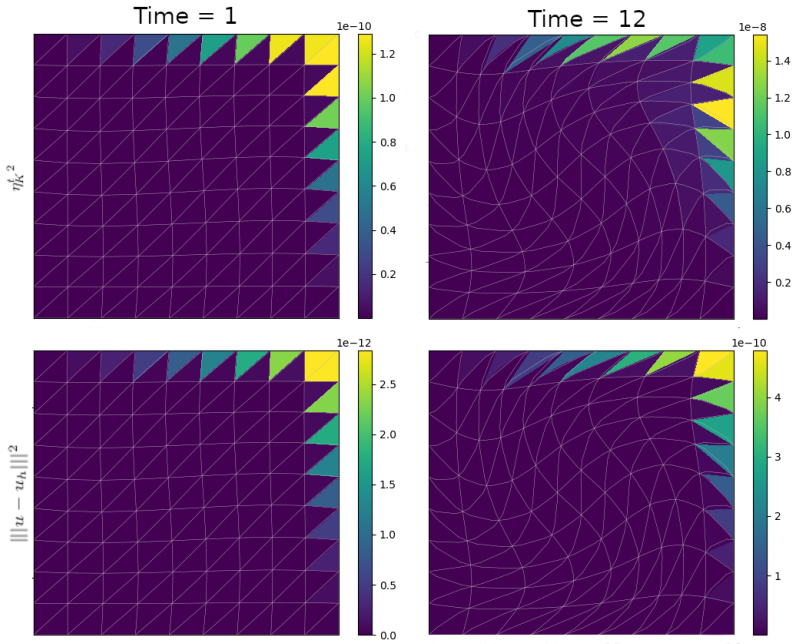

Figure 4.7: Plot of the error and the criterion after one and after twelve time steps when the mesh moves

A first thing we can notice in Figure 4.7 is that the moving mesh method is able to remain very accurate over the whole domain except for the boundary layer

where there is an error of the order of $10^{-3}|||u|||$ constant over time. Similarly, the error criterion has a value of the order of $10^{-2}|||u|||$, constant over time. We conclude that $|||u - u_h||| \approx 10^{-1}\eta_K^t$. After one time step, this error is very well predicted by the error criterion, after twelve time steps, the boundary layer is still caught by the error criterion, but the deformation changes the cell that is predicted to have the largest error. This can be related to the fact that the criterion is reliable but not efficient: the criterion predicts an additional error on the highly deformed cells of the right boundary. Finally, one sees that the error is not distributed in the sense that even if the mesh moves, the neighbouring cells do not end up with larger errors.

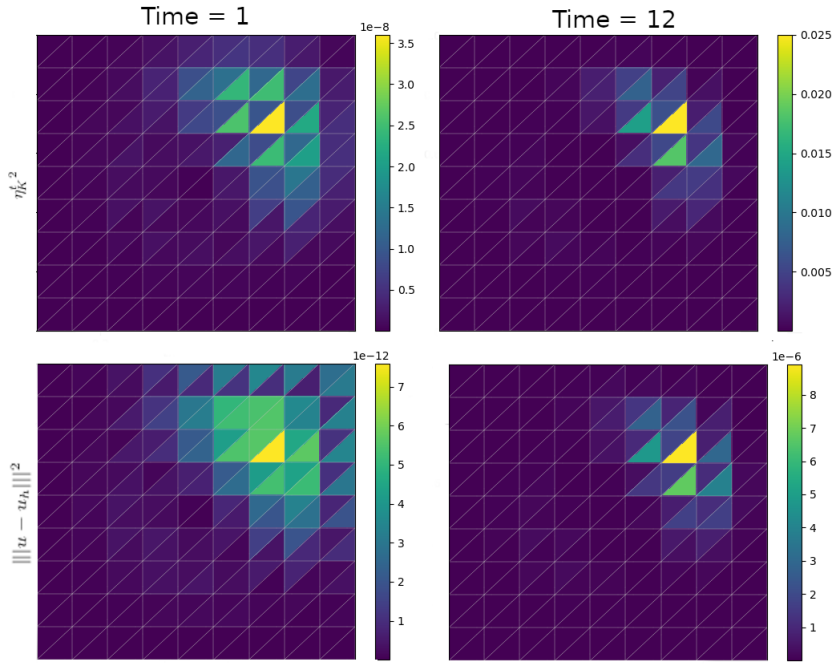

Figure 4.8: Plot of the error and the criterion after one and after twelve time steps when the mesh is static

This is very different for the static mesh method from Figure 4.8, where the bulk of the error is located where the advection velocity is greater: the black curve from Figure 4.6 crosses the large values of u at point $x \approx (0.78, 0.78)$, in the yellow cell. Even though the boundary layer is still present and predicted after one time step, the fact that most of the error is due to advection in the centre of the grid would make a refinement procedure mainly active in this region. After six time steps, the boundary layer is no longer present in the error and in the criteria.

We can conclude that both the DG method and the error criteria are able to

capture the boundary layer even when the grid is highly deformed.

5 - 4 Example 4: Performance with strong deformations

In this subsection we will proceed as in section **3 - 3.3** and see how the error develops with time. Recall that in section **3 - 3.3**, we exhibited the reliability of the criteria but underlined the loss in efficiency.

To do so, we let the model run until longer time with a very steep mesh velocity in the center of the mesh. We define the test case as follows:

- $\Omega = [0,1]^2$, $\Gamma_D = \partial\Omega$, $\Gamma_N = \emptyset$
- $H(s) = -\frac{3}{2} \cdot \frac{\tanh(\beta y(s))}{y'(s)}$, $H_M = \max(H(s))$, $\beta = 3$
- $y(s) = \frac{s-0.5}{(c+s)(1+c-s)}$, $c = 0.4$
- $V_{\text{aux}} = (2H_M, 2H_M)^T - 0.2(x - \frac{1}{2}, y - \frac{1}{2})^T$
- $V(x,y) = V_{\text{aux}} + (H(x)(1 - \frac{H'(y)}{H'(0)}), H(y)(1 - \frac{H'(x)}{H'(0)}))^T$
- $g = V \cdot \begin{pmatrix} 1 \\ 1 \end{pmatrix} + \partial_t u$, $\varepsilon = 0.01$
- $u(x) = (e^{-0.02} - e^{-t})(1 + x + y)$

$$\tilde{V}(t,x) = \begin{pmatrix} (H(x) - H(0)\cos(\pi x))(1 - \frac{H'(y)}{H'(0)} + \pi \frac{H(0)}{H'(0)} \sin(\pi y)) \\ (H(y) - H(0)\cos(\pi y))(1 - \frac{H'(x)}{H'(0)} + \pi \frac{H(0)}{H'(0)} \sin(\pi x)) \end{pmatrix}$$

This construction is first done so the speed $\tilde{V}$ has an area with strong contractions in the center. Additionally the term V_{aux} has two effects: the remaining advection is never equal to 0 and the energy-norm associated to the problem has a component proportionnal to the L^2-norm. We first plot the remaining advection speed and the mesh velocity's divergence.
Notice in Figure 4.9 that the mesh will shrink in the middle and that the remaining advection speed $|V - \tilde{V}|$ has two maxima (in $(0.5, 0)$ and $(0, 0.5)$) and two minima (in $(0.5, 1)$ and $(1, 0.5)$). To check what happens for longer time and see strong deformations, we initialized the case differently: we computed the mesh movement for 200 time steps and project the solution on this mesh. From there

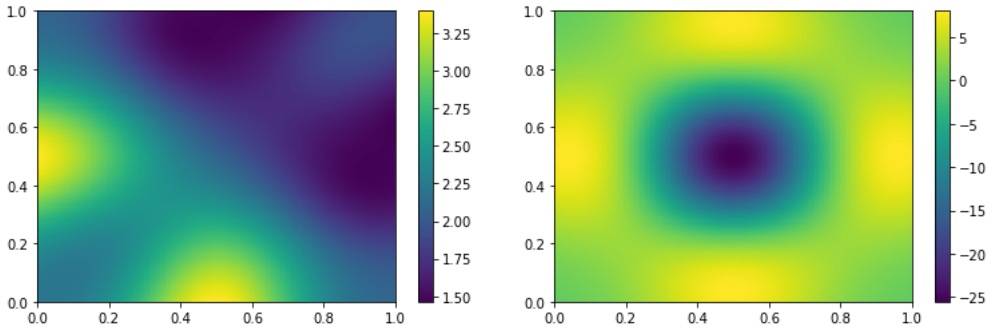

Figure 4.9: Values of the remaining advection speed (right) and the mesh velocity's divergence (left)

the simulation runs normally. In Figure 4.10 are plotted the values of the squares of the criteria and energy-error after 201 time steps, 206 time steps and 221 time steps. The simulations run on a regular mesh of 338 triangles ($= 2 \times 13^2$) and the time step is $\Delta t = \frac{1}{10000}$.

One sees in Figure 4.10 that the error criteria is able to detect the zones where the error is the largest. When focusing on the plots after 201 time steps, the criteria and the error have the following structure: an area up-right with the largest errors (due to the fact that $\max |u(t,\cdot)| = u(t,1,1)$) than some areas around $(1, 0.5)$ and $(0.5, 1)$ where the error is intermediate and finally the central zone around $(0.5, 0.5)$ where there is little error and some higher values for the criteria. The error from the central area occurs from the mesh's deformation.

When the computation runs for longer times, the error in the central area becomes predominant which is well represented by the criteria.

What is not that well represented by the criteria is that, in the energy-error after 206 and 221, there is still some large values around $(0.5, 1)$, $(1, 0.5)$ and in particular $(1, 1)$. These slowly disappear from the picture of the criteria. We can relate that to the fact that the criteria are not reliable: much similarly to the 1D case in section **3 - 3.1**, the error criteria over-evaluate the error in the center, which in contrast makes the error in the other areas under-evaluated.

When comparing the scales of the criteria and the total error we approximately have the following values

time	$\max \eta_K / \|\|\|u - u_h\|\|\|_K$
201	9
206	5
221	4

The order of $\max \eta_K / |||u - u_h|||_K$ does not change and tells us that the error

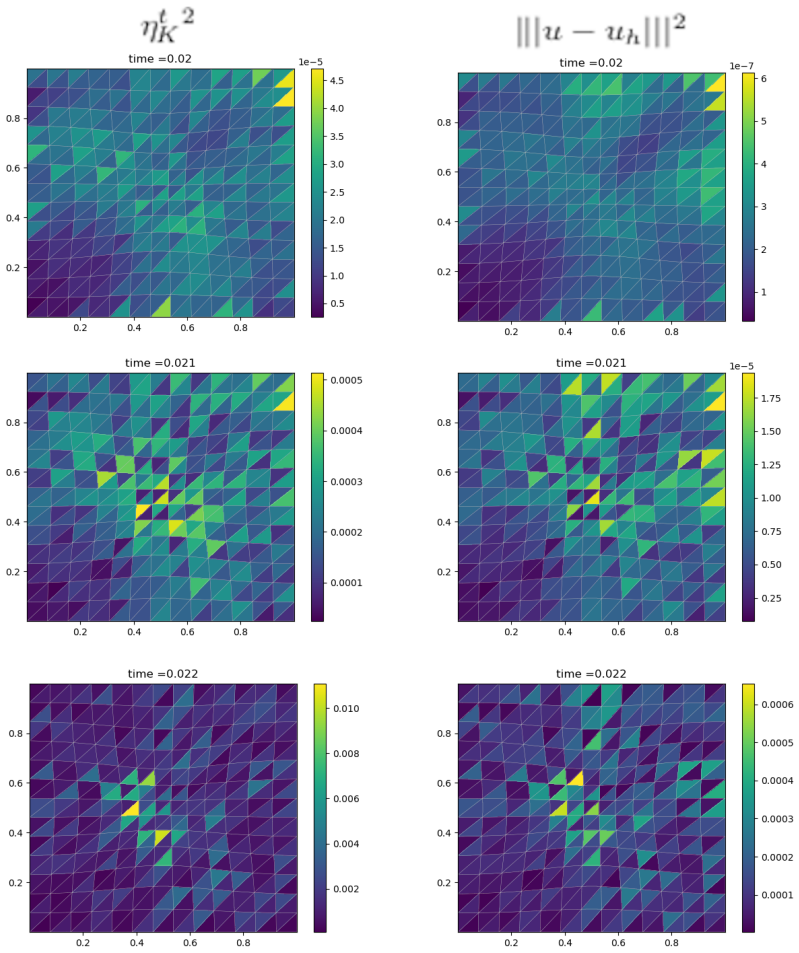

Figure 4.10: Values of the squares of the criteria (right) and energy-error (left) after 201 time steps (first row), 206 time steps (second row) and 221 time steps (third row)

and the criteria evolve similarly.

In this section, through the development of several test cases we were able to test the method and the criteria.

In particular, we initially focused on the effect of the mesh movement on the error. In Example 1 we could outline that the L^2-error is increasingly dependent of the divergence of the mesh velocity and remaining advection speed. We could finally outline the presence of a balance between these two values in a third test case

Example 2 dealt with a comparison with a SL method. Major focus was put on the effect of the numerical flux on the H^1-error of a moving mesh and SL method.

By comparing what happens when there is some remaining advection velocity or not and when the moving mesh velocity is divergence-free or not, we showed that the DG methods implemented here required a specific focus on the value of the numerical fluxes. Specifically, the numerical fluxes need to be adapted to the deformation of the mesh and to the non-conservative situation.
Example 3 proved that the implemented DG methods were able, similarly to those on static meshes, to resolve boundary layers and additionally that the error criteria were able to detect these boundary layers. By comparing the boundary layer test case on a moving mesh with the same solved on a static mesh, we proved that the moving mesh method can help the approximation in this kind of situation: since the error is scaled by the local advection speed, in the situation of static meshes, most of the error did not arise from the boundary layer but from the advection term, this effect disappears when the mesh moves and the solution is resolved so that the error only occurs from the boundary layer.
Finally Example 4 confirmed the reliability of the error criteria: when computed on a very deformed mesh, the error criteria can detect the error occurring from the deformation of the mesh and they are still able to detect the error occurring from the scheme (in the sense that they do not appear because of the mesh's deformation but because of the DG approximation). This can still be improved since the error in the deformed areas is over-evaluated and in contrast makes the error coming from the scheme under-evaluated.

Chapter 5

Conclusions and future works

1 Conclusion

In this thesis we established interior penalty discontinuous Galerkin methods for the semi-discretisation of an Arbitrary Lagrangian-Eulerian formulation in unsteady advection-diffusion problems. By discretising the problem via a dynamically deforming map, we used the existing analytic techniques for advection-diffusion problems with continuous diffusion tensors. This lead us to derive *a priori* error estimates that indicates the choice of the deforming velocity and made the establishment of *a posteriori* error criteria possible. The reliability of both the *a priori* and *a posteriori* error estimations were then discussed in numerical tests.

By focusing on the available data, we derived specific *a posteriori* criteria for the moving mesh method in one and two spatial dimensions. The robustness of these error criteria in terms of the mesh's Peclet number allowed us to scale the error criteria with the square of the local remaining advection speed (called δ). This behaviour is confirmed by the test cases where the error in terms of the energy-norm appears to strongly depend on this local speed.

Similarly in Chapter 4, we studied the ability of the DG methods on static meshes to resolve boundary layers and the capability of the error criteria to detect them. We marked that the DG methods formulated in the ALE framework, and the derived error criterion, suitably inherit from these properties. We specifically underlined that the DG method needed the mesh movement in order to resolve the boundary layer when the advection velocity has spatial variations.

Additionally, the developed *a priori* and *a posteriori* estimates outline a balance between the remaining advection speed and the norm of the gradient of the mesh movement. This balance is outlined when the given advection has large

spatial variations, leading to the need of a moving mesh velocity with large spatial variations as well. This is discussed in the test cases where we see that the effect of unbalanced mesh velocity occurs before the effect of entanglement.

SL methods were interpreted in terms of the ALE framework. In the comparison of the SL with the moving mesh method, we underlined the necessity of the accurate fluxes' computation when using a SLDG method for advection-dominated advection-diffusion equations. In the test cases, both in one and two spatial dimensions, we saw that most of the gain or loss of the moving mesh method is done in the expression of the numerical fluxes. The moving mesh method gains accuracy by approximating the fluxes more precisely but pays this gain by loosing consistency. The novelty here is that not only we consider the polynomial discretisation to be deforming but also the cells and especially the fluxes both in one and two spatial dimensions. Furthermore, the development of reliable *a posteriori* error criteria sets the scene for remainder-based h-refinement in SLDG methods.

2 Future works

A natural development of this ALE method is the development of a SL method for the resolution of advection-dominated flows. By more carefully approximating the characteristics and determinant of the deformation map, we can expect to measure the fluxes more accurately. The first step in this direction is to formulate the fully discretised problem and to find a suitable method to better link the computation of the characteristics with the computation of the determinant of the deformation map. Once this is achieved, by adding the reliable error criteria to the study, we can implement a semi-Lagrangian method that uses the principles of remainder-based adaptive mesh refinement.

Another topic we want to investigate, originating from the comparison with SL method, is to try to reduce the inconsistency occurring from the computation of the fluxes. We saw in the test cases that for small deformations of the map, the inconsistency dominates. Therefore, we want to investigate a moving mesh method that remains fully consistent where the deformations are small and that is inconsistent only where the deformations of the map are large.

Finally a topic that has not been adressed here is the study of the development of efficient error criteria. Here the deformation of the map made it impossible to achieve efficiency without more information on the deformation. Since the criteria on static meshes are robust in terms of the mesh's Peclet number, we can

expect to find reliable and efficient error criteria when the deformation remains small.

Bibliography

[1] V.Dolejší, M.Feistauer. *Discontinuous Galerkin Method*, Springer, 2015.

[2] P. Clement. *Approximation by finite element functions using local regularization*, Revue française d'automatique, informatique, recherche opérationnelle. Analyse numérique, 9, no 2 (1975), p. 77-84.

[3] B.Cockburn, C.-W.Shu. *TVB Runge-Kutta Local Projection Discontinuous Galerkin Finite Element Method for Conservation Laws II: General Framework* Mathematics of Computation, Vol. 52, No. 186 (Apr., 1989), pp. 411-435.

[4] B.Cockburn, C.-W.Shu. *Runge-Kutta discontinuous Galerkin methods for convection-diffusion problems*, Journal of Scientific Computing, 16 (2001), pp.173-261.

[5] W.H. Reed, T.R. Hill, *Triangular mesh methods for the neutron transport equation*, Tech. Report LA-UR-73–479, Los Alamos Scientific Laboratory, 1973.

[6] D.N.Arnold, F.Brezzi, B.Cockburn,L. Donatella Marini. *Unified Analysis of Discontinuous Galerkin Methods for Elliptic Problems*, SIAM J. Numer. Anal. Vol. 39, No. 5, pp. 1749–1779 (2002)

[7] M.F.Wheeler, *An Elliptic Collocation-Finite Element Method with Interior Penalties*, SIAM J. Numer. Anal. Vol. 15, No. 1, pp. 152-161 (1978)

[8] V.Dolejší, M.Feistauer, C.Schwab. *A finite volume discontinuous Galerkin scheme for nonlinear convection-diffusion problems*, Calcolo, 39 (2002), pp.1-40.

[9] V.Dolejší, M.Feistauer. *Error estimates of the discontinuous Galerkin method for nonstationary convection-diffusion problems*, Numerical Functional Analysis and Optimization, 26 (2005), pp.349-383.

[10] M.Feistauer, J.Hájek, K.Švadlenka. *Space-time discontinuous Galerkin method for solving nonstationary convection-diffusion-reaction problems*, Applications of Mathematics, 52 (2007), pp.197-233.

[11] V.Dolejší. *hp-DGFEM for nonlinear convection-diffusion problems*, Mathematics and Computer in Simulation, 87 (2013), pp.87-118.

[12] F.Naddei, M. de la Llave Plata, V.Couaillier, F.Coquel. *A comparison of refinement indicators for the p-adaptive simulation of steady and unsteady flows with discontinuous Galerkin methods*, (2018), hal-01787788.

[13] P.Houston, C.Schwab, E.Süli. *Stabilized hp-finite element methods for first-order hyperbolic problems*, SIAM J. Numer. Anal., 37 (2000), pp.1618-1643.

[14] P.Houston, E.Süli. *hp-adaptive discontinuous Galerkin finite element methods for first-order hyperbolic problems*, SIAM J. on Sci. Comput., 23 (2001), pp.1226-1252.

[15] P.Houston, E.Süli. *Adaptive Lagrange-Galerkin Methods for Unsteady Convection-Diffusion Problems*, Mathematics of Computation, Vol. 70, No. 233 (Jan., 2001), pp. 77-106.

[16] R.Verfürth. *A posteriori error estimators for convection-diffusion equations*, Numer. Math., 80 (1998), pp.641-663.

[17] R.Verfürth. *Robust a posteriori error estimators for a singularly perturbed reaction-diffusion equation*, Numer. Math., 78 (1998), pp.479–493.

[18] R.Verfürth. *Error Estimates for some Quasi-Interpolation operators*, M2AN, 33 (1999), pp.695-713.

[19] R.Verfürth. *Robust a posteriori error estimates for nonstationary convection-diffusion equations*, SIAM J. Numer. Anal., 43 (2005), pp.1783-1802.

[20] D.Schötzau, L.Zhu. *A robust a posteriori error estimator for discontinuous Galerkin methods for convection-diffusion equations*, Applied Numerical Mathematics, 59 (2009), pp.2236–2255.

[21] R.Araya, P.Venegas. *An a posteriori error estimator for an unsteady advection-diffusion-reaction problem*, Computers and Mathematics with Application, 66 (2014), pp.2456-2476.

[22] A.Karakashian, F.Pascal. *A posteriori error estimates for a discontinuous Galerkin approximation of second-order elliptic problem*, SIAM J. Numer. Anal., 41 (2003), pp.2374-2399.

[23] T. Warburton, J. S. Hesthaven. *On the constants in hp-finite element trace inverse inequalities*, Comput. Methods Appl. Mech. Engrg., 192 (2003), pp.2765–2773.

[24] A.Cangiani, E.H.Georgoulis, S.Metcalfe. *Adaptive discontinuous Galerkin methods for nonstationary convection-diffusion problems*, IMA Journal of Numerical Analysis, 34 (2014), pp.1578-1597.

[25] T.F.Dupont, Y.Liu. *Symmetric error estimates for moving mesh Galerkin methods for advection-diffusion equations*, SIAM J. Numer. Anal., 40 (2002), pp.914-927.

[26] M.Bause, P.Knabner. *Uniform error analysis for Lagrange-Galerkin approximations of convection-dominated problems*, SIAM J. Numer. Anal., 39 (2002), pp.1954-1984.

[27] K.Chrysafinos, N.J.Walkington. *Error estimates for the discontinuous Galerkin methods for parabolic equations*, SIAM J. Numer. Anal., 44 (2006), pp.349-366.

[28] K.Chrysafinos, N.J.Walkington. *Lagrangian and moving mesh methods for the convection-diffusion equation*, ESAIM: Mathematical Modeling and Numerical Analysis, 42 (2008), pp.25-55.

[29] V.Kučera, M.Feistauer, J.Prokopová. *The discontiunuous Galerkin method for convection-diffusion problems on time-dependant domains*, Numerical Mathematics and Advanced Applications, (2009), pp.551-559. Springer, Berlin, Heidelberg.

[30] J.J.Sudirham, J.J.W.van der Vegt, R.M.J.van Damme. *Space-time discontinuous Galerkin method for advection-diffusion problems on time-dependant domains*, Applied Numerical Mathematics, 56 (2006), pp.1491-1518.

[31] A.Bonito, I.Kyza, R.H.Nochetto. *A DG approach to higher order ALE formulations in time*, in Recent Developments in Discontinuous Galerkin Finite Element Methods for Partial Differential Equations, X.Feng, O.Karakashian, Y.Xing pp.223-258, Springer, Heidelberg, 2012.

[32] A.Bonito, I.Kyza, R.H.Nochetto. *Time-discrete high-order ALE formulations: stability*, SIAM J. Numer. Anal., 51 (2013), pp.577-604.

[33] A.Bonito, I.Kyza, R.H.Nochetto. *Time-discrete high-order ALE formulations: a priori error analysis*, Numer. Math., 125 (2013), pp.225-257.

[34] M.Balászová, M.Feistauer, M.Vlasák. *Stability of the ALE space-time discontinuous Galerkin method for nonlinear convection-diffusion problems in time-dependant domains*, ESAIM: Mathematical Modeling and Numerical Analysis, 52 (2018), pp.2327-2356.

[35] S.Srivastava, S.Ganesan. *Local projection stabilization with discontinuous Galerkin method in time applied to convection dominated problems in time-dependant domains*, BIT Numerical Mathematics, 60 (2020), pp.481-507.

[36] S.Ganesan, S.Srivastava, *ALE-SUPG finite element method for convection-diffusion problems in time-dependent domains: Conservative form*, Applied Mathematics and Computation, Volume 303, 15 June 2017, Pages 128-145.

[37] S.Ganesan, S.Srivastava, *ALE-SUPG finite element method for convection-diffusion problems in time-dependent domains: Non-conservative form*, arXiv, 1603.00632 (2016).

[38] L.Zhou, Y.Xia., C.-W.Shu. *Stability analysis and error estimates of arbitrary Lagrangian-Eulerian discontinuous Galerkin method coupled with Runge-Kutta time-marching for linear conservation laws*, ESAIM: M2AN 53 (2019) 105–144.

[39] L.Zhou, Y.Xia. *Arbitrary Lagrangian-Eulerian local discontinuous Galerkin method for linear convection-diffusion equations*, Journal on Scientific Computing, 90 (2022), 21.

[40] E.Rozier, J.Behrens: *Adaptive discontinuous Galerkin methods for 1D unsteady convection-diffusion problems on a moving mesh.* To appear in: Modeling, Simulation and Optimization of Fluid Dynamic Applications, A. Iske and T. Rung (eds.), Chapter 3, Springer, Heidelberg, 2023.

[41] J-F. Remacle,J. E. Flaherty, M. S. Shephard, *An adaptive discontinuous Galerkin technique with an orthogonal basis applied to compressible flow problems*, SIAM Review, 45 (2003), pp.53-73.

[42] S. Faghih-Naini, V. Aizinger, *p-adaptive discontinuous Galerkin method for the shallow water equations with a parameter-free error indicator*, Int J Geomath 13, 18 (2022).

[43] A. Cangiani, Z. Dong, E. H. Georgoulis, P. Houston, *hp-Version Discontinuous Galerkin Methods on Polygonal and Polyhedral Meshes*, Springer, 2017.

[44] W. Huang, R. D. Russel, *Adaptive Moving Mesh Methods*, Springer, 2011.

[45] P.Houston, C.Schwab, E.Süli. *Discontinuous hp-Finite Element Methods for Advection-Diffusion-Reaction Problems*, SIAM J. Numer. Anal., 39 (2002), pp.2133-2163.

[46] E. H. Georgoulis, A. Lassis. *A note on the design of hp-version interior penalty discontinuous Galerkin finite element methods for degenerate problems*, IMA J. Numer. Anal., 26 (2006), pp.381-390.

[47] A. Ern, A. Stephansen, P. Zunino. *A Discontinuous Galerkin method with weighted averages for advection-diffusion equations with locally vanishing and anisotropic diffusivity*, IMA J. Numer. Anal., 29 (2005), pp.235-256.

[48] E.Burman, P. Zunino. *A domain decomposition method based on weighted interior penalties for advection-diffusion-reaction problems*, J. Numer. Anal. 44 (2006) 1612-1638.

[49] A. Ern, A. Stephansen, M.Vohralík. *Guaranteed and robust discontinuous Galerkin a posteriori error estimates for convection–diffusion–reaction problems*, J. Comput. App. Math. 234 (2010) 114–130.

[50] C.J.Budd, W.Huang, R.D.Russell. *Adaptivity with moving grids*, CambriDGe University Press, Acta Numerica (2010).

[51] M.J.Baines, M.E.Hubbard, P.K.Jimack. *Velocity-Based Moving Mesh Methods for Nonlinear Partial Differential Equations*, Commun. Comput. Phys., 10 (2011), pp.509-576.

[52] E.Gaburro, W.Boscheri, S.Chiocchetti, C.Klingenberg, V.Springel, M.Dumbser. *High order direct Arbitrary-Lagrangian-Eulerian schemes on moving Voronoi meshes with topology changes*, J. Comput. Phys., 407 (2020), pp.109-167.

[53] M.Tavelli, W.Boscheri. *A high order parallel problems Eulerian-Lagrangian algorithm for advection-diffusion problems on unstructured meshes*, Int. J. Numer. Met. Fluids, 00 (2019), pp.1-16.

[54] François Vilar, P.H. Maire, Remi Abgrall. *Cell-centered discontinuous Galerkin discretizations for two-dimensional scalar conservation laws on unstructured grids and for the one-dimensional Lagrangian hydrodynamics.* Computers and Fluids, 2010, pp.Article in Press.

[55] Walter Boscheri, Michael Dumbser. *Arbitrary-Lagrangian-Eulerian discontinuous Galerkin schemes with a posteriori subcell finite volume limiting on moving unstructured meshes* J. Comput. Phys., 346 (2017), pp.449-479.

[56] Michael Dumbser, Walter Boscheri. *High–Order Unstructured Lagrangian One–Step WENO Finite Volume Schemes for Non–conservative Hyperbolic Systems: Applications to Compressible Multi–Phase Flows*, arXiv, 1304.4816.

[57] Christian Klingenberg, Gero Schnücke, Yinhua Xia. *Arbitrary Lagrangian-Eulerian discontinuous Galerkin method for conservation laws: Analysis and application in one dimension*, Mathematics of Computation 86(305):1 (2015).

[58] L.Formaggia, F.Nobile. *A stability analysis for the arbitrary Lagrangian Eulerian formulation with finite elements*, East-West J. Numer. Math., 7 (1999), pp. 105-131.

[59] L.Formaggia, F.Nobile. *Stability analysis of second-order time accurate schemes for ALE–FEM*, Comput. Methods Appl. Mech. Engrg. 193 (2004) 4097–4116.

[60] Christian Klingenberg, Gero Schnücke, Yinhua Xia. *An Arbitrary Lagrangian–Eulerian Local Discontinuous Galerkin Method for Hamilton–Jacobi Equations*, J Sci Comput (2017) 73:906–942.

[61] C. W. Hirt, A. A. Amsden, and J. L. Cook. *An arbitrary Lagrangian–Eulerian computing method for all flow speeds*, J. Comput. Phys. 14, 227 (1974).

[62] J.M.Hyman, B.Larrouturou. *Dynamic rezone methods for partial differential equations in one space dimension*, Applied Numerical Mathematics, 5 (1989)pp.435-450.

[63] J.M.Hyman, S.Li, L.R.Petzold. *An adaptive moving mesh method with static rezoning for partial differential equations*, Computers and Mathematics with Applications, Volume 46, Issues 10–11, November–December 2003, Pages 1511-1524.

[64] I. Lomtev, R. M. Kirby, and G. E. Karniadakis. *A Discontinuous Galerkin ALE Method for Compressible Viscous Flows in Moving Domains*, J. Comput. Phys. 155, 128–159 (1999).

[65] P.Fu, G.Schnücke, Y.Xia, *Arbitrary Lagrangian-Eulerian discontinuous Galerkin method for conservation laws on moving simplex meshes*, Mathematics of Computation, 88 (2019), pp.2221–2255.

[66] M. Uzunca, B.Karasözen, T.Küçükseyhan, *Moving mesh discontinuous Galerkin methods for PDEs with traveling waves*, Applied Mathematics and Computation 292 (2017) 9–18.

[67] S.Badia, R.Codina, *Analysis of a stabilized finite element approximation of the transient convection-diffusion equation using an ALE framework*, SIAM J. NUMER. ANAL.Vol. 44, No. 5, pp. 2159-2197 (2006).

[68] M.Lesoinne, C.Farhat, *Geometric conservation laws for flow problems with moving boundaries and deformable meshes, and their impact on aeroelastic computations.*, Comput. Methods Appl. Mech. Eng. 1996; 134(1-2):71-90.

[69] J.Donea, A.Huerta, J.-Ph.Ponthot, A.Rodríguez-Ferran, *Arbitrary Lagrangian-Eulerian methods*, The Encyclopedia of Computational Mechanics, Wiley, Vol. 1, Chapter 14, pp. 413-437, 2004.

[70] Springel,V., *E pur si muove : Galilean-invariant cosmological hydrodynamical simulations on a moving mesh*, Monthly Notices of the Royal Astronomical Society, Volume 401, Issue 2,Pages 791–851, January 2010.

[71] B.K.Kometa (2011). *Semi-Lagrangian methods and new integration schemes for convection-dominated problems* [Doctoral dissertation, Norwegian University of Science and Technology, Trondheim]. NTNUopen. https://ntnuopen.ntnu.no/ntnu-xmlui/bitstream/handle/11250/258968/506206_FULLTEXT01.pdf?sequence=1

[72] L.Bonaventura, *An introduction to semi-Lagrangian methods for geophysical scale flows*, Lecture Notes, MOX - Applied Mathematics Laboratory, Department of Mathematics, Politecnico di Milano, (luca.bonaventura@polimi.it), mox.polimi.it/ bonavent/archive/lezlag000.pdf, Italy.

[73] A.Staniforth, J.Cote, *semi-Lagrangian integration schemes for atmospheric models*, Monthly Weather Review 119 (1991), 2206–2223.

[74] M.Restelli, L.Bonaventura, R.Sacco, *A semi-Lagrangian discontinuous Galerkin method for scalar advection by incompressible flows*, J. Comput. Phys. 216, 195-215 (2006).

[75] S.P. Cook et al., *The moving mesh semi-Lagrangian MMSISL method*, J. Comput. Phys. (2019), https://doi.org/10.1016/j.jcp.2019.01.037

[76] Bonaventura, L., Calzola, E., Carlini, E. et al. *Second Order Fully Semi-Lagrangian discretisations of Advection-Diffusion-Reaction Systems.* J Sci Comput 88, 23 (2021).

[77] X.Cai, W.Guo, J.Qiu, *Comparison of Semi-Lagrangian Discontinuous Galerkin Schemes for Linear and Nonlinear Transport Simulations.* Communications on Applied Mathematics and Computation (2022) 4:3–33.

[78] Morton, K. W., Priestley, A., Suli, E. *Stability of the Lagrange-Galerkin method with non-exact integration.* M2AN - Modélisation mathématique et analyse numérique, Volume 22 (1988) no. 4, pp. 625-653. http://www.numdam.org/item/M2AN_1988__22_4_625_0/

[79] Petera, J., Nassehi, V., *A new two-dimensional finite element model for the shallow water equations using a lagrangian framework constructed along fluid particle trajectories.* Int. J. Numer. Meth. Engng., 39: 4159-4182 (1996).

[80] F.X.Giraldo, *The Lagrange–Galerkin method for the two-dimensional shallow water equations on adaptive grids.* Int. J. Numer. Meth. Fluids 2000; 33: 789–832.

[81] M.El-Amrani, A.El-Kacimi, B.Khouya, M.Seaid, *Bernstein-Bézier Galerkin-Characteristics Finite Element Method for Convection-Diffusion Problems*, Journal of Scientific Computing (2022) 92:58.

[82] M.Ding, X.Cai, W.Guo, J.Qiu (2020). *A semi-Lagrangian discontinuous Galerkin (DG) – local DG method for solving convection-diffusion equations.* Journal of Computational Physics. 409. 109295. 10.1016/j.jcp.2020.109295.